N81-22076

STUDY OF THERMAL CONTROL SYSTEMS FOR ORBITING POWER SYSTEMS

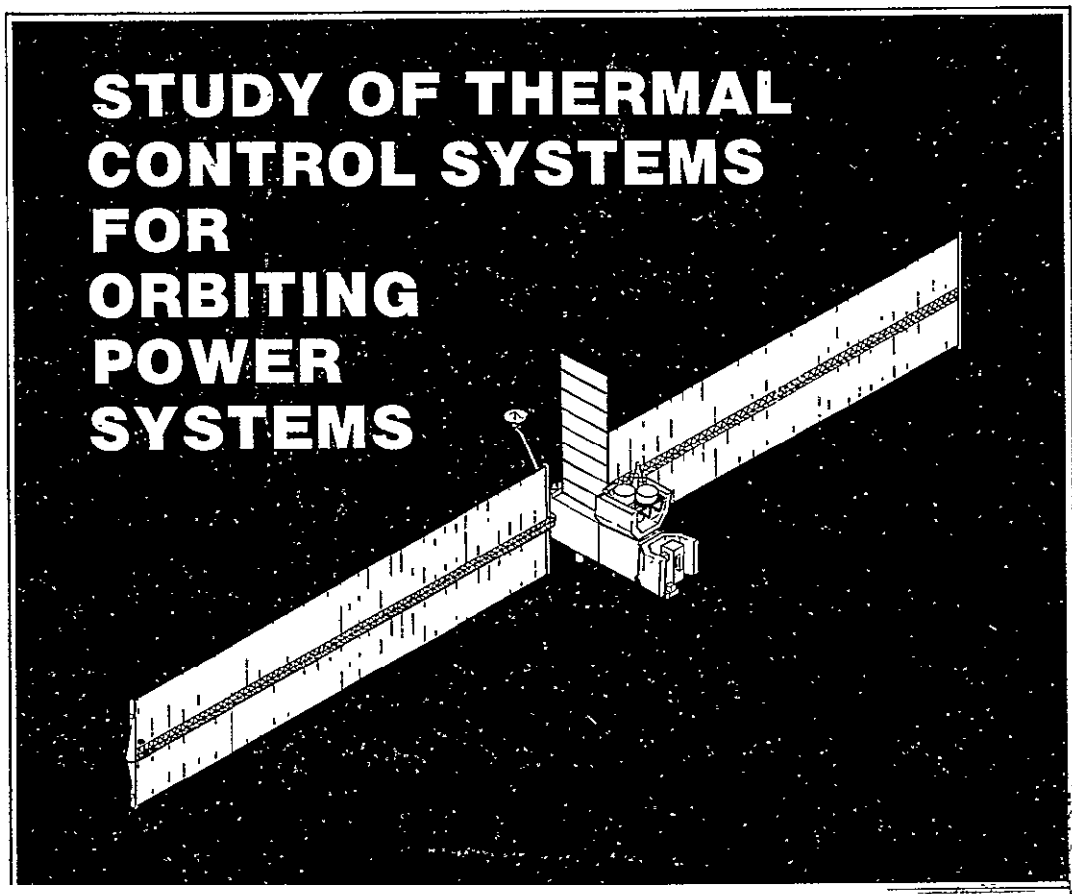

FINAL REPORT CONTRACT NAS8-33560

REPORT NO. 2-53020/1R-52666

16 FEBRUARY 1981

Prepared for
The National Aeronautics and Space Administration
Marshall Space Flight Center

by

VOUGHT CORPORATION
an LTV company

(NASA-CR-161751) STUDY OF THERMAL CONTROL SYSTEMS FOR ORBITING POWER SYSTEMS Final Report (Vought Astronautics, Dallas, Tex.) 168 p HC A08/MF A01 CSCL 22B

N81-22076

Unclas
G3/15 42252

169

G0-1078

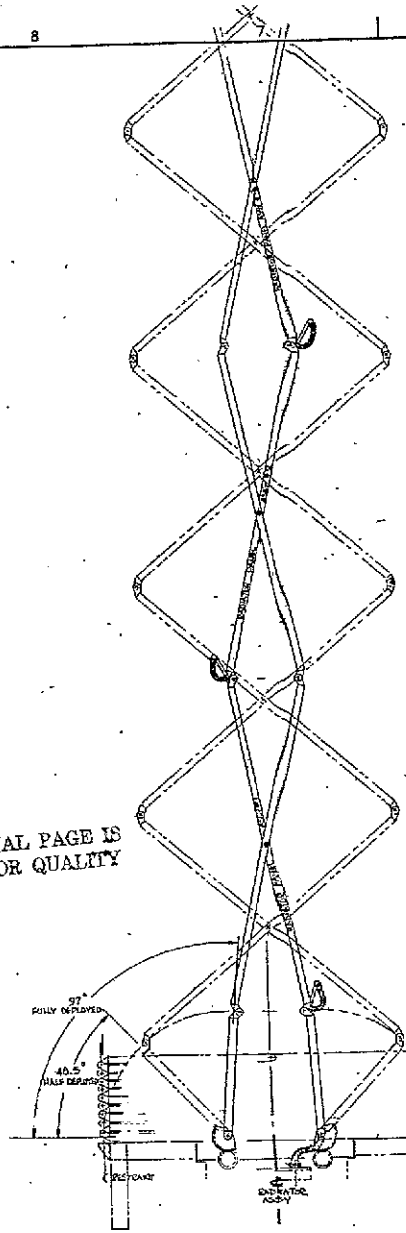

DETAIL "D"
SCALE 1/8
SHOWING DEPLOYED ARRANGEMENTS

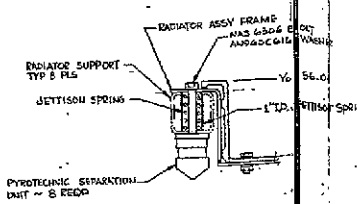

SECTION J-J
ZONE G4 SHT 1
SCALE 1/2

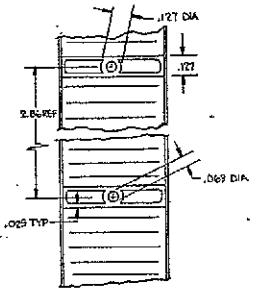

DETAIL H
ZONE D2 SHT 1
SCALE 4/1

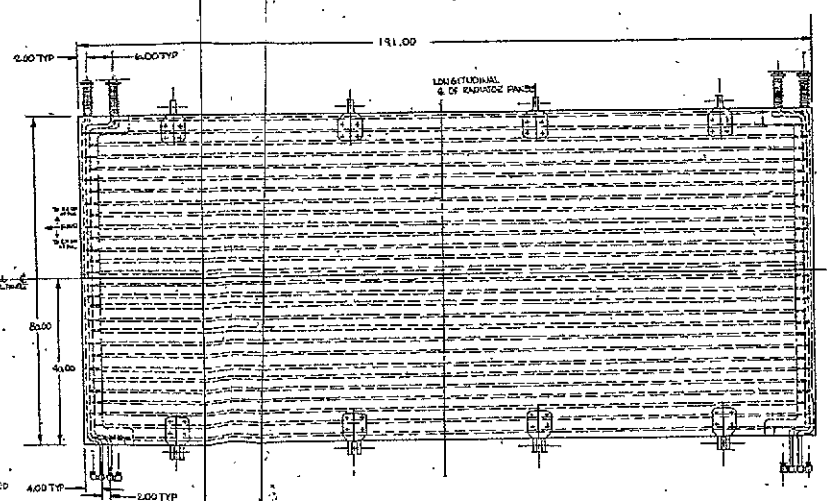

VIEW-F RADIATOR PANEL ASSY (ROTATED 90° CW)
(ZONE D-8 SHT-1)
SCALE 1/10

FOLDOUT FRAME

FOLDOUT FRAME

VOUGHT CORPORATION			
RADIATOR CONFIGURATION FOR SCISSOR HINGE DEPLOY PARALLEL PUMPED FLUID CONCEPT			
DRAWING NO. E180378	SPEC NO. 221-60113	REV	
SCALE 1/10 AND RATIO	SHEET 2 OF 2		

159 A

159 B

ORIGINAL PAGE IS OF POOR QUALITY

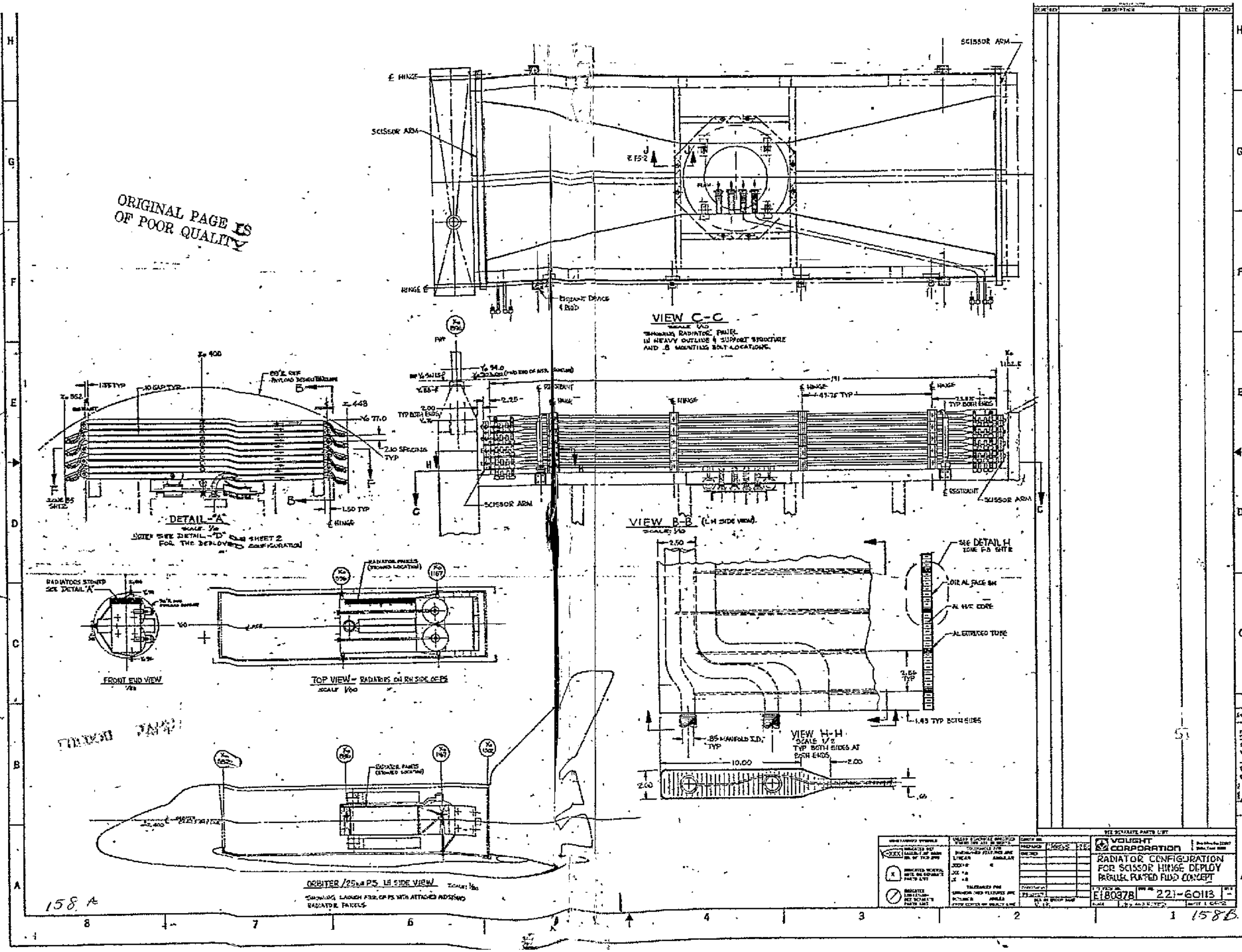

DWG 155-60113

N 81.22076

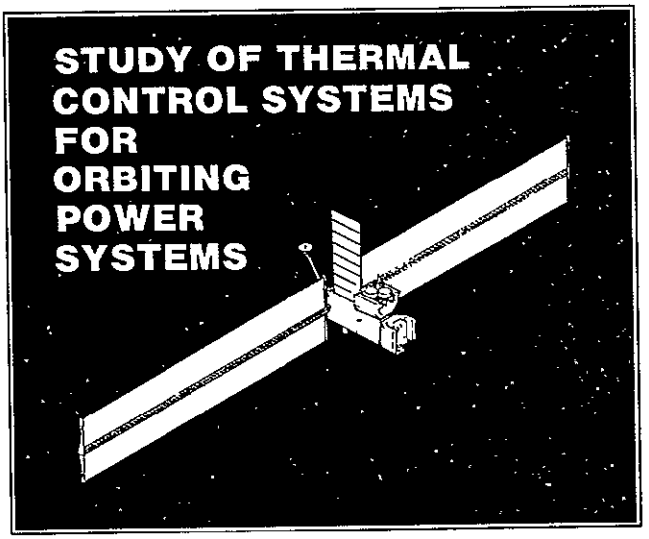

FINAL REPORT CONTRACT NAS8-33560

REPORT NO. 2-53020/1R-52666

16 FEBRUARY 1981

Prepared for
The National Aeronautics and Space Administration
Marshall Space Flight Center

PREPARED BY:

H. R. Howell
H. R. Howell

REVIEWED BY:

J. A. Oren
J. A. Oren

APPROVED BY:

R L Cox
R. L. Cox

TABLE OF CONTENTS

LIST OF TABLES

LIST OF FIGURES

LIST OF FIGURES (CONT'D)

1.0 SUMMARY

This report presents the results of a study of the Thermal Control System for the initial and growth versions of the 25 kW Power System. The long operating life and higher reliability requirements of the Power System impose new design criteria on the thermal control system, particularly the space radiator. Relatively large radiator areas will be exposed to the meteoroid hazard for five or more years resulting in high probabilities of fluid passage penetrations for conventional radiator designs.

Two major thermal control system design issues were addressed during the study: (1) whether the space radiator should be a heat pipe or a pumped fluid design, and (2) whether the heat rejection should be centralized on the Power System or distributed between the Power System and its payloads. Concepts for the thermal interface between the Power System and the payloads are also evaluated. Finally, a preliminary design of the thermal control system, with emphasis on the radiator and radiator deployment mechanism, was conducted.

An advanced heat pipe radiator concept that provides a 15% weight reduction over conventional heat pipe designs has been compared to "meteoroid bumpered" pumped fluid radiator designs. The trade study results indicate that for heat rejection rates up to about 50 kW, the weight advantage of the advanced heat pipe design over the bumpered pumped fluid design is less than 10%. A cost comparison of the advanced heat pipe, conventional heat pipe and bumpered pumped fluid designs shows a cost advantage for the pumped fluid design. Based on this cost advantage, the bumpered pumped fluid radiator is recommended for the initial 25 kW Power System and intermediate growth versions up to 50 kW. For advanced Power Systems with heat rejection rates above 50 kW the lower weight of the advanced heat pipe radiator offsets the higher cost and this design is recommended.

The Power System/Payloads heat rejection allocation studies show that a centralized heat rejection system is the most weight and cost effective approach. The Power System should provide all of the payload active cooling requirements although some specialized payloads with unique cooling requirements may require payload kit radiators or may lend themselves to passive cooling. The multiple launch requirements of the payload heat rejection systems is the primary driver in the selection of the centralized system. It is recommended that relocatable heat rejection modules that remain on orbit to provide payload cooling be considered for advanced Power Systems.

A concept for a contact heat exchanger that eliminates fluid transfer between the Power System and its payloads has been developed. Pressure drop and weight data for a unique flex hose reel design that provides multiple rotational capabilities for the payloads is also presented.

The Thermal Control System preliminary design studies show that two Orbiter pumps operating in parallel can provide 6400 lb/hr of R-21 coolant flow with adequate pressure drop margin for design maturity. A thermally actuated flow control valve is used to regulate payload heat rejection and allow single or multiple payload cooling with over temperature protection for the Power System. The nine panel radiator system is deployed on orbit from a compact stack by a scissors arm mechanism driven by redundant electric motors. The scissor arms have been sized to provide a deployed system natural frequency of 0.10 hertz to preclude interaction with the Power System attitude control system.

Additional effort is recommended in the area of the panel and deployment system structural analysis and design. A breadboard test of the thermal control loop components is recommended to identify design problems and provide verification of the component life characteristics.

Areas identified for technology development include fluid swivels, contact heat exchangers, space constructable radiators, redundant thermally actuated temperature control valves, redundant fluid accumulators and reduced cost heat pipes.

2.0 INTRODUCTION

The 25 kW Power System being developed by NASA Marshall Space Flight Center will provide electrical power, attitude control, communications and heat rejection to payloads on orbit. Figure 1 shows a Power System configuration based on the NASA Reference Concept (Reference 1). The Power System remains on orbit for at least 5 years to provide services to various attached payloads delivered and retrieved by the Space Shuttle Orbiter or to provide services to the Orbiter payloads with the Orbiter docked to the Power System.

The long life requirements and the transfer of heat from one spacecraft to another imposes unique design requirements on the Power System Thermal Control System (TCS). Previous radiator designs are not appropriate for long life systems. New radiator designs are required to prevent meteoroid penetration of the radiator fluid passages and loss of cooling capability.

This report presents the results of a parametric trade study of heat pipe radiators and meteoroid protected pumped fluid radiators. Representative design configurations are established for each of the design concepts and parametric weight and cost analyses are conducted to identify operating conditions for which the heat pipe or pumped fluid radiators are most effective.

Parametric trade data are presented for centralized heat rejection systems where the payload and Power System heat load is rejected by a central radiator system located on the Power System and a distributed heat rejection system where the Payload and Power System have separate radiator systems. Concepts for the thermal interface between the Power System and the Payloads are also presented. The results of preliminary design studies of the Power System TCS for the concepts selected are presented and areas requiring technology and hardware development are identified.

3.0 REQUIREMENTS, GUIDELINES AND CONSTRAINTS

Although the specific design requirements (heat load, temperature, flowrates, structural loads, etc.) for the Power System Thermal Control System are still evolving from design studies, several general requirements have been established. Table 1 lists the design guidelines established jointly by Vought and NASA MSFC to be used in the Thermal Control System (TCS) Study.

A high reliability (0.99 probability of success) TCS with a life of five years is required. In addition to the overall system reliability a radiator panel meteoroid reliability (probability of no meteoroid penetration) of 0.99 is required. The meteoroid reliability applies only to the coolant loop passages; penetration of heat pipes is allowed. The heat pipe radiator panels are oversized to allow for meteoroid penetration and random failure and still provide full heat rejection capability at the end of the mission. Reference 2, NASA SP8013, "Meteoroid Environment Model - 1969 (Near Earth to Lunar Surface): is used for the meteoroid environment. The TCS should remain operational after the first failure and the power processing equipment cooling should be retained after the first failure.

On-orbit maintenance of the TCS is available with the Orbiter Remote Maneuvering System or EVA. Replacement of the radiator panels is allowed only as a contingency operation. Replacement of the other TCS components is unscheduled maintenance, i.e., planned maintenance intervals are not desirable.

The Power System will be transported to orbit by the Space Shuttle requiring that the launch weight of the TCS be minimized. The Power System radiator will be stowed in the Orbiter cargo bay during launch and will require deployment on-orbit; the stowed volume and weight must be minimized. A completely self-contained radiator deployment mechanism capable of partial or full deployment and multiple deploy/retract cycles for quiscent operation or reboost activities is required. A manual back-up capability for deployment/retraction is desired and in the event the back-up capability fails, a radiator jettison feature is included to allow the Power System to be retrieved from orbit.

A stated design objective is to minimize cost. Development of new concepts is to be considered only if existing technology cannot meet the design objectives.

Heat rejection requirements are summarized in Table 2. The 25 kW Power System heat load is 12 kW with the breakdown shown on Table 2. It is

recognized that the battery heat loads and some power processing (chargers and regulators) heat loads do not occur simultaneously. However, due to the preliminary design phase of these components, the full 12 kW heat load was selected for the trade studies as a representative heat load. Also shown on Table 2 are the maximum allowable coldplate outlet temperatures for the Power System equipment.

Payload heat load will vary from partial up to 25 kW. The Power System coolant loop supply temperature to the payload heat exchanger is 35°F to provide a minimum payload coolant return temperature of 45°F. The maximum Power System coolant return temperature from the payload heat exchanger is 100°F. The thermal interface between the Power System and the payloads can incorporate either fluid quick disconnects and liquid-to-liquid heat exchangers or contact heat exchangers. Payload rotation relative to the Power System is not a firmly established requirement, but gimballed joints are to be considered.

4.0 HEAT PIPE/PUMPED FLUID TRADE STUDY

The primary design driver for the Power System radiator is the survivability of the radiator in the meteoroid environment. Based on the penetration model suggested by NASA (Reference 2), a spherical meteoroid as small as 0.011 inch diameter (1.1×10^{-8} lb) would penetrate an aluminum tube with a conventional wall thickness of 0.035 in. The specified meteoroid mass-flux model (Reference 2) would result in a mean time fluid tube penetration rate of approximately 403 days for a 25 kW radiator with unprotected fluid tubes. The probability of such a conventional radiator surviving the meteoroid hazard for five years is 0.37. It is evident that new radiator designs are required to achieve the high reliability (0.99) specified for the Power System.

The most obvious design improvement would be to provide protection of the fluid passages from the impacting meteoroids. Leach and Stalmach (Reference 3) have shown that meteoroid bumpers are the most weight effective method as opposed to armor protection. The bumper is designed to fragment the high velocity meteoroids and dissipate their kinetic energy. The bumper is spaced at sufficient distances from the fluid tube to permit fragments from the meteoroid to spread out over a larger area, thus minimizing the damage. The design challenge for meteoroid bumper protected radiators is to provide a low cost, lightweight, thermally efficient bumper.

The second radiator design concept involves the use of heat pipes to distribute the heat over the radiator surface rather than flow tubes. The heat pipe concept is attractive because meteoroid penetration of an individual heat pipe will result in only minimal loss in total heat rejection due to a localized reduction in fin effectiveness. This concept is termed a hybrid because a coolant loop is still required to collect the vehicle waste heat and transport it to the radiator. The interface between the coolant loop and the heat pipes is on the radiator panel. The fluid passage at the interface is vulnerable to the meteoroid hazard, but the exposed area is greatly reduced from the pumped fluid concept. The design challenge for the hybrid heat pipe concept is to obtain a low cost, lightweight, thermally efficient interface between the coolant loop and the heat pipe.

4.1 Thermal Control System Reliability Study

The design reliability requirement for the Power System Thermal Control System is a probability of success of 0.99 for five years. In order to determine the design meteoroid reliability (probability of no meteoroid penetration of a fluid passage) for the radiator panels, a study of coolant loop configurations was conducted to determine the required component redundancy and/or maintenance. Figure 2 shows two coolant loop concepts and the components included in the reliability study. The first concept is a single coolant loop (Figure 2a) with the option of redundant components and/or maintenance on the components to improve reliability. The second concept (Figure 2b) utilizes a redundant standby loop with the option of redundant components and/or component maintenance in each loop to improve reliability.

Table 3 shows the range of component failure rates and the resulting probabilities of success for (1) single loops with no redundant components, (2) single loops with redundant components, (3) redundant loops with no redundant components, and (4) redundant loops with redundant components in each loop. The probability of success (reliability) of the single loop was computed by the Poisson distribution function.

$$R = e^{-\Sigma\lambda t} \tag{1}$$

where λ is the failure rate and t is the mission time. The reliability of the redundant standby pumps is given by

$$R = e^{-\lambda_p t} + \frac{\lambda_p}{\lambda_s}\left[e^{-\lambda_p t} - e^{-(\lambda_p + \lambda_s)t}\right] \tag{2}$$

where λ_p is the failure rate of the pump and λ_s is the failure rate of the failure detection and switch system. The use of the Orbiter pumps will require the operation of two pumps in parallel with redundancy provided by a single standby pump. The reliability for this case is

$$R = e^{-2\lambda_p t} + \frac{2\lambda_p}{\lambda_s}\left[e^{-2\lambda_p t} - e^{-(2\lambda_p + \lambda_s)t}\right] \tag{3}$$

A concept for a redundant temperature control valve is shown in Figure 3. Both temperature control valve elements operate simultaneously. In case of failure any one of the elements can provide control. The elements are designed to close the bypass port in the failed position, thus allowing the remaining element to provide control.

Figure 4 shows a redundant bellows fluid accumulator. The fluid and gas space are separated by two independent bellows. In the event of failure of either bellows, fluid or gas leaks into the area between the bellows and accumulator shell and functional capability is retained. A second bellows failure is required before functional capability is lost. As in the redundant temperature control valve, both bellows operate simultaneously but only one is required. No failure detection and switch system is required and the reliability is given by

$$R = 2e^{-\lambda t} - e^{-2\lambda t} \qquad (4)$$

Redundancy for the temperature sensors is accomplished by providing three sensors and utilizing the majority vote concept. If one of the three indicated temperatures does not agree with the other two, it is ignored. The reliability for the redundant temperature sensors is computed from

$$R = e^{-3\lambda t} + 3e^{-2\lambda t}(1-e^{-\lambda t}) \qquad (5)$$

It should be noted that the temperature sensors are required for system health monitoring only. They are not required for system operation per se, but if an over or under temperature were indicated the system would be shutdown to prevent equipment damages.

The redundant loop reliability is computed as the product of the reliability of the active components and the dormant components.

$$R = R_A R_D \qquad (6)$$

Although the redundant loop is not operating, all components except the

pump are exposed to their failure mechanism and are considered active for reliability calculations. The radiator tubes are exposed to the meteoroid hazard and the structure is exposed to space environment. The redundant loop fluid in the radiator, coldplates and heat exchangers goes through the same temperature fluctuations as the operating loop; thus the accumulator will be active. Temperature variations at the temperature control valve in the redundant loop are likely not to be as severe due to the stagnant fluid and isolation from the active loop. However, for conservatism it is assumed that the valve is operating for reliability calculations. Similarily, the temperature sensors in the redundant loop are assumed to be active. The reliability of the active components in the redundant loop is given by

$$R_A = 3e^{-\Sigma\lambda_A t} + e^{-\lambda_s t} - e^{-(\Sigma\lambda_A + \lambda_s)t} - e^{-2\Sigma\lambda_A t} - 1 \quad (7)$$

The reliability of the dormant components (the pump) is found from equation (2).

Figure 5 shows the effect of maintenance on the pumps and temperature sensor, the two highest failure rate components on the overall reliability.

The reliability study results indicate that the highest expected single loop reliability with redundant components and without maintenance is 0.9385 (Table 3). Maintenance on the pumps and temperature sensor have a small effect on loop reliability since with redundancy the failure rate of these components is already small. Figure 5 shows that the single loop reliability is increased from 0.9385 to approximately 0.953 for one year maintenance period. Maintenance on the single loop without redundant components has a more significant effect on the loop reliability as shown by Figure 5. However, the highest obtainable single loop reliability with maintenance and with redundant components is below the design requirement of 0.99. Therefore, a redundant standby loop is required. Table 3 shows that the redundant standby loop reliability with redundant components in each loop has a reliability range of 0.9903 to 0.9959. Thus the required reliability could be met with this concept. Maintenance on the redundant standby loop concept without redundant components will not increase the reliability to the desired 0.99 (Figure 5). The selected concept is the redundant standby loop with redundant components. Maintenance will not be required but could provide some additional

margin on the loop reliability.

The failure rate data of Table 3 shows an assumed radiator panel meteoroid penetration reliability of 0.99. In order to test the validity of this assumption the effect of different meteoroid reliabilities on the Thermal Control System reliability was determined. Figure 6 shows this effect for the redundant standby loop concept. Improving the meteoroid probability of penetration from 0.01 to 0.001 (probability of no meteoroid penetration from 0.99 to 0.999) will have negligible effect on the Thermal Control System reliability. If there were no probability of meteoroid penetrations (reliability = 1.0) the Thermal Control System reliability would increase from 0.99 to 0.990099. Thus radiator meteoroid penetration reliabilities greater than 0.99 are not required.

A third coolant loop concept involves the use of a heat collection loop which interfaces with multiple heat rejection loops (Figure 7). The use of multiple heat rejection loops offers two advantages. First, the radiator meteoroid protection requirements are reduced for smaller independent radiator loops. The meteoroid penetration rate varies directly with radiator area; the probability of no meteoroid penetration for given bumper configuration is a function of e^{-A}. The second advantage is that the system reliability can be increased above the individual heat rejection loop reliability by oversizing. Thus, a system made up of smaller less reliable heat rejection subsystems is potentially lighter weight than a single high reliability heat rejection system.

The total thermal control system reliability is the product of the heat collection subsystem reliability and the multiple heat rejection subsystem reliability. It is evident that both subsystems must have reliabilities greater than 0.99 to meet the overall reliability requirement of 0.99. A redundant heat collection loop with redundant pumps in each loop will yield probabilities of 0.9896 to 0.9949 (Table 4). The parametric weight studies were conducted with a collection subsystem probability of 0.995 and the heat rejection subsystem oversized to yield a probability of 0.995. Thus total system probability is 0.99 (0.995 x 0.995) and the total system weights can be compared directly to the single subsystem concept with no oversizing.

TABLE 4

HEAT COLLECTION LOOP RELIABILITY

Pump	.0635	-	.6184
Accumulator	.00085	-	.00389
Fill Drain	.05		
Lines/Fittings	.05		
	.16435		.72229
Single Loop	.9928		.9689
Redundant Loop*	.9949	-	.9896

*Switch System Reliability = .995 - .99

The amount of oversizing required to achieve a given system reliability is given by

$$P_S = \sum_{i=r}^{N} \binom{N}{i} P_{SS}^{\,i} (1 - P_{SS})^{N-i} \qquad (8)$$

where: P_S = system probability of success

P_{SS} = subsystem probability of success

N = total number of subsystems

r = required number of subsystems

$\binom{N}{i} = \frac{N!}{i!(N-i)!}$

The pumped fluid radiator panels are designed with bumpered meteoroid protection of the fluid tubes and manifolds to provide a reliability of 0.99. The hybrid panels are designed with bumpered meteoroid protection of the coolant

loop/heat pipe interface to provide a reliability of 0.99. In addition, the number of heat pipes are increased to allow for loss of heat rejection capability due to meteoroid penetration of the heat pipes. The amount of heat pipe oversizing is determined by equation (8) where the subsystem probability (P_{SS}) is the probability of meteoroid penetration of each heat pipe and r is the required number of heat pipes.

4.2 Pumped Fluid Panel Design

Representative panel tube/fin or heat pipe/fin cross section configurations have been established to serve as the basis for the radiator trade studies. Important considerations in evolving candidate configurations were ease and cost of manufacturing, lightweight meteoroid protection, and thermal performance. An assessment of the candidate panel crossections for both the pumped fluid and the heat pipe panels was made to select representative designs that will produce meaningful trade results in the study.

Figure 8 illustrates four tube/fin panel crossections considered for the pumped fluid radiator. Concept A utilizes an extruded tube/bumper design which is adhesively bonded or welded to the radiator fin. An I-beam type tube extrusion bonded to a fin is shown in Concept B with the meteoroid bumper provided by the top and bottom of the I and the fin. The fin could be eliminated from this concept and the I extrusions joined by welding or bonding. Concepts C and D are based on use of Orbiter technology in which tubes are adhesively bonded in an aluminum honeycomb/facesheet layup.

All four concepts appear competitive on the basis of weight, thermal performance, ease of manufacturing, and cost, except for Concept C which is heavier and not as thermally efficient as the others. Concepts A and B may require structural stiffening to withstand handling and Orbiter launch loads and could incur an additional weight penalty. Concept D was selected for the trade studies. This concept is known to have good stiffness, with minimum panel thickness (minimizes stowage volume) and the manufacturing processes and procedures are well established. The uniform panel surface also facilitates the application of the radiator thermal control coating. Figure 9 summarizes the pumped fluid panel design that is used for the trade studies. The panel consists of an aluminum honeycomb panel with extruded aluminum flow tubes. The honeycomb and tube extrusions are bonded to an aluminum facesheet, 0.011 in. thick, on each side of the panel. The panel thickness is determined from the

extrusion height which results from the panel weight optimization of tube diameter and thickness.

4.3 Hybrid Heat Pipe Panel Design

Figure 10 shows three concepts for the hybrid heat pipe panel cross section. These concepts have been evaluated by Alario and Haslett (Reference 4). Their test element data, reproduced in Table 5, indicates that the bonded honeycomb concept thermal performance compares favorably with the other concepts. It has the highest heat rejection per unit area which would minimize the launch stowage volume and deployed area requirements for the Power System radiators. The heat rejection rate per unit weight for the honeycomb panel is also near the maximum.

TABLE 5

COMPARISON OF HEAT PIPE PANEL CROSS-SECTION THERMAL PERFORMANCE

	T_{in} = 38°C	
	W/m^2	W/kg
Concept A (bonded fin)	297	67.5
Concept B (flanged extrusion)	339	63.1
Concept C (honeycomb)	394	67.2

The bonded fin and flanged extrusion concepts are likely to require additional structural stiffeners which would increase their weight. The bonded honeycomb concept was selected for the radiator trade studies. This will provide for structural consistency between the pumped fluid and heat pipe panels and should cause other differences between the two concepts to become more visible.

The radiator panels for the hybrid concept contain the fluid-to-heat pipe interface heat exchangers and the heat pipes which distribute heat from the fluid out onto the panels. The design of the fluid-to-heat pipe interface heat exchanger to achieve good thermal performance while minimizing weight, volume, and cost is critical to the success of the hybrid approach. Two concepts have been selected for the radiator trade studies. These are the simple, low cost heat pipe with a compact heat exchanger shown in Figure 11 and a center core wick heat pipe with integral evaporator and manifold shown in Figure 12.

The simple heat pipe concept, Figure 11, consists of straight heat pipes bonded into a 1.0 in. thick honeycomb panel. The heat pipes have a flat surface on the side adjacent to the honeycomb facesheet to provide good heat transfer to the fin. Heat pipe diameters are optimized in the trade study. The heat exchanger contains two layers of 0.125 in. compact core material for a total core thickness of 0.25 in. The fluid flow passage width is varied in the radiator optimization. The heat exchanger is made with "saddles" within which the heat pipes are bonded as shown in Section A-A of Figure 11. These "saddles" provide inherent meteoroid protection for the heat exchanger passages as well as inhancing the heat transfer. Each heat pipe interfaces both redundant flow passages so that either loop utilizes the entire radiator area. Honeycomb is included between the heat exchanger core and the face sheets between the saddles. The design should be relatively inexpensive since one bonding operation is required for the entire panel layup including heat exchangers, honeycomb, heat pipes, and face sheets.

The integral manifold concept, shown in Figure 12, consists of a heat pipe made in a "T" shape with the evaporator of the heat pipe around the outside of the heat transport fluid manifold. This approach is thermally and weight efficient. The heat pipe surrounds the fluid heat exchanger and acts as a meteoroid bumper. The heat pipe design is a center core wick, aluminum heat pipe with the wick extending around the outside diameter of the fluid manifold as shown in Figure 12. Thermal vacuum tests of a radiator panel element incorporating the integral manifold design have been conducted to verify this design concept.

The radiator panel test element (Figure 13) was made up of 0.5 in. aluminum honeycomb (3.1 lb/ft^3) with 0.011 in. aluminum facesheets bonded to it. Orbiter bonding techniques were used to bond the condenser sections of the heat pipes. The heat pipes were made of Type 304 stainless steel. In order to allow for the different thermal expansion coefficients of the heat pipe and the radiator facesheet, each facesheet was split into 6 individual sections to lessen the buildup of thermal stress. The heat pipes were charged subsequent to the bonding of the panel because of the high vapor pressure of ammonia at the bonding temperature. The panel was painted with White Velvet 401 paint to provide a known surface emissivity.

The heat pipes and radiator were instrumented with a total of 17 thermocouples as shown in Figure 14. In addition, 2 immersion thermocouples were installed in the heat exchanger inlet and outlet and a thermocouple was attached to the exterior of the heat exchanger between the two heat pipes. Four thermocouples were attached directly to each of the two heat pipes to allow accurate measurement of the condenser temperatures. Four thermocouples mounted on the facesheet directly over the heat pipes allowed determination of the heat pipe-to-facesheet temperature drop. All of the surface mounted thermocouples were welded to the test article.

The heat input into the heat pipes was provided by Freon 21 flowing through the spiral-finned heat exchanger at controlled temperatures and flowrates.

The fluid temperature drop through the heat exchanger was measured with delta-connected, immersion, copper-constantan thermocouples. The thermocouple output was measured with a digital multimeter with a resolution of 0.001 mv. This corresponds to a temperature resolution of 0.05°F.

The absolute thermocouple readings were recorded on a Brown strip recorder with a temperature range of 0°F to 150°F. The estimated accuracy of the temperature readings is ± 3°F.

TABLE 6

INTEGRAL MANIFOLD THERMAL VACUUM TEST RESULTS

	1	2	3
Flowrate, lb/hr	2000	300	2000
Inlet Temp, °F	52.6	51.5	58.4
Q_{REJ}, BTU/hr	400	369	427
Q_{REJ}, BTU/hr-ft^2	37.1	34.2	39.6
ΔT-Fluid-To-Heat Pipe, °F	8.8	19.3	14.1
Predicted ΔT, °F	9.8	17.0	11.3
UA Fluid-to-Heat Pipe, BTU/hr-°F	22.7	9.6	15.1
UA (Predicted), BTU/hr-°F	17.8	9.6	17.6

Table 6 summarizes the results of the integral manifold thermal vacuum tests. The measured fluid to heat pipe conductances are greater than or equal to the calculated values in two out of the three test points. The

measured value of test point 3 is approximately 14% lower than predicted. The average value of test points 1 and 3 which should be approximately equal is 7% greater than the predicted conductance. Although the test data is limited, the result tend to confirm the thermal performance of the integral manifold heat pipe concept.

4.4 Parametric Weight Analysis of Concepts

The radiator panels that resulted from the concept development discussed above must be optimized in order to obtain fair and meaningful trade comparisons. Parametric data providing weight optimized panels for different radiator heat loads, operating temperatures and environment temperatures are required for each concept. Specialized computer routines were used for the parametric weight optimization of both the pumped fluid and hybrid concepts.

The items included in the weight of the pumped fluid radiator are facesheets, honeycomb, bonding adhesive, panel thermal control coatings, flow tube extrusions, manifolds, Freon 21 and equivalent pumping power penalty. The tube extrusion dimensions were determined based on a bumper distance (facesheet to tube outside surface) of 0.225 in. This basic dimension plus the computed tube inside diameter and tube thickness required for meteoroid protection determines the extrusion dimensions and the honeycomb thickness. The facesheet thickness that resulted in the minimum weight was also determined. A minimum thickness of 0.01 in. was specified for manufacturing ease and for most cases this limit was used by the computer routine.

The hybrid panel weight included the facesheets, honeycomb, bonding adhesive, panel thermal control coating, heat pipe, heat pipe fluid, coolant loop manifold and heat exchanger, Freon 21 and equivalent pumping power penalty. Weights of aluminum-ammonia heat pipes with a wall thickness of 0.036 in. were used for all cases except the high operating temperatures. Aluminum-acetone heat pipe weights were used for the high temperature (250°F) case.

In order to compare the single subsystem and the multiple subsystem with oversizing, thermal control system components common to both subsystems are included in the weight values rather than just radiator panel weight. Multiple subsystems will require more, although smaller, pumps, accumulators, and temperature control valves than the single subsystem. The multiple subsystem weights also include the heat exchangers for heat transfer from the collection loop to the heat rejection loops. The following algorithims

are used to estimate the TCS component weights:

Heat Exchanger Weight = 2 lb/kW

Pump = 5.5 lb

Accumulator = .605 x fluid weight

Tubing = 40 lb (100 ft of 5/8" x .028" SS tube)

Temperature Control Valve = 4 lb

A study of heat pipe sizes indicated that smaller heat pipes are more weight effective. Figure 15 shows the effect of heat pipe size on optimized radiator panel weight. For the integral manifold concept it appears that heat pipes below 0.25 in. diameter would further reduce panel weight. However, center core wick heat pipes smaller than this were not considered practical. Furthermore, the required capacity for the smaller heat pipes is higher than is currently available. Figure 16 shows center core heat pipe capacity as a function of diameter. As indicated on Figure 15, a 0.25 in. O.D. heat pipe would require a capacity of 1528 watt-in, whereas the estimated capacity of existing center core wick designs for this diameter is 1000 watt-in. A 0.375 in. heat pipe for the optimized radiator panel weight would require a capacity of approximately 1800 watt-in. This is close to the capacity of existing designs and should be achievable. Therefore, the hybrid panels were optimized with 0.375 in. heat pipes. Development of smaller sized higher capacity center core wick heat pipes could potentially reduce the radiator panel weight by approximately 10%.

Figures 17, 18 and 18a present the results of the radiator panel weight optimizations for the three concepts considered. The range of parameters analyzed were:

Heat Load - 1-250 kW

Operating Temperatures - T_{in}/T_{out} = 40°F/0°F, 100°F/40°F and 250°F/130°F

Environment Temperatures - -8°F, 40°F, -80°F

In general, the integral manifold heat pipe panels are lighter than the compact heat exchanger-heat pipe panels by 10-15 percent. Exceptions are at the high radiator operating temperature (T_{in}/T_{out} = 250°F/130°F) where the difference is 5 percent or less. The weight differences decrease at the low load conditions and there are cases of high temperature and low load where the compact heat exchanger-heat pipe panels are slighly lighter than the integral

manifold panels.

The required radiator area has a large effect on the relative weight of the three radiator types. This effect is due to the direct relationship between radiator area and meteoroid protection requirements. For relatively small areas, whether due to low heat loads or a large difference in radiator and sink temperatures, the pumped fluid panels are lighter than the heat pipe panels. At intermediate heat loads, radiator sink temperatures and area requirements, the differences in weight of the two concepts are small. For larger heat loads and high radiation sink temperatures the hybrid heat pipe panels weigh significantly less than the pumped fluid panels. This is illustrated by Figure 19 which shows the regions (heat load and average radiator temperature) for which the pumped fluid or heat pipe panels are weight optimum. As indicated by Figure 19, there is a wide region in which there is less than 10% difference in the weight of the two concepts. The anticipated operating region of the initial 25 kW Power System is seen to fall within this region. Above about 50 kW heat load the heat pipe panels show a definite weight advantage.

Figures 20 and 21 show the effect of meteoroid probability on radiator weight for 16 kW and 32 kW heat loads. As previously discussed (Figure 6), the radiator meteoroid probability can be reduced from 0.99 to 0.90 and the overall TCS reliability is reduced only from 0.99 to 0.98. Thus, it may be desirable to design to a lower radiator meteoroid probability. Figures 20 and 21 indicate a radiator weight savings of approximately 50 lbs. for a 16 kW heat load and approximately 200 lbs. for a 32 kW heat load for a 5 year life. Data are also shown for 10 year life radiators, showing more significant weight savings.

4.5 Parametric Cost Analysis of Concepts

Comparative costs of the three thermal control systems were obtained from the PRICE routine (Reference 5). This routine provides a consistent estimation of development and manufacturing costs of the radiator panels as well as the other components. Costs were obtained for both the single subsystem and multiple subsystem concepts. Thus all thermal control system components are included in order to compare the single and multiple subsystem. The components included in the cost analysis were:

Radiator Panels
Heat Pipes
Pumps
Accumulators
Temperature Control Valve
Temperature Sensor
Heat Exchanger
Inter-panel Flex Hoses
Radiator Deployment Mechanism

Table 7 summarizes the PRICE input data. The engineering and manufacturing complexity factors input to PRICE for the radiator panels was based on historical cost for the Space Shuttle Orbiter radiator panels produced by Vought. Table 8 summarizes the complexity factors used for all components. Heat pipe and pump cost data were obtained from vendors and input directly to PRICE. Heat pipe costs based on data obtained from Hughes are summarized in Table 9. Pump costs obtained from Sundstrand are summarized in Table 10.

Figure 22 compares the cost of the three concepts as a function of heat load. The pumped fluid concept is seen to be the lowest cost system for heat loads up to 250 kW. The cost differential for the three concepts is not significant at the higher heat loads except for the multiple subsystem pumped fluid concept. This concept costs 17% less ($4,000,000) than the integral manifold concept at 250 kW.

Table 11 shows a comparative cost breakdown of the three concepts for a 25 kW system. The integral manifold heat pipe concept cost is $1,307,000 (18%) greater than the pumped fluid concept for a 25 kW heat rejection system. The cost differential is due primarily to the cost of the heat pipes. This is illustrated by Table 12 which compares the cost of the radiator panels only. Development costs for the heat pipe panels are somewhat higher since manufacturing methods of incorporating charged heat pipes into the panel or charging the heat pipes after assembly will have to be developed. The low technology heat pipe concept cost includes the cost of the compact heat exchangers, thus production costs are slightly higher. The pumped fluid radiator panel cost is $1,136,000 less than the weight competitive integral manifold heat pipe radiator panel. The primary difference is the $897,000 cost of the heat pipes.

Tables 13 through 24 present comparative cost breakdowns of the three concepts for 25 kW, 50 kW, 100 kW and 250 kW heat rejection systems. Data are included for both the single system and multiple heat rejection subsystem concepts.

5.0 BODY MOUNTED ALL HEAT PIPE/PUMPED FLUID TRADE STUDY

Although the Power System body surface area is not sufficient for total heat rejection, use of this area would reduce the deployed radiator area. Heat pipe radiators utilizing the Power System structure could provide cooling of the power processing equipment or batteries thus reducing the coolant loop heat load and fluid requirements. Figure 23 shows two baseline candidate schematics and body mounted heat pipe radiator concepts. Use of the body mounted heat pipe radiators to cool the power processing equipment and the Power System equipment results in the minimum deployed radiator area. Removal of the batteries from the coolant loop reduces the heat load only by 3.5 kW and does not allow the radiator outlet to be increased since a low temperature is also required for the payload heat exchanger.

5.1 Heat Pipe Radiator Design

Figure 24 illustrates the body mounted heat pipe radiator concept. The cross-hatched area shown results in a total area availability of approximately 634 ft^2. The available body area does not have a good view to space due to the solar arrays and the deployed radiators. Analysis indicates that the average radiation sink temperature of the body area is approximately 10°F with radiant interchange with the solar arrays and deployed radiators included. For the reference Power System attitude of X-axis perpendicular to the orbit plane and Z-axis parallel to the sun line, the sides of the Power System (Y-axis) will alternately face the earth and deep space resulting in a radiation sink temperature variation from -8°F to 46°F. Table 25 shows the variation in radiation sink temperature for all four sides of the Power System with orbit position. In order to provide environment averaging a perimeter or hoop heat pipe arrangement as shown on Figure 24 is required. The reference 25 kW Power System skin will be load carrying panels of either honeycomb or skin and stringer design (Reference 1). This same basic skin could be used for radiator area by integration of the heat pipes. Evaluation of the body mounted heat pipe radiators considered the additional weight of the heat pipes only. Utilization of the existing skin as the radiator fin was assumed.

An equipment mounting concept is shown in Figure 25. Six equipment mounting locations or interface between the feeder heat pipes and the radiator panel are provided around the periphery. Variable conductance heat pipes between the radiator and the equipment coldplate are used to provide temperature control and prevent low temperatures during equipment dormant periods. Five feeder heat pipes are used at each of the six interfaces, with only four required, to yield a reliability of 0.999. This is based on a heat pipe random failure rate of 0.25 per 10^6 hours. For six sets of feeder heat pipes the total feeder heat pipe reliability is 0.994. A radiator reliability of 0.996 will yield an overall system reliability of 0.99.

5.2 Body Mounted Heat Pipe Weight Analysis

Figure 26 shows the results of a parametric weight analysis of the body mounted all heat pipe concept. Weight data are presented for three different radiation sink temperatures and radiator operating temperatures. Comparative weight of a pumped fluid coolant loop is also shown for the 10°F heat pipe radiator sink temperature. The curves on Figure 26 end at the maximum heat rejection allowed based on the total available body area.

The weight of the body mounted all heat pipe system includes the weight of the radiator heat pipes (but not the fin), the thermal control coating (silver Teflon), the perimeter heat pipes and the variable conductance feeder heat pipes. The number of radiator heat pipes for each combination of radiator temperature and sink temperature which yielded a minimum radiator fin effectiveness of 0.90 was determined to obtain the radiator panel heat pipe weight. An axial grooved 0.25 inch ammonia/aluminum heat pipe was used for the radiator panel. The design limited the capacity of the heat pipe to 1600 watt-inches.

The perimeter heat pipes were sized to provide the maximum heat transfer from one face to another based on the radiation sink temperatures of Table 25. An aluminum/ammonia, 0.5 inch heat pipe as shown in Details A and B of Figure 24 was used. The perimeter heat pipes resulted in a weight of 0.12 lb/ft^2 of radiator area.

Variable conductance, 0.5 in., stainless steel/ammonia heat pipes were used for the feeder heat pipes with a weight of 0.25 lb/ft. Flanged heat pipes are used at the radiator/feeder heat pipe interfaces to provide approximately 1°F temperature drop at the contact area. The feeder heat pipe weight included an allowance of 12 inches of adiabatic length between the contact

interface and the equipment mounting coldplate, but did not include the coldplate or the heat pipe length in the coldplate since the fluid loop system weights do not include the coldplates or the fluid in the coldplates. The feeder heat pipe weight is 0.041 lb/watt.

Table 26 compares the weight of the body mounted heat pipe and reduced capacity pumped fluid loop to the all fluid loop weight. The weight comparison is made for a total heat load of 25 kW representative of the reference Power System. The body mounted heat pipe load was taken as 8.5 kW representing maximum utilization of the available body area. The body mounted heat pipe concept is seen to be heavier for all fluid loop concepts and radiation sink temperatures except for the -40°F fluid loop radiator sink temperature and -10°F heat pipe radiator sink temperature with either the pumped fluid or low cost hybrid radiator panels.

5.3 Body Mounted Heat Pipe Cost Analysis

The RCA PRICE routine (Reference 5) was used to determine the cost of the body mounted heat pipe thermal control system. Estimated costs of the heat pipes were input to the routine based on informal data from heat pipe vendors. Heat pipe cost data are as follows:

Variable Conductance Feeder Heat Pipes	- $1500 each
Perimeter Heat Pipes	- $ 300 each
Radiator Heat Pipes	- $ 150 each

Figure 27 shows the body mounted heat pipe cost as a function of heat load. The cost includes the development and manufacturing cost of the body mounted radiator panels, feeder heat pipes, and perimeter heat pipes. Inclusion of the entire cost of the radiator panels overstates the cost since the cost of the skin panels will be eliminated if they are replaced with heat pipe radiator panels. This cost difference will be partially offset by the cost of development and integration of the heat pipes into the panel. Also, the increased vehicle integration costs are not included in the PRICE analysis of the all heat pipe system. The equipment mounting restrictions and feeder heat pipe and perimeter heat pipe integration with the vehicle basic structure will be more costly than installation and integration of fluid lines.

A lower limit of the body mounted heat pipe cost is obtained by deleting the radiator panel cost as shown on Figure 27. Table 27 compares the cost of a fluid loop TCS supplemented by the body mounted heat pipe radiator

to the all fluid loop TCS with a 25 kW heat load. The high and low range of the body mounted heat pipe radiator costs are included for comparison. The all fluid loop TCS is seen to be cheaper than the reduced capacity fluid loop supplemented by the body mounted heat pipe radiator for all fluid loop concepts. The 25 kW pumped fluid radiator results in a cost savings of $1,700,000 to $4,300,000 over the body mounted heat pipe radiator concept.

5.4 All Heat Pipe/Fluid Loop Concept Selection

The all fluid loop concept provides a weight and cost advantage over the concept of a reduced capacity fluid loop supplemented by a body mounted heat pipe radiator. The deployed radiator size is reduced by the body mounted heat pipe radiator. This has some potential advantages of reducing attitude control requirements and providing better payload viewing angles. However, the total radiator area is increased, requiring more surface area to have a thermal control coating. Plume contamination potential of the thermal control coating during Orbiter docking and re-boost phases is also increased. Equipment cooled by the body mounted heat pipe radiator will be restricted to locations near the surface and must be equally distributed around the periphery of the Power System. The reference Power System configuration appears to be easily adapted to these restrictions.

The advantages of the body mounted heat pipe radiator appear to be limited; due to weight and cost considerations the all fluid loop concept is selected for the Power System.

6.0 POWER SYSTEM/PAYLOAD HEAT REJECTION ALLOCATION

The Power System is required to support Orbiter sortie missions and attached payloads in the free flying mode by supplying power, heat rejection, attitude control and data communications. A nominal 25 kW of electrical power will be supplied to the payloads. Essentially, all of this power must be dissipated as waste heat. Structural heat leaks or gains from the environment will reduce or increase the payload heat load depending on the payload thermal design, operating temperature and orbital attitude. It is anticipated that the payload heat load on the TCS will be 16 kW to 25 kW. Processing of the payload power (battery charging and voltage regulation) and communication and attitude control equipment power dissipation results in a Power System equipment cooling requirement of approximately 9 kW to 12 kW. Thus, the total heat load is in

the range of 25 kW to 37 kW. The objective of this study is to conduct parametric weight and cost studies of the effect of including portions or all of the payload heat rejection on the Power System heat rejection system. The study does not include a payload heat rejection requirements investigation, but is parametric to allow evaluation of payloads heat loads up to a maximum of 25 kW.

Figure 28 illustrates a centralized heat rejection system in which all of the active heat rejection is contained on the Power System. Payloads docked to the Power System have no active heat rejection capability. All payload waste heat is transferred to the Power System and rejected via the Power System radiator. Figure 29 shows a concept in which each payload has its own independent heat rejection system. The radiators are transported to and from orbit with each payload launch. Thermal interfaces between the Power System and the payloads are eliminated, but each payload must pay the radiator procurement cost and multiple launch costs of the radiator are incurred. The radiator design is simplified since only a 90 day life (assumed payload mission duration) is required rather than the 5 year life of the Power System radiator.

A concept for separate Power System and payload radiator systems is shown on Figure 30. The payload radiator remains on-orbit, requiring only one procurement and launch. The thermal interface between the Power System and payloads is eliminated, but a thermal interface between the payload and the radiator system is still required. The concept shown utilizes the Science and Applications Space Platform (SASP) structure for radiator mounting.

6.1 Centralized and Distributed TCS Weight Comparison

Figure 31 compares the weight of a centralized and a distributed TCS utilizing the concept of Figure 30. Both the centralized and distributed TCS are designed for a five year life. A Power System heat load of 12 kW was used for this analysis with a variable payload heat load. The centralized and distributed TCS weights are comparable if both systems have the same operating temperatures, with the distributed TCS showing a slight weight advantage for higher payload heat loads. If the payload requirements allow a high temperature radiator to be used, then the distributed system shows a definite weight advantage. The only high temperature payload anticipated for the Power System at this time is the Materials Experiment Carrier (MEC).

Thus a Power System dedicated solely to MEC, or a high temperature payload, should have a distributed TCS for weight effectiveness.

The weight analysis shown on Figure 31 assumes that the total payload heat load is rejected by the distributed system. It may be desirable to have a basic centralized system that rejects less than the full 25 kW payload heat load, but would accommodate a majority of payloads that have less than a 25 kW heat load. Figure 32 shows the TCS weight as a function of payload heat rejection where the total heat load is 37 kW. The effect of the high temperature payload is also shown along with the weight savings available with a 90 day payload radiator design. A centralized 37 kW TCS weight is also shown for comparison. Again, the high temperature payload distributed TCS provides a considerable weight savings over the centralized system. A high temperature, 5 year life, 10 kW distributed TCS saves approximately 450 lbs. and a 25 kW high temperature distributed TCS saves 1000 lbs. over the centralized TCS. The 90 day distributed TCS weighs approximately 200 lbs. less than the 5 year distributed TCS with a payload heat rejection of 25 kW. The difference between the 90 day and 5 year high temperature distributed TCS is less (85 lbs. at 25 kW) due to the smaller radiator and the strong sensitivity of meteoroid protection to radiator area.

The reference Power System has three berthing ports and can conceivably accommodate up to three payloads. Figure 33 shows the effect of multiple distributed TCS's. The total payload heat rejection is assumed to be equally divided between the 2 or 3 payloads in this analysis. Multiple distributed TCS's are seen to have a small effect on the distributed TCS weight (about 20 lbs. for the low temperature payload and 45 lbs. for the high temperature payloads) although they do decrease the distributed TCS weight advantage over the centralized TCS.

As previously discussed, the payload heat load may be less than 25 kW due to passive structural heat leaks. Figure 34 shows the effect of lower heat rejection rates on the centralized and distributed TCS weight trades. As the total heat load is reduced by lower payload heat loads, the weight advantage of the distributed TCS is reduced. For a total heat load of 25 kW (12 kW for power processing and 13 kW for the payload) the centralized and distributed TCS's have essentially the same weight.

The centralized radiator is mounted on the Power System body in a manner that provides passive solar avoidance. Direct solar radiation on the radiators is avoided by the Power System attitude which provides solar exposure of the solar arrays. A distributed system, especially the type shown on Figure 29, may not have a radiator environment as favorable as the centralized system. Figure 35 shows the effect of payload radiator sink temperature on the TCS weight. All previous trade data has been for a radiator sink temperature of -40°F for both the centralized and the distributed TCS. As indicated by Figure 35, the distributed TCS weight varies considerably. The 25 kW distributed TCS weight ranges from 1820 lbs. to 2490 lbs. as the sink temperature increases from -80°F to -10°F. It is apparant that the payload radiator design should be restricted to mounting locations and deployment methods that prevent direct solar flux on the radiator.

The weight data presented on Figure 32 indicates that a distributed TCS with 90 day payloads has a weight advantage over the centralized and distributed 5 year TCS's. However, the total weight to orbit of the distributed 90 day TCS is obviously much greater than a centralized or 5 year distributed TCS. Figure 36 shows that the 20 launches required of a 90 day payload during a 5 year period results in a total weight to orbit of 25,000 lbs.

6.2 Centralized and Distributed TCS Cost Comparison

A comparison of the centralized and distributed TCS costs indicates a cost advantage for the centralized TCS. Figure 37 summarizes the cost trade study results. The initial procurement cost of the centralized system is less since the distributed system requires the procurement of at least two separate systems and the burden of two development costs are incurred. It may be possible to share development costs of the Power System and Payload TCS's, but it is likely that the two systems will have different design requirements due to different life times, meteoroid protection, sink temperatures, operating temperatures, stowage volumes and deployment mechanism design.

The cost analysis assumes that the payload will have a coolant loop for heat collection and transport to the Power System payload heat exchanger for rejection from the centralized TCS. Thus, the additional cost incurred by distributing the heat rejection to the Payload will include a radiator, radiator deployment system and a radiator temperature control valve. The

cost of a larger capacity accumulator to accommodate temperature changes in the radiator is not included in the distributed system costs.

The parametric cost data generated in the heat pipe/pumped fluid trade studies have been utilized in the centralized and distributed TCS cost study. Table 28 shows a cost breakdown for various payload heat rejection levels. As shown by Table 28, the development cost of the distributed TCS is approximately $10 million regardless of the heat rejection allocated to the payload, whereas, the development cost of the centralized TCS is $7 million. Thus, there is a $3 million savings resulting from having to develop only one centralized TCS instead of two separate TCS's required for the distributed concept. If several unique payloads are used which require unique TCS's, then the development cost advantage of the centralized TCS will increase.

Production costs for the distributed TCS includes systems for two payloads. As a minimum at least one payload will be exchanged each 90 days requiring one payload TCS on orbit and one waiting for transfer to orbit. Operational considerations and the use of multiple payloads could dictate that additional payload TCS's be required. Production costs for the payload TCS are dependent on the amount of heat rejection (radiator size) and ranges from approximately $0.45 million for 5 kW to $1.0 million for 25 kW.

Single launch costs for the centralized and distributed TCS are comparable with about a $0.2 million advantage for the distributed TCS due to its weight advantage. The costs increase significantly for the multiple launches required by the distributed TCS. A $17.4 million launch cost is incurred for a 25 kW payload heat rejection system during the five year life of the Power System.

6.3 Centralized/Distributed TCS Concept Selection

Selection of the centralized or distributed TCS concept requires consideration of the payload requirements, cost and weight and evolutionary growth potential.

Figure 38 summarizes the payload requirements which influences the centralized/distributed TCS selection. Although the payloads are expected to use the full 25 kW of electrical power available, it is anticipated that passive heat rejection will account for 20% to 40% of the total heat load for many payloads. Passive heat rejection is dependent on the payload design

and temperature control requirements of the individual components. Additional payload requirements studies are required to fully definitize the payload heat loads.

As summarized on Figure 38, consideration of the science, space construction, manned modules and materials processing payloads indicates that a centralized Power System heat rejection system providing 10-16 kW of cooling should satisfy essentially all of the early mission requirements. This heat rejection rate will also meet the Orbiter Sortie Mission requirements.

For those payloads requiring additional heat rejection a payload kit radiator (Figure 39) could be used. The payload kit radiators are designed to interface with the Spacelab Pallet or the SASP non-deployable truss and would be installed on the ground as a kit for particular payloads as required.

Trade studies indicate that the centralized TCS is the most weight and cost effective system. Single launch weight differences between the centralized and distributed TCS's are small for low temperature payloads. The distributed TCS is significantly lighter for high temperature payloads (single launch), however, there is only one high temperature payload (Materials Experiment Carrier) presently planned for the Power System. Consideration of the multiple launch requirements for the distributed TCS shows a clear weight advantage for the centralized system (Figure 36).

Cost comparisons show that development costs for separate Power System and Payload TCS's increase the initial procurement price of the distributed system. If more than one payload TCS development is required the cost differential will be greater. Again the multiple launch requirements of the distributed TCS make the costs of this concept prohibitive (Figure 37).

The multiple launch penalties of the distributed TCS suggests the use of a heat rejection module for payload cooling that would remain on-orbit with the Power System. Two concepts for a relocatable heat rejection module are shown in Figure 40.

Figure 41 summarizes the TCS growth scenario. It is recommended that the initial 25 kW Power System TCS be centralized. The heat rejection capability should meet the requirements of the majority of the payloads with consideration of the passive heat rejection capability. Specialized payloads may require kit radiators. Intermediate growth versions of the Power System

should utilize increased centralization with possible use of a relocatable heat rejection module for specialized payloads. Long term growth versions should be highly centralized and include thermal management of all energy producers and users.

7.0 POWER SYSTEM/PAYLOAD THERMAL INTERFACE STUDY

Figures 42-44 show three concepts for the thermal interface between the Power System and the payloads. There are three berthing ports on the reference Power System and a payload heat exchanger is located at each port. An alternative would be to have one central payload heat exchanger with fluid lines to each port. The central heat exchanger would be more complex due to the redundant coolant loops in the Power System and at least three independent loops for each of the payloads. Redundant coolant loops for the payloads would require eight independent flow loops in the central heat exchanger. Also the central heat exchanger design would be further restricted by the requirement of a 45°F return temperature for all payloads.

Any combination of the three payload heat exchangers, from one to three, may be used at the same time with any combination of heat loads. A thermally actuated flow control valve to provide this control is shown schematically on Figure 42. The three payload heat exchangers are flowed in parallel. The flow control valve immediately downstream of each heat exchanger restricts flow to a trickle when the heat exchanger is not in use. Cold fluid from the radiator outlet flows through the heat exchanger to the valve which is contracted to restrict flow. If the heat exchanger is in use the fluid is heated and the valve expands to allow more flow to heat exchanger. At full capacity the heat exchanger outlet is restricted to 100°F. If the upper temperature limit is exceeded the valve expands against a stop, restricting flow to the heat exchanger. Thus the valve insures that the maximum allowable return temperature is not exceeded and protects the Power System loop from an over temperature condition. The burden of payload overtemperature protection is placed on the payload since the valve will terminate cooling if the payload overheats the Power System.

If only one heat exchanger is in use then all flow is routed to it and full heat rejection capacity can be utilized by one payload. Heat rejection is automatically divided according to demand when two or three

payloads are present. When no payloads are present, then all flow is routed to the parallel Power System equipment flow paths.

The flow control valve is used to regulate the payload heat rejection with either a contact heat exchanger (Figure 42) or a fluid heat exchanger (Figure 43). The contact heat exchanger requires no fluid transfer between spacecraft and would be leak-free. The payload TCS can be either a pumped coolant loop, with or without a supplementary radiator, or an all heat pipe TCS.

The fluid heat exchanger concept requires fluid quick disconnects at the Power System/Payload interface. A pumped coolant loop is required for the payload TCS. All payloads are required to use the same coolant and a small amount of fluid will be exchanged with each payload from the residual in the lines from the Power System/Payload interface to the payload heat exchanger. An accumulator or fluid expansion device will be required for these lines.

Figure 44 shows a concept for a direct fluid coupling to the payload. An intermediate cooling loop is used to prevent payload damage or contamination of the Power System loop. The payload TCS would not require a pump or loop controls but would include plumbing, coldplates and an accumulator.

Table 29 summarizes the advantages and disadvantages of the three thermal interface concepts.

7.1 Contact Heat Exchanger Concept

Figure 45 compares the weight of a contact heat exchanger to a conventional liquid-to-liquid heat exchanger. It is seen that the contact heat exchanger weight is about 20 lbs heavier than the liquid-to-liquid at moderate heat exchanger effectivenesses (below 0.90). At higher effectiveness the weight differences are large with the fluid-to-fluid heat exchanger being much lighter. Since a 35°F radiator outlet temperature will probably be required for battery cooling, a high effectiveness payload heat exchanger may not be necessary. The required 45°F payload heat exchanger outlet can be met with the contact heat exchanger for an approximately 20 lb weight penalty. Elimination of the fluid quick disconnects and the transfer of fluid between the payload and the Power System for a 20 lb weight penalty would appear to make the contact heat exchanger an attractive alternative.

7.2 Rotating Joint Concepts

Earth viewing payloads will require rotation relative to the Power System. Thus, it is desirable to provide fluid transfer across a rotating joint. This can be accomplished with a fluid swivel or, for limited rotation, flexible hoses.

Figure 46 shows a four pass fluid swivel design that would allow redundant coolant loops in both the Power System and the payloads. The design features redundant seals between the fluid and the ambient and between the redundant loops. Single seals are used between the supply and return since leakage is not critical at this interface. Stainless steel is used to minimize the heat transfer between the supply and return lines.

Although the number of rotations and rotational speeds are modest compared to existing commercial fluid swivels, long life vacuum dynamic seal technology has not been proven. Flex hoses provide a proven alternate method of transferring fluid across a joint with limited rotational capability. Figure 47 shows a drum and flex hose reel concept that would provide several 360° rotations. The hose unwinds from one drum, is routed across the rotating joint, and rewinds on the opposite drum. The drum is made up of a stack of four concentric reels to provide for an active and redundant loop supply and return.

Figures 48 and 49 show the weight and volume of the hose reel mechanism. The weight is seen to increase rapidly with hose diameter and allowable revolutions. Figure 50 presents the device pressure drop. A hose diameter on the order of 0.75 inch is required to yield reasonable pressure drops (10 psi, or less). Thus the weight penalty (Figure 48) will be 120 lbs to 250 lbs depending on the number of revolutions desired. A single revolution flex hose weight would be more competitive with the fluid swivel weight but would incur more operational constraints.

Figure 51 illustrates the flex hose reel concept integrated with a contact heat exchanger concept. A conical contact heat exchanger plug on the payload is inserted into the receptacle on the Power System as the two spacecraft are docked. The Power System receptacle is allowed to rotate with the rotating joint on the Power System. Figure 52 details the contact heat exchanger interface. A jackscrew/guide is used for the initial contact and retention. Final contact pressure between the mating heat exchanger

surfaces is provided by a pressurized stainless steel diaphragm. Expendable nitrogen is used to pressurize the diaphragm after berthing and the nitrogen is vented to space for undocking.

8.0 PRELIMINARY DESIGN STUDIES

The parametric trade study results have been used to develop a thermal control system preliminary design. Consideration has been given to the flow and pressure drop of the TCS loop, the radiator thermal environment, the thermal design of the radiator, and mechanical design of the radiator deployment mechanism including the dynamics of the deployed panels.

8.1 Coolant Loop Preliminary Design

Figure 53 shows the coolant loop schematic. Redundant flow loops are used; one active and one standby to provide the desired reliability. The Power System equipment is located in four parallel flow paths with 778 lb/hr in each leg. The batteries are located in the upstream position of each of the four legs to provide a maximum battery coldplate fluid outlet temperature of 50°F.

The payload heat exchangers are plumbed to form a fifth parallel leg with a flow of 3288 lb/hr. Each of the payload heat exchangers are flowed in parallel with the payload heat exchanger flow control valve, described in Paragraph 7.0, controlling the flow to each heat exchanger.

Figure 54 shows the approximate location of each component, as described in the Reference Concept (Reference 1), and the lines routing. The line sizes were weight optimized to minimize wet weight and pumping power penalty.

Coldplate pressure drop was based on the Spacelab coldplate data shown in Figure 55. At the design flow rate of 778 lb/hr, each coldplate has a pressure drop of approximately 0.12 psi. The highest pressure drop leg contains 16 coldplates in series with a flow of 778 lb/hr and 3 coldplates in series at a flow of 1556 lb/hr for a total pressure drop of 3.2 psi.

Coldplate overall thermal conductance at 778 lb/hr is approximately 33 BTU/hr-ft^2-°F (Figure 56) which will provide adequate performance. The maximum heat dissipation component is the 30 V regulator which has a heat removal requirement of 587 BTU/hr-ft^2. A fluid-to-baseplate temperature difference of approximately 18°F is obtained and the maximum baseplate

temperature is below 100°F.

Two Orbiter pumps operating in parallel provide a total R-21 flowrate of 6400 lb/hr (3200 lb/hr each pump). A third pump is included in the pump package for redundancy. Thus, two pump failures are allowed before the standby loop is activated. Full capacity is still provided after three pump failures. Even after four failures, near full capability can be obtained by operating one pump in each loop and partial capability is available from one pump in one loop.

The pressure head provided by the Sunstrand Orbiter pump is 64 psi at 3200 lb/hr (Figure 57). Total system pressure drop is estimated as:

Component	ΔP-PSI
Radiator	30.0
TCV	6.0
GSE H/X	3.0
Lines	8.8
Coldplates	3.2
	51.0

Thus, a 13.0 psi margin is available for design maturity. The redundant thermally actuated temperature control valve and the payload heat exchanger control valve will require development and the preliminary design pressure drop estimates for these components could change.

8.2 Radiator Environment Studies

Analyses have been conducted to determine the effective steady state design radiation sink temperature for the radiators. The analysis includes the effect of the thermal mass of the panels and radiant interchange with the Power System including the solar arrays. An orbital heating and radiant interchange model (Figure 58) was developed to determine the orbital transient heat flux on the radiator panels and Power System surfaces. The Space Shuttle Orbiter docked to the Power System was included in the model as a representative payload. The heat fluxes include the effect of blockage and reflected energy.

The computed heat fluxes and radiation exchange factors are input to a SINDA model for a transient temperature analysis. Adiabatic surface temperatures are computed for the Orbiter and Power System surfaces. The Orbiter radiator surfaces were held at a constant 70°F. Transient temperatures

of the Power System solar arrays and radiator surfaces were computed. The radiator temperatures were calculated with no fluid flow and a radiator weight of 1 lb/ft^2. The resulting orbital temperature variation is the effective radiator transient sink temperature. The maximum orbital temperature yields the radiator effective steady state design sink temperature. Figure 59 summarizes the analysis results for the two orbits considered with variable Beta angles and solar absorptivity. A silver/Teflon coating with α/ε = .76/.11, was assumed for the radiator coating. The results indicate that the design condition (highest sink temperature) is for a Beta angle of 0° with the Z-axis parallel to the sun line. Since the Power System is always oriented with the solar arrays toward the sun, the radiators are always parallel to the sun's rays and receive only earth albedo and solar reflected from the Power System surfaces. The effect of higher solar absorptance coatings on the radiator sink temperature is also shown on Figure 59 for the 0° Beta angle condition. It is seen that large increases in α have a small effect on the radiator sink temperature due to the minimal solar flux.

Figure 60 shows the effect of solar absorptivity on radiator performance. Area requirements for a 25 kW heat load are shown along with the heat rejection, from a radiator designed for 25 kW with an α of 0.11, as a function of α. Increasing the α from 0.11 to 0.20 results in only a 4.6% increase in radiator area requirements. For an α of 0.30 the area increase is 10.3%. Thus, it would appear that cheaper thermal control coatings with higher solar absorptances are applicable to the Power System radiators.

For coarse solar alignment of the Power System the effect of α is more pronounced and low α radiator coatings or solar avoidance designs are beneficial. Figure 61 shows the radiator area savings resulting from an oriented radiator for various solar absorptances as a function of the solar misalignment angle. Considerable area savings are ewalized at high misalignment angles and absorptivities by orienting the radiator out of the sun. This data is for the X-axis parallel to sun line orbit. In the Z-axis parallel to sun line orbit, the radiators are shaded by the Power System body and solar arrays and performance is not changed by the solar misalignment.

Another radiator orientation concept is shown in Figure 62. In this concept the radiators are oriented to view the edge of the solar arrays to minimize radiant heating and solar reflections from the arrays. The area savings are not a strong function of α because much of the radiator heating from the array is in the infrared region. An area reduction of approximately 100 ft^2 results from this re-orientation even at the lowest solar absorptivity. This appears to be an effective orientation for reducing radiator area, but requires that the radiators be re-oriented to the area allocated for the re-boost propulsion system on the reference 25 kW Power System Concept.

8.3 Radiator Panel Design

The specific radiator design conditions resulting from the coolant loop preliminary design and the radiator environment studies have been used to determine the weight optimum radiator design. A centralized radiator with a total heat load of 28 kW was selected based on the study results of paragraph 6.0, Power System/Payload Heat Rejection Allocation. This provides for 12 kW cooling for the Power System equipment and 16 kW cooling for the payload. For 25 kW of electrical power provided to the payload, the passive payload heat rejection is 36% or 9 kW. The 16 kW payload cooling also meets the Power System/Orbiter sortie mission requirements.

The design conditions of:

$$T_{in} = 93.5°F$$
$$T_{out} = 35°F$$
$$\dot{w} = 6400 \text{ lb/hr R-21}$$
$$Q = 28 \text{ kW}$$
$$T_{sink} = -57°F$$

were input to the specialized computer routine described in Paragraph 4.4, for weight optimization of the radiator. Figure 63 shows the panel details. A nine panel system flowed in parallel with a total area of 955 ft^2 is obtained. Since the manifold area incorporates bumpers for meteoroid protection and does not have good thermal contact with the manifolds or flow tubes, the effective radiation area is reduced. It is estimated that the 45 ft^2 of manifold area is approximately 50% effective; thus the effective radiation area of the panels is approximately 932.5 ft^2. Each panel weighs 137.16 lbs. The nine panel total weight is 1234.4 lb.

8.4 Radiator Deployment System Design

Four radiator deployment concepts have been examined for application to the Power System. The first concept involves the use of spring loaded hinges to deploy the radiator from a panel stack as illustrated in Figure 64. A drum and cable system controls the deployment and retraction. This concept requires only a single motor for deployment and retraction and has good reliability and low mechanical complexity. A preliminary analysis of the hinge line shear and torque generated by the Power System maneuvers is summarized on Figure 65. The interface hinge at the base is required to have a torque of 9213 in-lbs and exert a shear force of 23.5 lb. It is estimated that a coil spring on the order of 6.5 inches in diameter with a wire diameter of 1.3 inches is required to provide this torque at the base. Furthermore, the spring constant required to obtain a natural frequency of 0.1 Hz is estimated to be 4000 in-lb/deg at the base. For a 90° deployment the base spring torque requirement is 360,000 in-lb resulting in an impractical spring size. Thus, the only feasible design is to utilize mechanical latches at the hinges to provide the required stiffness. The latches will require solenoid activation/deactivation which tends to negate the mechanical simplicity and high reliability of the spring loaded hinge concept.

The second deployment concept is a power hinge at each radiator panel. This concept is similar to the Orbiter payload bay door hinge and could utilize Orbiter technology and hardware. An advantage of this concept is that each panel could be deployed individually as required and the other panels would remain in the stack. The disadvantage is that electric motors are required at each hinge line, and system reliability is dependent on the reliability of multiple motors. The deployment of the baseline 9 panel radiator system would require the operation of 9 electric motors. Growth to more panels would require additional electric motors.

The third deployment concept is a scissors arm similar to the Skylab solar panel deployment mechanism. A single drive motor can be used for this concept resulting in a high reliability. The scissors arms (Figure 66) provide good structural stiffness and reduce the panel and hinge stiffness requirements of the other concepts.

Figure 67 shows a boom deployment concept. The radiator panels are deployed from a folded stack by a telescoping boom. The boom supplies all of the stiffness and the radiator panels can be a non-structural design.

The mast is identical to the solar array mast used on the reference 25 kW Power System described in Reference (1). It is estimated that the stowed mast length would be approximately 78 inches and have a diameter of 26 inches.

Table 30 compares the characteristics of the four candidate deployment concepts. Although the scissors deployment concept is heavier, it will allow the use of minimum panel structure and should result in a total system weight savings. The power hinge and spring hinge concept will require additional panel stiffness to meet the natural frequency requirements of the deployed radiator system. The scissors concept is also the most reliable when the latch mechanism for the spring hinge concept is considered.

Another radiator deployment method involves the construction of the radiator array on orbit by EVA or RMS activity. Figure 68 illustrates a space constructed radiator array for a large multi-kilowatt space station. The radiator array is built up from 4 kW submodules which contain the fluid loops. The individual heat pipe radiator panels are inserted into the submodule and interface with the coolant loop through a cylindrical contact heat exchanger. Figure 69 shows the submodule details. A nitrogen pressurization system is used to supply the contact heat exchanger pressure.

System weight for the space constructable radiator concept is shown in Figures 70 and 71. Figure 70 shows the system weight with the radiator panel length restricted to 45 ft. and Figure 71 shows the weight with the panel length optimized. Both curves show that a panel width of 6 in. is close to the optimum width. The space constructable concept is not weight competitive with the mechanical deployment concepts for heat load below about 50 kW. For higher heat loads the weight savings are significant. However, the constructable concept requires the development of a high capacity heat pipe radiator and the contact heat exchanger. The concept is applicable to future high heat load Power Systems or Space Stations, but does not appear feasible for the initial 25 kW Power System.

The scissors deployment concept is selected for preliminary design analyses. A dynamics analysis of the deployed radiator has been conducted to determine the fundamental vibration frequency.

The radiator configuration evaluated consists of 8 hinged panels which are actuated by means of a scissors linkage. The baseline individual panels are 6.7 feet by 16 feet bonded aluminum honeycomb-facesheet construction. Panel thickness is 1 inch. The aluminum actuation I-beams are hinged to the panels, and are sized in this analysis as 2 inch by 2 inch cross-section with 0.3-inch flange and web. The transition sections between the base and the lower panel and beams are represented as plates equivalent to 2-inch thick bonded aluminum honeycomb-facesheet panels. The transition section is assumed to be mounted to a rigid base.

Reactions to maneuver acceleration loads at the transition section base pivots are presented in Table 31. In addition, loads are presented in Table 32 for the lower linkage at its intersection with the transition section, and with the first radiator panel.

Vibration mode shapes are presented for the deployed configuration in Figures 72 - 75, and for the partially deployed configuration in Figures 76 - 79. The fundamental mode for the deployed configuration is bending out-of-plane, and occurs at a frequency of 0.11 Hz which exceeds the criteria of 0.10 Hz. The fundamental mode for the partially deployed configuration is an extension mode, and occurs at 0.12 Hz which also exceeds the criteria. It is concluded that the preliminary design has adequate stiffness.

8.5 Preliminary Design Summary

Figure 80 summarizes TCS preliminary design. The scissors deployment concept is used to deploy 9 radiator panels to provide 28 kW of heat rejection. A weight estimate of the panels and deployment mechanism yields a total weight of 1883 lb. Design layouts of the selected scissors deployment mechanism and the radiator panels have been made and are presented in Appendix A. The stowed and deployed configurations and interface with the Orbiter are shown for the reference Power System configuration. The stack height of the stowed 9 panels is 21 inches. In the deployed position the radiator height is 843.5 in. The overall length of the panels and scissors arms is 195.5 in. The layouts include the interpanel flex hose plumbing. Panel fittings and flex hose arrangements have been designed to provide the proper dynamic bend radius to accommodate multiple deployment/retraction cycles. Meteoroid protection of the flex hoses is provided by a multi-layer

Teflon wrap. Figure 81 shows the Teflon thickness requirements as a function of reliability. A thickness of approximately 0.11 in. will provide a reliability of 0.995 (probability of puncture = 0.005).

A one-tenth scale feasibility demonstration model of the deployment system has been built. Figures 82, 83 and 84 are photographs of the model in the stowed, partially deployed and fully deployed positions.

The preliminary design layouts and demonstration model have verified that there are no major design problems associated with the deployment concept. Areas for design improvement include the reduction of the stowed panel stack height and increased deployed stiffness by weight/stiffness optimization of the scissors arms and simplified interpanel plumbing design.

9.0 CONCLUSIONS AND RECOMMENDATIONS

Based on the study results the following conclusions are made:

(1) A pumped fluid radiator with meteoroid protection should be used for the initial and intermediate growth versions of the Power System.

(2) All of the payload active heat rejection should be provided by the Power System with a centralized radiator.

(3) There are no major technical problems associated with the Power System Thermal Control System. Orbiter pumps and radiator technology can be effectively utilized by the Power System.

(4) Thermal Control System component life and operating characteristics need to be established through a early breadboard test program.

A new heat pipe radiator concept has been developed and verified by element testing. The advanced design provides a weight savings of 10-15% over existing heat pipe radiator designs. A pumped fluid radiator with meteoroid bumpers can insure a 99% probability of no meteoroid penetration of the fluid passages for five years. The advanced heat pipe design also has a weight advantage over the bumpered pumped fluid radiators for heat rejection rates greater than about 25 kW. In the range of 50 kW to 110 kW the advanced heat pipe radiator is more than 10% lighter than the bumpered

pumped fluid radiator. Above 110 kW the pumped fluid radiator with multiple subsystems weight is again within 10% of the advanced heat pipe radiator design.

The cost of the advanced heat pipe radiator and the conventional heat pipe radiator are greater than the bumpered pumped fluid radiator over the entire range of heat loads considered. The weight competitive advanced heat pipe radiator cost is 17% to 25% greater than the pumped fluid radiator.

The bumpered pumped fluid radiator design is recommended for the initial 25 kW Power System based on its cost advantage. The weight advantage of the advanced heat pipe design becomes significant between 50 kW and 110 kW and this concept is recommended for the 50 kW to 100 kW range. The bumpered pumped fluid design with multiple subsystems is recommended for the 110 kW to 250 kW heat rejection range.

The Power System/Payload heat rejection allocation studies have shown that a centralized heat rejection system which meets the Power System and payload active cooling requirements is the most weight and cost effective system. The single launch weight of the centralized heat rejection system is comparable to the payload distributed system unless the payload radiator can operate at a much higher temperature. Since only one high temperature payload (Materials Experiment Carrier) has been identified this is not considered a design driver unless a Power System is dedicated for use entirely by the Materials Experiment Carrier. Consideration of the multiple launch requirements of the distributed heat rejection system shows that the centralized system reduces the total weight to orbit requirement by 23,000 lbs for a fully distributed system.

The cost of the distributed TCS involves the development and procurement of the Power System heat rejection system and numerous payload systems. Even with the optimistic assumption that each payload can utilize the same heat rejection system design and that only two systems are required, it has been shown that the centralized system cost is still 24% less than the distributed system. A more realistic scenario with development costs for more than one system and procurement costs for more than two systems will significantly increase the cost advantage of the centralized system.

It is recommended that the heat rejection system be centralized and that the Power System provide all of the active heat rejection of the majority of the payloads. Occasional payloads with low passive heat rejection

can be accommodated with payload kit radiators as required. A payload heat rejection requirements study is recommended to determine the design values for the Power System radiators. Consideration of relocatable heat rejection modules to meet evolving requirements is also recommended. The relocatable modules would remain on orbit to provide cooling for payloads located extended distances from the Power System to avoid long fluid transfer lines and associated penalties.

Heat transfer between the Power System and its payloads is best accomplished through a fluid-to-fluid heat exchanger located on the Power System. Fluid transfer to the payload is accomplished through fluid quick disconnects. A flex hose reel design concept that provides up to 28 continuous revolutions has been formulated to meet possible payload rotation requirements. A concept for a contact heat exchanger that eliminates fluid transfer between the Power System and payloads has been shown to be weight competitive with the fluid-to-fluid heat exchanger.

It is concluded from the preliminary design studies that the Orbiter R-21 pumps can be effectively used in the Power System coolant loop. Two Orbiter pumps operating in parallel provide a total flow of 6400 lb/hr to meet the flow and fluid temperature requirements of all components. Total loop pressure drop is 13 psi below the pump head at this flow.

The preliminary design studies have also shown that there are no major design problems associated with the radiator deployment mechanism. The honeycomb panels and scissors arms are sized to provide adequate stiffness with deployed vibration frequencies that will preclude interaction with the attitude control system and still maintain a compact stowage volume consistent with Orbiter launch requirements.

The study has identified several areas in which technology development is required for design improvement. The use of fluid swivels for interpanel fluid transfer instead of flex hoses would provide a reduced stowed volume, better meteoroid protection and design simplicity. Fluid swivels are also applicable to the Power System/Payload interface to provide payload rotation capabilities.

Contact heat exchanger development is also recommended. Elimination of fluid transfer between the Power System and payloads is desirable to reduce fluid leakage and aliviate the complexity of fluid line connect/disconnect designs. A related technology involves the development of space

constructable radiators which utilize contact heat exchangers. Space constructable radiators would provide for more flexible launch storage, elivainate the deployment mechanism, allow on orbit replacement of panels and enhance modular growth capabilities.

Redundant thermally actuated temperature control valves and redundant fluid accumulators have been identified as desirable to meet the long life high reliability requirements of the Power System. Development of these components is recommended.

The heat pipe/pumped fluid radiator trade studies showed that the cost of the heat pipes is the primary drawback to the use of heat pipe radiators. A weight advantage for small diameter high capacity heat pipes was also shown. It is recommended that radiator heat pipe technology development be directed towards reduced cost, small diameter high capacity heat pipes.

Recommended future effort for the Power System TCS includes detailed thermal and structural optimization of the radiator panel and deployment mechanism. Further studies are needed in the selection of the radiator thermal control coating including long term degradation due to solar and plume impingement from multiple reboost and Orbiter docking activities. Transient coolant loop/radiator analysis in a wider range of orbits is recommended to insure that all operational requirements are met by the design.

A breadboard test of the thermal control loop components is recommended to verify system and component operating characteristics and design requirements. An early assessment of the component life characteristics is essential to the successful development and design which will insure a reliable five year system operation.

10.0 REFERENCES

(1) "25 kW Power System Reference Concept", NASA George C. Marshall Space Flight Center, PM-001, September 1979.

(2) Cour-Palais, B.G., "Meteoroid Environment Model - 1969 (Near Earth to Lunar Surface):, NASA SP 8013, March 1969.

(3) Leach, J. W. and Stalmach, D. D., "Optimum Design of Spacecraft Radiators for Large Capacity or Long Duration Mission Applications", ASME Paper No. 79-ENAs-10, 9th Intersociety Conference on Environmental Systems, July 1979.

(4) Alario, J. and Haslett R., "Modular Heat Pipe Radiators for Enhanced Shuttle Mission Capabilities", ASME Paper No. 79-ENAs-17, 9th Intersociety Conference on Environmental Systems, July 1979.

(5) "PRICE 84", RCA PRICE Systems

TABLE 1

THERMAL CONTROL SYSTEM REQUIREMENTS, GUIDELINES AND CONSTRAINTS

RELIABILITY

- TOTAL SYSTEM - 0.99 for 5 YRS.
- PROBABILITY OF NO MICROMETEOROID FLUID PASSAGE PENETRATION - 0.99 FOR 5 YRS.
- HEAT PIPE RADIATOR PANELS OVERSIZED TO ALLOW FOR RANDOM FAILURE
- FAIL OPERATIONAL
- RETAIN POWER PROCESSING COOLING AFTER FIRST FAILURE

ON-ORBIT MAINTENANCE

- EVA OR ORBITER RMS CAPABILITY
- REPLACEMENT OF RADIATOR PANELS IS CONTINGENCY MAINTENANCE
- REPLACEMENT OF OTHER COMPONENTS IS UNSCHEDULED MAINTENANCE

STOWAGE VOLUME

- STORAGE REQUIREMENTS CONSISTENT WITH ORBITER LAUNCH
- MAXIMUM RADIATOR PANEL STOWED LENGTH 32 FT.

RADIATOR DEPLOYMENT

- SELF CONTAINED CAPABILITY FOR PARTIAL OR FULL DEPLOYMENT OR RETRACTION
- MANUAL (EVA) BACKUP FOR DEPLOYMENT/RETRACTION
- JETTISON FEATURE

MICROMETEOROID ENVIRONMENT

- NASA SP 8013

COST

- TRADE PARAMETER OF MAJOR IMPORTANCE. CONSIDER EXISTING TECHNOLOGY. COST TO ORBIT $700/LB

WEIGHT

- MINIMIZE WEIGHT

GENERAL

- MINIMIZE OBSTRUCTION OF PAYLOAD EARTH, SOLAR AND STELLAR VIEWING
- MINIMIZE AERODYNAMIC DRAG
- MINIMIZE MOMENTS OF INERTIA

TABLE 2

HEAT REJECTION REQUIREMENTS

- 25 kW POWER SYSTEM EQUIPMENT

BATTERIES	3.5
POWER PROCESSING EQUIP	6.5
COMMUNICATIONS EQUIP	2.0
	12.0 kW

MAX BATTERY COLDPLATE TEMP = 50°F
ALL OTHER EQUIPMENT = 90°F

- PAYLOAD

PARTIAL TO TOTAL HEAT REJECTION BY POWER SYSTEM (25 kW MAXIMUM)

PAYLOAD COOLANT RETURN TEMPERATURE = 45°F

HEAT EXCHANGER INTERFACE

- CONTACT
- LIQUID-TO-LIQUID

CONSIDER GIMBAL JOINTS

- TOTAL SYSTEM

QUISCENT OPERATION, PUMPS ONLY	0.7 kW
NOMINAL (12 kW PS + 16 kW P/L)	28 kW
MAXIMUM (12 kW PS + 25 kW P/L)	37 kW
CONSIDER GROWTH VERSIONS TO	250 kW

TABLE 3
FLUID LOOP RELIABILITY CHARACTERISTICS

COMPONENT	FAILURE RATE $\lambda \times 10^6$ HRS	REDUNDANT COMPONENT FAILURE RATE $\lambda \times 10^6$ HRS
Rad Panel Struct Integrity (8 Panels)	.8 - 1.6	
Rad Panel Meteoroid	.23	
Pump/Motor/Inverter	1.39 - 4.48	.0439* - .4082*
Accumulator/Filter	.14 - .30	.00085 - .00389
Temp Control Valve	.34 - .52	.00498 - .0116
Fill Drain Valve, Pair	.05	
Temp Sensor**	1.50	.27
Lines/Fittings	.05	
	4.5 - 8.73	1.450 - 2.625
Single Loop Probability of Success (5 Years)	.8211 - .6822	.9385 - .8916
Redundant Loop Probability of Success*	.9811 - .9523	.9959 - .9903

*Switch System P_o = .995 - .99
**Required For Health Monitoring Only

TABLE 7

ASSUMPTIONS FOR COST ANALYSIS
OF
POWER SYSTEM THERMAL CONTROL SYSTEM

- RCA PRICE ROUTINE USED
- SCHEDULE FOR PROGRAM FOR ALL CASES
  - DEVELOPMENT START : JAN '81
  - PROTOTYPE COMPLETE : JAN '82
  - DEVELOPMENT COMPLETE : JAN '83
  - PRODUCTION START : FEB '83
  - DELIVERY : AUG '84
- YEAR OF ECONOMICS : 1979
- YEAR OF TECHNOLOGY : 1981
- TOTAL SYSTEM COST IS PRIME CONTRACTOR HARDWARE ACQUISITION COST. NO VEHICLE LEVEL TESTS, FLIGHT SUPPORT OR MAINTENANCE COSTS ARE INCLUDED.
- COMPLEXITY FACTORS FOR PRICE ROUTINE DERIVED FROM HISTORICAL COSTS WHERE AVAILABLE AND ROM QUOTES ON COMPONENTS.

TABLE 8

PRICE COMPLEXITY FACTORS

- PRICE ROUTINE INPUTS

COMPONENT	ENGINEERING COMPLEXITY	MANUFACTURING COMPLEXITY	PLATFORM FACTOR
RADIATOR PANELS	1.5	7.2	2.5*
HEAT PIPES	← VENDOR ROM →		
PUMP/MOTOR	← VENDOR ROM →		
ACCUMULATOR	1.566	5.4	2.5
TEMP CONTROL VALVE	.866	9.1	2.5
TEMP SENSORS	1.37	6.1	2.5
HEAT EXCHANGER	0.865	9.1	2.5
FLEX HOSES	1.633	5.2	2.5
DEPLOYMENT MECHANISM	1.361	6.1	2.5
INTEGRATION & TEST	1.162	7.020	2.5

*PLATFORM OF 2.5 IS MANNED SPACE

TABLE 9

HEAT PIPE COSTS

	DEVELOPMENT COST	UNIT PRODUCTION COST
LOW TECHNOLOGY HEAT PIPE	$100,000	$375/HEAT PIPE
INTEGRAL MANIFOLD HEAT PIPE	$600,000	$550/HEAT PIPE

TABLE 10

SUNDSTRAND PUMP ROM COSTS

PUMP	QTY	NON-RECURRING (SPECIAL DATA AND INSPECTION)	NON-RECURRING (DEVELOPMENT)	ROM PRICE EACH
2500 lb/hr, Dual Centrifugal Motor Driven, Based on Sundstrand Model 145660-300	12	$175,000	0	$35,000
	36	$175,000	0	$30,000
	60	$175,000	0	$25,000
5000 lb/hr Dual Centrifugal Motor Driven Similar to Model 145660-300	30	$175,000	$750,000	$35,000
	40	$175,000	$750,000	$32,000
		$175,000	$750,000	$30,000
10,000 lb/hr Dual Centrifugal Motor Driven Similar to Model 145660-300	20	$175,000	$850,000	$40,000
	30	$175,000	$850,000	$37,500
	40	$175,000	$850,000	$35,000

TABLE 11

25 kW THERMAL CONTROL SYSTEM COST COMPARISON

THOUSANDS OF 1979 DOLLARS

COMPONENT	PUMPED FLUID			LOW TECH HEAT PIPE			INTEGRAL MANIFOLD HEAT PIPE		
	DEV.	PROD	TOTAL	DEV.	PROD	TOTAL	DEV.	PROD	TOTAL
Radiator Panels	2196	406	2603	2567	519	3086	2439	403	2842
Heat Pipes	-	-	-	100	189	289	600	297	897
Pumps	925	140	1065	925	140	1065	925	140	1065
Accumulator	482	6	488	482	6	488	482	6	488
Temp Control Valve	120	46	166	120	46	166	120	46	166
Temp Sensor	70	10	80	70	10	80	70	10	80
Flex Hoses	198	8	205	198	8	205	198	8	205
Deployment Mechanism	1680	38	1718	1680	38	1718	1680	38	1718
Integration & Test	884	44	928	1245	63	1307	1044	54	1099
			$7253			$8404			$8560

VOUGHT

VOUGHT

TABLE 12

25 kW THERMAL CONTROL SYSTEM COST COMPARISON

THOUSANDS OF 1979 DOLLARS

CONCEPT	DEVELOPMENT	PRODUCTION	SUBTOTAL	TOTAL
Pumped Fluid				
Radiator Panels	2196	406	2603	$2603
Low Technology Heat Pipe				
Radiator Panels	2567	519	3086	
Heat Pipes (505)	100	189	289	$3375
Integral Manifold Heat Pipe				
Radiator Panels	2439	403	2842	
Heat Pipes (540)	600	297	897	$3739

TABLE 13 25 kW PUMPED FLUID COST ANALYSIS

T_{IN} = 100, T_{OUT} = 40, T_S = -40°F

COST-THOUSANDS OF DOLLARS

COMPONENT	MULTIPLE (4,8.33 kW) SUBSYSTEMS			SINGLE SUBSYSTEM		
	DEVELOPMENT	PRODUCTION	TOTAL	DEVELOPMENT	PRODUCTION	TOTAL
RADIATOR PANELS	2299	638	2938	2196	406	2603
HEAT PIPES	-	-	-	-	-	-
HR LOOP PUMP	175	560	735	925	140	1065
COLLECTION LOOP PUMP		140	1065			
HR LOOP ACCUMULATOR	329	9	338	482	6	488
COLLECTION LOOP ACCUM.	410	5	415			
TEMPERATURE CONTROL VALVE	153	178	331	120	46	166
TEMPERATURE SENSOR	89	16	105	70	10	80
HEAT EXCHANGER	405	496	901			
FLEX HOSES	198	12	210	198	8	205
DEPLOYMENT MECHANISM	1191	84	1275	1680	38	1718
INTEGRATION AND TEST	722	87	809	884	44	928
			9122			7253

TABLE 14 50 kW PUMPED FLUID COST ANALYSIS

T_{IN} = 100, T_{OUT} = 40, T_S = -40°F

COST-THOUSANDS OF DOLLARS

COMPONENT	MULTIPLE (7, 833 kW) SUBSYSTEMS			SINGLE SUBSYSTEM		
	DEVELOPMENT	PRODUCTION	TOTAL	DEVELOPMENT	PRODUCTION	TOTAL
RADIATOR PANELS	2299	1022	3321	2131	873	3004
HEAT PIPES	-	-	-	-	-	-
HR LOOP PUMP	175	980	1155	1025	160	1185
COLLECTION LOOP PUMP	1025	160	1185			
HR LOOP ACCUMULATOR	329	14	343	721	10	732
COLLECTION LOOP ACCUM.	613	9	622			
TEMPERATURE CONTROL VALVE	153	283	436	120	46	166
TEMPERATURE SENSOR	89	18	107	70	10	80
HEAT EXCHANGER	405	792	1197			
FLEX HOSES	198	20	218	198	17	215
DEPLOYMENT MECHANISM	1191	133	1324	1680	72	1752
INTEGRATION AND TEST	722	128	850	1627	89	1716
			10758			8850

TABLE 15 100 kW PUMPED FLUID COST ANALYSIS

T_{IN} = 100, T_{OUT} = 40, T_S = -40°F

COST-THOUSANDS OF DOLLARS

COMPONENT	MULTIPLE (9, 12.5 kW) SUBSYSTEMS			SINGLE SUBSYSTEM		
	DEVELOPMENT	PRODUCTION	TOTAL	DEVELOPMENT	PRODUCTION	TOTAL
RADIATOR PANELS	2690	1920	4610	2734	1865	4598
HEAT PIPES	-	-	-	-	-	-
HR LOOP PUMP	175	1080	1255	1125	280	1405
COLLECTION LOOP PUMP	1125	280	1405			
HR LOOP ACCUMULATOR	421	24	445	1050	17	1067
COLLECTION LOOP ACCUM.	893	15	908			
TEMPERATURE CONTROL VALVE	153	349	502	120	46	166
TEMPERATURE SENSOR	89	19	108	70	10	80
HEAT EXCHANGER	545	1400	1945			
FLEX HOSES	202	35	237	202	31	233
DEPLOYMENT MECHANISM	1216	167	1383	1730	152	1882
INTEGRATION AND TEST	975	209	1184	3070	185	3256
			13982			12687

TABLE 16 250 kW PUMPED FLUID COST ANALYSIS

T_{IN} = 100, T_{OUT} = 40, T_S = -40°F

COST-THOUSANDS OF DOLLARS

COMPONENT	MULTIPLE (21, 12.5 kW) SUBSYSTEMS			SINGLE SUBSYSTEM		
	DEVELOPMENT	PRODUCTION	TOTAL	DEVELOPMENT	PRODUCTION	TOTAL
RADIATOR PANELS	2690	3913	6604	3741	5821	9561
HEAT PIPES	-	-	-	-	-	-
HR LOOP PUMP	175	2200	2375	1225	400	1625
COLLECTION LOOP PUMP	1225	400	1625			
HR LOOP ACCUMULATOR	421	35	456	1724	35	1759
COLLECTION LOOP ACCUM.	1465	32	1497			
TEMPERATURE CONTROL VALVE	153	707	861	120	46	166
TEMPERATURE SENSOR	89	25	114	70	10	80
HEAT EXCHANGER	545	2864	3409			
FLEX HOSES	202	69	271	202	66	268
DEPLOYMENT MECHANISM	1216	340	1556	2260	306	2566
INTEGRATION AND TEST	975	401	1376	8087	579	8666
			20144			24691

TABLE 17 25 kW INTEGRAL MANIFOLD HEAT PIPE COST ANALYSIS

T_{IN} = 100, T_{OUT} = 40, T_S = -40°F

COST-THOUSANDS OF DOLLARS

COMPONENT	MULTIPLE (4, 8.33 kW) SUBSYSTEMS			SINGLE SUBSYSTEM		
	DEVELOPMENT	PRODUCTION	TOTAL	DEVELOPMENT	PRODUCTION	TOTAL
RADIATOR PANELS	2865	651	3516	2439	403	2842
HEAT PIPES	600	418	1018	600	297	897
HR LOOP PUMP	175	560	735	925	140	1065
COLLECTION LOOP PUMP	925	140	1065			
HR LOOP ACCUMULATOR	329	9	338	482	6	488
COLLECTION LOOP ACCUM.	410	5	415			
TEMPERATURE CONTROL VALVE	153	178	331	120	46	166
TEMPERATURE SENSOR	89	16	105	70	10	80
HEAT EXCHANGER	405	496	901			
FLEX HOSES	198	12	210	198	8	205
DEPLOYMENT MECHANISM	1191	84	1275	1680	38	1718
INTEGRATION AND TEST	731	93	833	1044	54	1099
			10742			8560

TABLE 18 50 kW INTEGRAL MANIFOLD HEAT PIPE COST ANALYSIS

T_{IN} = 100, T_{OUT} = 40, T_S = -40°F

COST-THOUSANDS OF DOLLARS

COMPONENT	MULTIPLE (5, 12.5 kW) SUBSYSTEMS			SINGLE SUBSYSTEM		
	DEVELOPMENT	PRODUCTION	TOTAL	DEVELOPMENT	PRODUCTION	TOTAL
RADIATOR PANELS	3260	1105	4365	2761	789	3550
HEAT PIPES	600	756	1356	600	589	1189
HR LOOP PUMP	175	700	875	1025	160	1185
COLLECTION LOOP PUMP	1025	160	1185			
HR LOOP ACCUMULATOR	421	14	435	721	10	731
COLLECTION LOOP ACCUM.	613	9	622			
TEMPERATURE CONTROL VALVE	153	214	367	120	46	166
TEMPERATURE SENSOR	89	17	106	70	10	80
HEAT EXCHANGER	545	853	1398	-		
FLEX HOSES	198	14	212	198	8	205
DEPLOYMENT MECHANISM	1216	102	1318	1680	72	1752
INTEGRATION AND TEST	975	203	1178	2080	125	2205
			13417			11063

TABLE 19 100 kW INTEGRAL MANIFOLD HEAT PIPE COST ANALYSIS

T_{IN} = 100, T_{OUT} = 40, T_S = -40°F

COST-THOUSANDS OF DOLLARS

COMPONENT	MULTIPLE (9, 12.5 kW) SUBSYSTEMS			SINGLE SUBSYSTEM		
	DEVELOPMENT	PRODUCTION	TOTAL	DEVELOPMENT	PRODUCTION	TOTAL
RADIATOR PANELS	3260	1812	5072	3041	1583	4624
HEAT PIPES	600	1361	1961	600	1183	1783
HR LOOP PUMP	175	1080	1255	1125	280	1405
COLLECTION LOOP PUMP	1125	280	1405			
HR LOOP ACCUMULATOR	421	23	444	979	16	995
COLLECTION LOOP ACCUM.	832	14	846			
TEMPERATURE CONTROL VALVE	153	349	502	120	46	166
TEMPERATURE SENSOR	89	19	108	70	10	80
HEAT EXCHANGER	545	1400	1945			
FLEX HOSES	202	23	225	202	31	233
DEPLOYMENT MECHANISM	1216	167	1383	1680	118	1798
INTEGRATION AND TEST	975	209	1184	3616	196	3812
			16330			14896

TABLE 20 250 kW INTEGRAL MANIFOLD HEAT PIPE COST ANALYSIS

T_{IN} = 100, T_{OUT} = 40, T_S = -40°F

COST-THOUSANDS OF DOLLARS

COMPONENT	MULTIPLE (21, 12.5 kW) SUBSYSTEMS			SINGLE SUBSYSTEM		
	DEVELOPMENT	PRODUCTION	TOTAL	DEVELOPMENT	PRODUCTION	TOTAL
RADIATOR PANELS	3260	3694	6954	3235	4317	7551
HEAT PIPES	600	3176	3776	600	3267	3867
HR LOOP PUMP	175	2200	2375	1225	400	1625
COLLECTION LOOP PUMP	1225	400	1625			
HR LOOP ACCUMULATOR	421	35	456	1724	35	1759
COLLECTION LOOP ACCUM.	1465	32	1497			
TEMPERATURE CONTROL VALVE	153	707	861	120	46	166
TEMPERATURE SENSOR	89	25	114	70	10	80
HEAT EXCHANGER	545	2864	3409			
FLEX HOSES	202	69	271	202	66	268
DEPLOYMENT MECHANISM	1216	340	1556	2240	292	2532
INTEGRATION AND TEST	975	401	1376	7290	546	7836
			24269			25684

TABLE 21 25 kW LOW TECHNOLOGY HEAT PIPE COST ANALYSIS

T_{IN} = 100, T_{OUT} = 40, T_S = -40°F

COST-THOUSANDS OF DOLLARS

COMPONENT	MULTIPLE (4, 8.33 kW) SUBSYSTEMS			SINGLE SUBSYSTEM		
	DEVELOPMENT	PRODUCTION	TOTAL	DEVELOPMENT	PRODUCTION	TOTAL
RADIATOR PANELS	3148	814	3962	2567	519	3086
HEAT PIPES	100	240	340	100	189	289
HR LOOP PUMP	175	560	735	925	140	1065
COLLECTION LOOP PUMP	925	140	1065			
HR LOOP ACCUMULATOR	329	9	338	482	6	488
COLLECTION LOOP ACCUM.	410	5	415			
TEMPERATURE CONTROL VALVE	153	178	331	120	46	166
TEMPERATURE SENSOR	89	16	105	70	10	80
HEAT EXCHANGER	405	496	901			
FLEX HOSES	198	12	210	198	8	205
DEPLOYMENT MECHANISM	1191	84	1275	1680	38	1718
INTEGRATION AND TEST	863	101	964	1245	63	1307
			10641			8404

TABLE 22 50 kW LOW TECHNOLOGY HEAT PIPE COST ANALYSIS

T_{IN} = 100, T_{OUT} = 40, T_S = -40°F

COST-THOUSANDS OF DOLLARS

COMPONENT	MULTIPLE (5, 12.5 kW) SUBSYSTEMS			SINGLE SUBSYSTEM		
	DEVELOPMENT	PRODUCTION	TOTAL	DEVELOPMENT	PRODUCTION	TOTAL
RADIATOR PANELS	4102	1402	5504	2810	1012	3822
HEAT PIPES	100	450	550	100	476	576
HR LOOP PUMP	175	700	875	1025	160	1185
COLLECTION LOOP PUMP	1025	160	1185			
HR LOOP ACCUMULATOR	421	14	435	721	10	731
COLLECTION LOOP ACCUM.	613	9	622			
TEMPERATURE CONTROL VALVE	153	214	367	120	46	166
TEMPERATURE SENSOR	89	17	106	70	10	80
HEAT EXCHANGER	545	853	1398			
FLEX HOSES	198	14	212	198	8	205
DEPLOYMENT MECHANISM	1216	102	1318	1620	72	1692
INTEGRATION AND TEST	1123	154	1277	2166	113	2279
			13849			10736

TABLE 23 100 kW LOW TECHNOLOGY HEAT PIPE COST ANALYSIS

T_{IN} = 100, T_{OUT} = 40, T_S = -40°F

COST-THOUSANDS OF DOLLARS

COMPONENT	MULTIPLE (9, 12.5 kW) SUBSYSTEMS			SINGLE SUBSYSTEM		
	DEVELOPMENT	PRODUCTION	TOTAL	DEVELOPMENT	PRODUCTION	TOTAL
RADIATOR PANELS	4102	2302	6403	3176	1961	5138
HEAT PIPES	100	810	910	100	1079	1176
HR LOOP PUMP	175	1080	1255	1125	280	1405
COLLECTION LOOP PUMP	1125	280	1405			
HR LOOP ACCUMULATOR	421	23	444	979	16	995
COLLECTION LOOP ACCUM.	832	14	846			
TEMPERATURE CONTROL VALVE	153	349	502	120	46	166
TEMPERATURE SENSOR	89	19	108	70	10	80
HEAT EXCHANGER	545	1400	1945			
FLEX HOSES	202	23	225	202	31	233
DEPLOYMENT MECHANISM	1216	167	1383	1620	124	1744
INTEGRATION AND TEST	1123	235	1358	3870	233	4103
			16784			15040

TABLE 24 250 kW LOW TECHNOLOGY HEAT PIPE COST ANALYSIS

T_{IN} = 100, T_{OUT} = 40, T_S = -40°F

COST-THOUSANDS OF DOLLARS

COMPONENT	MULTIPLE (21, 12.5 kW) SUBSYSTEMS			SINGLE SUBSYSTEM		
	DEVELOPMENT	PRODUCTION	TOTAL	DEVELOPMENT	PRODUCTION	TOTAL
RADIATOR PANELS	4102	4698	8800	4529	4614	9143
HEAT PIPES	100	1890	1990	100	3040	3140
HR LOOP PUMP	175	2200	2375	1225	400	1625
COLLECTION LOOP PUMP	1225	400	1625			
HR LOOP ACCUMULATOR	421	35	456	1724	35	1759
COLLECTION LOOP ACCUM.	1465	32	1497			
TEMPERATURE CONTROL VALVE	153	707	861	120	46	166
TEMPERATURE SENSOR	89	25	114	70	10	80
HEAT EXCHANGER	545	2864	3409			
FLEX HOSES	202	69	271	202	66	268
DEPLOYMENT MECHANISM	1216	340	1556	1620	180	1800
INTEGRATION AND TEST	1123	451	1574	7803	503	8306
			24528			26287

TABLE 25

POWER SYSTEM BODY SINK TEMPERATURE

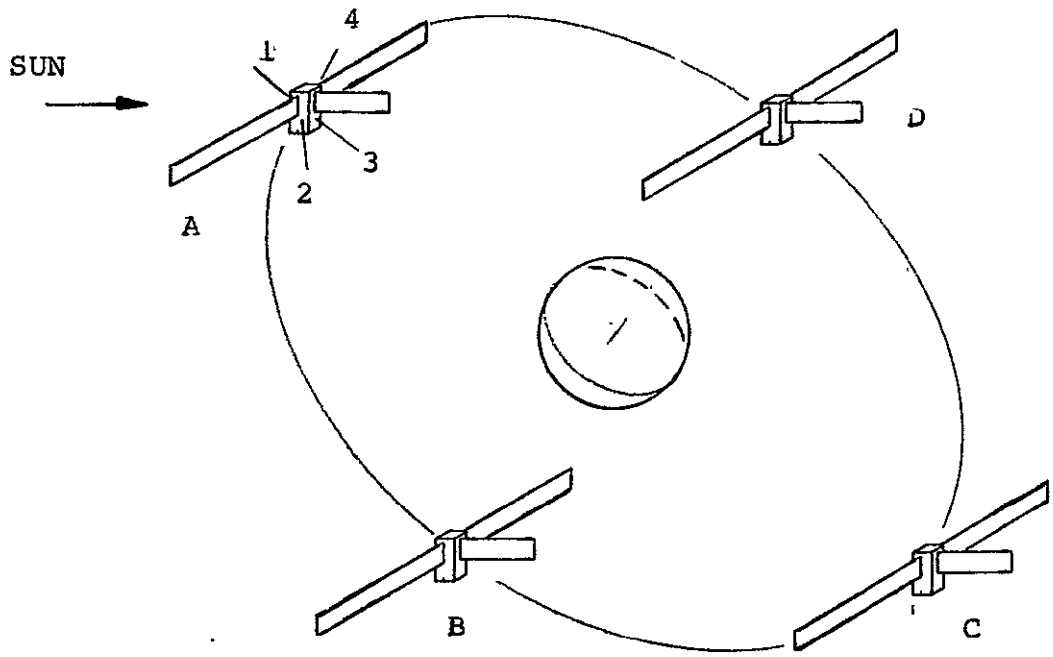

α = .1

ε = .8

β = 55°

270 N.M.

SINK TEMP - °F

ORBIT POSITION	SIDE			
	1	2	3	4
A	-20	- 8	- 3	- 8
B	11	46	-13	- 8
C	-55	- 5	-31	- 5
D	-20	- 8	-34	46

DARK SIDE DESIGN T_{SINK} = - 4°F

SUN SIDE = + 12°F

TABLE 26

WEIGHT COMPARISON OF BODY MOUNTED HEAT PIPE AND FLUID LOOP TCS

Total Heat Load = 25 kW
Tin = 100°F, Tout = 40°F
Weight-Lb

Sink Temperature - °F	TCS	FLUID LOOP CONCEPT		
		Pumped Fluid	Low Cost Hybrid	Int. Manifold Hybrid
-80°F Fluid Loop	16.5 kW Fluid Loop	770	870	760
-10°F BMHP	8.5 kW BMHP	495	495	495
		1265	1365	1255
-80°F Fluid Loop	16.5 kW Fluid Loop	770	870	760
10°F BMHP	8.5 kW BMHP	570	570	570
		1340	1440	1330
-80°F Fluid Loop	25 kW Fluid Loop	1160	1290	1110
-40°F Fluid Loop	16.5 kW Fluid Loop	915	1040	930
-10°F BMHP	8.5 kW BMHP	495	495	495
		1410	1535	1425
-40°F Fluid Loop	16.5 kW Fluid Loop	915	1040	930
10°F BMHP	8.5 kW BMHP	570	570	570
		1485	1610	1500
-40°F Fluid Loop	25 kW Fluid Loop	1421	1549	1390

TABLE 27

COST COMPARISON OF BODY MOUNTED HEAT PIPE AND FLUID LOOP TCS

COST - MILLIONS OF DOLLARS

TCS	RADIATOR CONCEPT		
	Pumped Fluid	Low Tech Hybrid	Int. Manifold Hybrid
16.5 kW Fluid Loop	6.40	7.45	7.65
8.5 kW BMHP	5.15 - 2.56	5.15 - 2.56	5.15 - 2.56
	11.55 - 8.96	12.60 - 10.01	12.80 - 10.21
25 kW Fluid Loop	7.25	8.56	8.34

TABLE 28 CENTRALIZED AND DISTRIBUTED TCS COST BREAKDOWN

	PROCUREMENT COST - $M			LAUNCH COST - $M		TOTAL COST - $M
	DEV	PRODUCTION	TOTAL	SINGLE LAUNCH	20 LAUNCHES	SINGLE LAUNCH/20 LAUNCHES
CENTRALIZED TCS						
37 kW P/S	7.04	0.98	8.02	1.547		9.57/9.57
DISTRIBUTED TCS						
12 kW P/S TCS	6.03	0.27	6.3	0.476	0.476	
25 kW P/L						
Rad Panels	2.19	0.812	3.00	0.847	16.94	
Rad Deploy	1.68	0.076	1.76			
TCV	0.12	0.092	0.21			
	10.02	1.25	11.27	1.323	17.416	12.59/28.69
17 kW P/S TCS	6.23	0.47	6.70	0.665	0.665	
20 kW P/L						
Rad Panels	2.15	0.700	2.85	0.672	13.44	
Rad Deploy	1.42	0.064	1.48			
TCV	0.12	0.092	0.21			
	9.92	1.326	11.24	1.337	14.105	12.58/25.35
22 kW P/S TCS	6.43	0.57	7.0	0.847	0.847	
15 kW P/L						
Rad Panels	2.13	0.56	2.69	0.501	10.01	
Rad Deploy	1.26	0.054	1.31			
TCV	0.12	0.092	0.21			
	9.94	1.296	11.21	1.348	10.857	12.56/22.07
27 kW P/L TCS	6.64	0.71	7.35	1.064	1.064	
10 kW P/L						
Rad Panels	2.11	0.48	2.59	0.340	6.79	
Rad Deploy	1.20	0.044	1.24			
TCV	0.12	0.092	0.21			
	10.07	1.326	11.39	1.404	7.85	12.79/19.25
32 kW P/S TCS	6.84	0.86	7.70	1.302	1.302	
5 kW P/L						
Rad Panels	2.10	0.36	2.46	0.174	3.472	
Rad Deploy	-	-	-			
TCV	0.12	0.092	0.21			
	9.06	1.312	10.37	1.476	4.77	11.85/15.14

TABLE 29

POWER SYSTEM/PAYLOAD FLUID INTERFACE CONCEPT SUMMARY

CONCEPT	ADVANTAGES	DISADVANTAGES
DIRECT FLUID CONNECTION	• BEST THERMAL EFFICIENCY • LIGHTEST WEIGHT • LOW COST • HIGH RELIABILITY ELIMINATES PUMPS	• LIMITS P/L RETURN TEMP TO 100°F • SOPHISTICATED HEAT REJECTION CONTROL • VARIABLE LOOP ΔP
FLUID/FLUID HEAT EXCHANGER	• ALLOWS HIGH TEMP PAYLOADS • SIMPLIFIED HEAT REJECTION CONTROL • THERMALLY EFFICIENT • STATE-OF-THE-ART TECH • LIGHTWEIGHT • ALLOWS INDEPENDENT P/L LOOP DESIGN	• FULL CAPACITY REQD AT EACH PORT • REQUIRES P/L PUMP
CONTACT HEAT EXCHANGER	• ELIMINATES FLUID CONNECTIONS & LEAKAGE POTENTIAL • ALLOWS ALL HEAT PIPE TCS FOR PAYLOADS • ALLOWS HIGH TEMP PAYLOADS • SIMPLIFIED HEAT REJECTION CONTROL • ALLOWS INDEPENDENT P/L LOOP DESIGN	• HIGHER TEMP DROP • FULL CAPACITY REQD AT EACH PORT • REQUIRES DEVELOPMENT • REQUIRES P/L PUMP • HEAVY

TABLE 30 RADIATOR DEPLOYMENT CONCEPT TRADE MATRIX

	DEPLOYMENT CONCEPT			
	POWER HINGE[1]	SCISSORS[2]	SPRING HINGE[3]	TELESCOPING BOOM[4]
WEIGHT - LB	159	440	163	194
SOLAR AVOIDANCE WT.	42	42	42	-
RETRACTED STACK HEIGHT - IN.	13.5	18.0	13.5	26.0
ELECTRIC MOTORS REQUIRED	9	1	1	1
MOTOR RELIABILITY WITH REDUNDANCY	0.9829	0.9995	0.9995	0.9995
MECHANICAL COMPLEXITY*	6	7	3	8
RELATIVE COST*	7	5	3	6

COMMENTS:

1 - . SIMILAR TO ORBITER DOOR/RAD DEPLOYMENT
. ALLOWS ONE PANEL AT A TIME TO BE DEPLOYED/RETRACTED
. RELIABILITY DECREASES FOR ADDITIONAL PANELS

2 - . SIMILAR TO SKYLAB SOLAR PANEL DEPLOYMENT
. CANNOT INCORPORATE SOLAR AVOIDANCE DUE TO INTERFERENCE WITH SOLAR ARRAYS

3 - . SYSTEM NATURAL FREQUENCY LOWER THAN ESTIMATED 0.1 Hz ALLOWED

4 - . SIMILAR TO SOLAR ARRAY MAST USED ON REFERENCE 25 kW POWER SYSTEM
. POSSIBLE USE OF COMMON HARDWARE
. EXCESSIVE STOWAGE VOLUME

*1 = LEAST, 10 = MOST

TABLE 31 BASE PIVOT ATTACHMENT LOADS FOR MANEUVER*

LOCATION		F_X (LBS)	F_Y (LBS)	F_Z (LBS)	M_X (IN-LBS)	M_Y (IN-LBS)	M_Z (IN-LBS)
FULLY DEPLOYED	(1)	-136	-4	150	-405	-1060	- 409
	(2)	136	-4	150	-405	1060	409
	(3)	65	-3	-150	-408	473	1892
	(4)	- 65	-3	-150	-408	- 473	-1892
PARTIALLY DEPLOYED	(1)	9	-4	116	354	308	10
	(2)	- 9	-4	116	354	- 308	- 10
	(3)	- 12	-3	-116	350	170	- 279
	(4)	12	-3	-116	350	- 170	279

TABLE 32 SCISSORS I-BEAM BOLT ATTACHMENT LOADS FOR MANEUVER*

LOCATION		F_X (LBS)	F_Y (LBS)	F_Z (LBS)	M_X (IN-LBS)	M_Y (IN-LBS)	M_Z (IN-LBS)
FULLY DEPLOYED	(5)	-30	146	24	0	33	541
	(6)	30	-256	-47	0	-41	718
PARTIALLY DEPLOYED	(5)	12	8	9	0	14	-552
	(6)	-13	-8	-19	0	-21	82

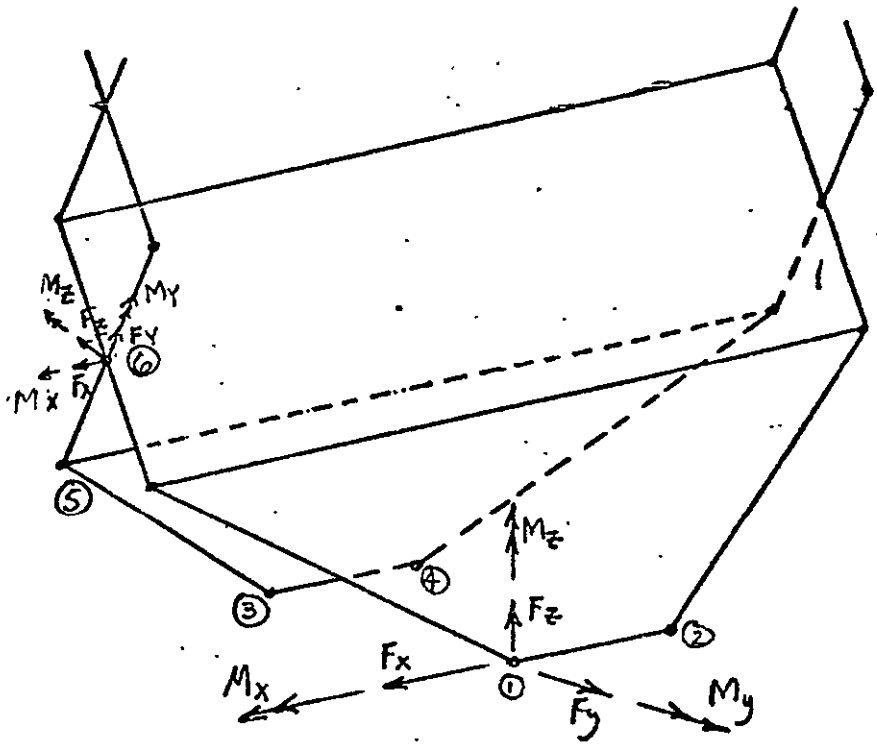

*NOTE: ACCELERATIONS AT POWER MODULE CG:

$\eta_y = .01g$

$\ddot{\theta}_x = -.01 \frac{DEG}{SEC^2}$

LOADS ARE LIMIT.

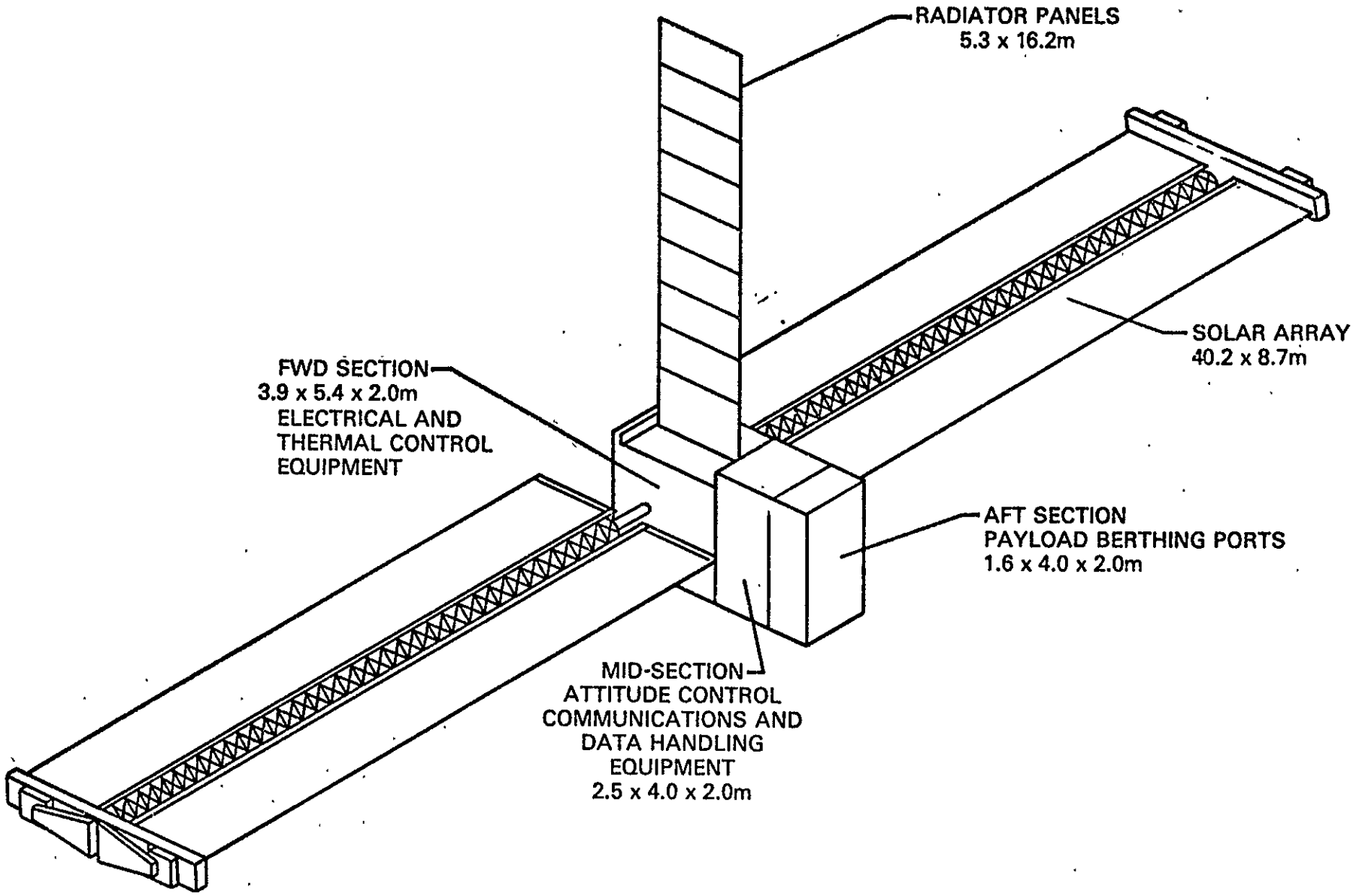

FIGURE 1 25kW POWER SYSTEM REFERENCE CONCEPT

FIGURE 2

FLUID LOOP CONCEPTS

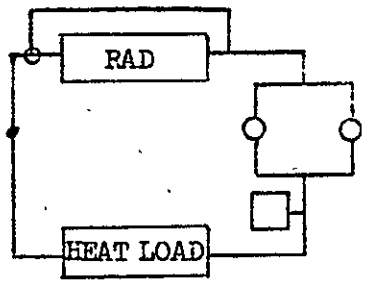

SINGLE LOOP

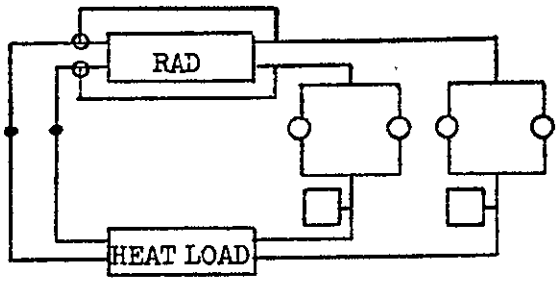

DUAL LOOP (ONE STANDBY)

REDUNDANT COMPONENTS

PUMPS	- 3, 2 REQD (ORBITER) 2, 1 REQD
TEMP SENSOR	- 3 OPERATE, 2 REQD (MAJORITY VOTE)
TEMP CONTROL VALVE	- 2 OPERATE, 1 REQD
ACCUMULATOR	- 2 OPERATE, 1 REQD

MAINTENANCE

PUMPS
TEMP SENSOR
TEMP CONTROL VALVE
ACCUMULATOR

FIGURE 3

REDUNDANT TEMPERATURE CONTROL VALVE

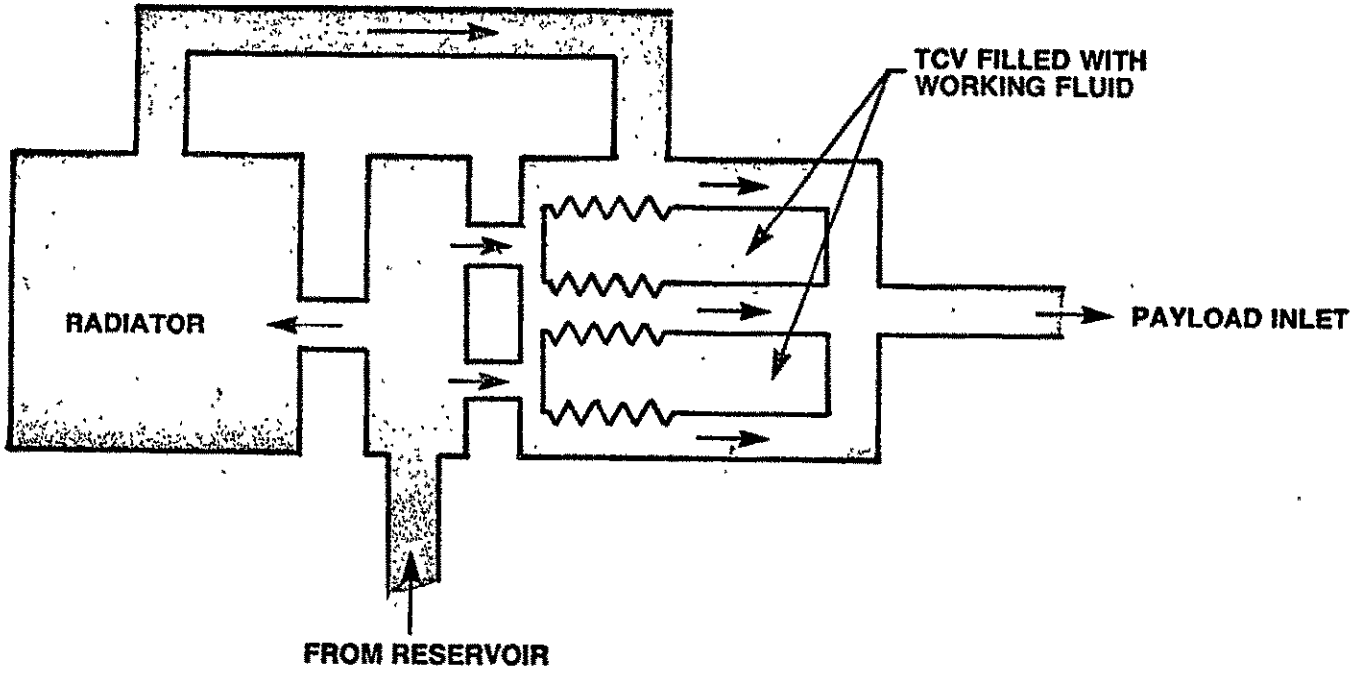

FAILURE RATE = $0.00498/10^6$ HRS

Sundstrand Energy Systems

FIGURE 4

REDUNDANT BELLOWS ACCUMULATOR

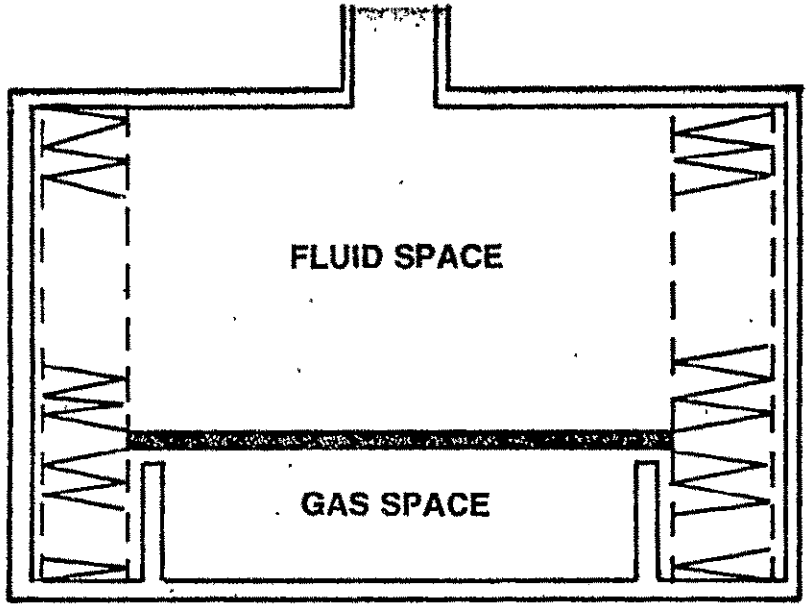

FAILURE RATE = $0.00085/10^6$ HRS

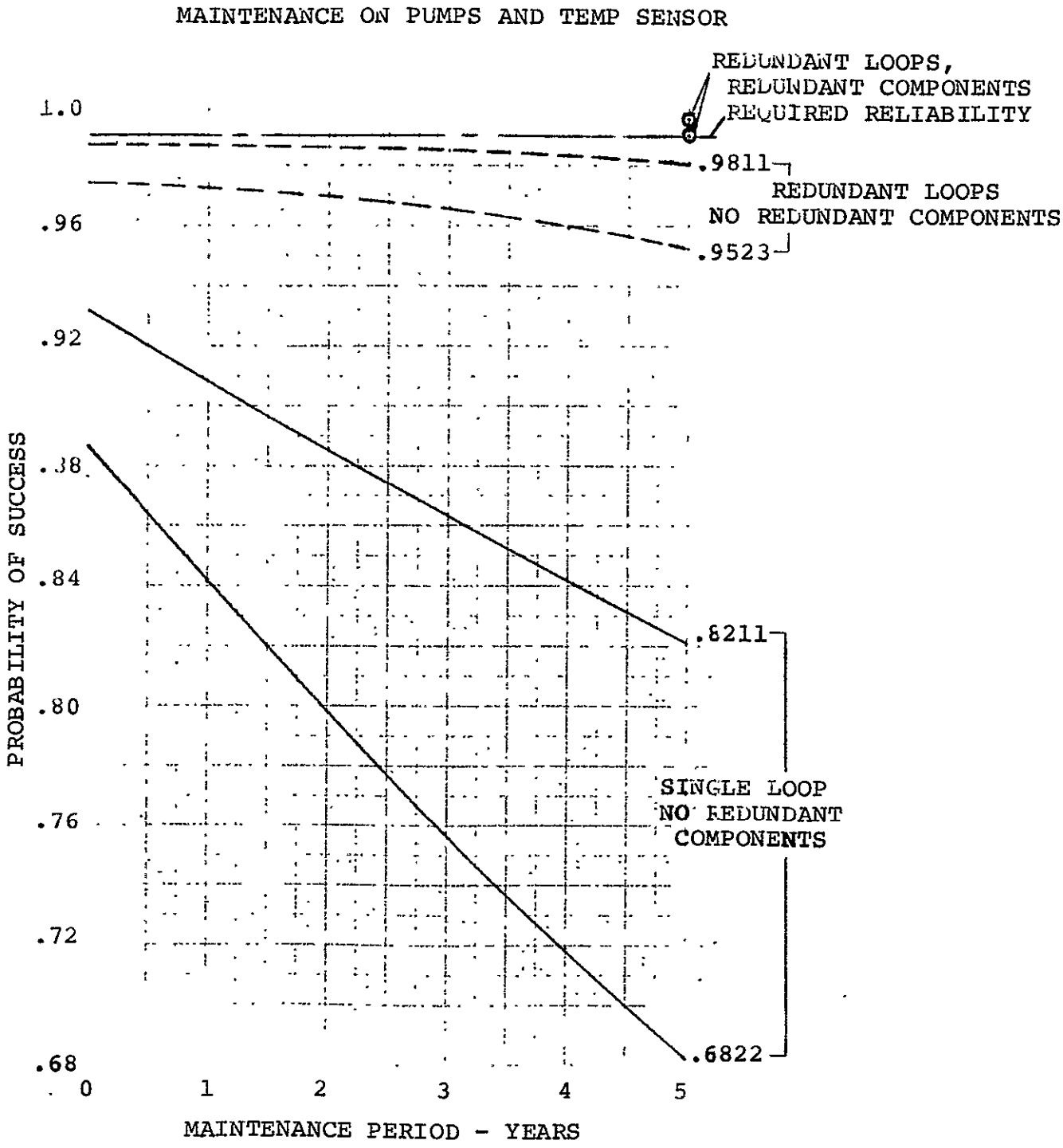

FIGURE 5 EFFECT OF MAINTENANCE ON FLUID LOOP RELIABILITY

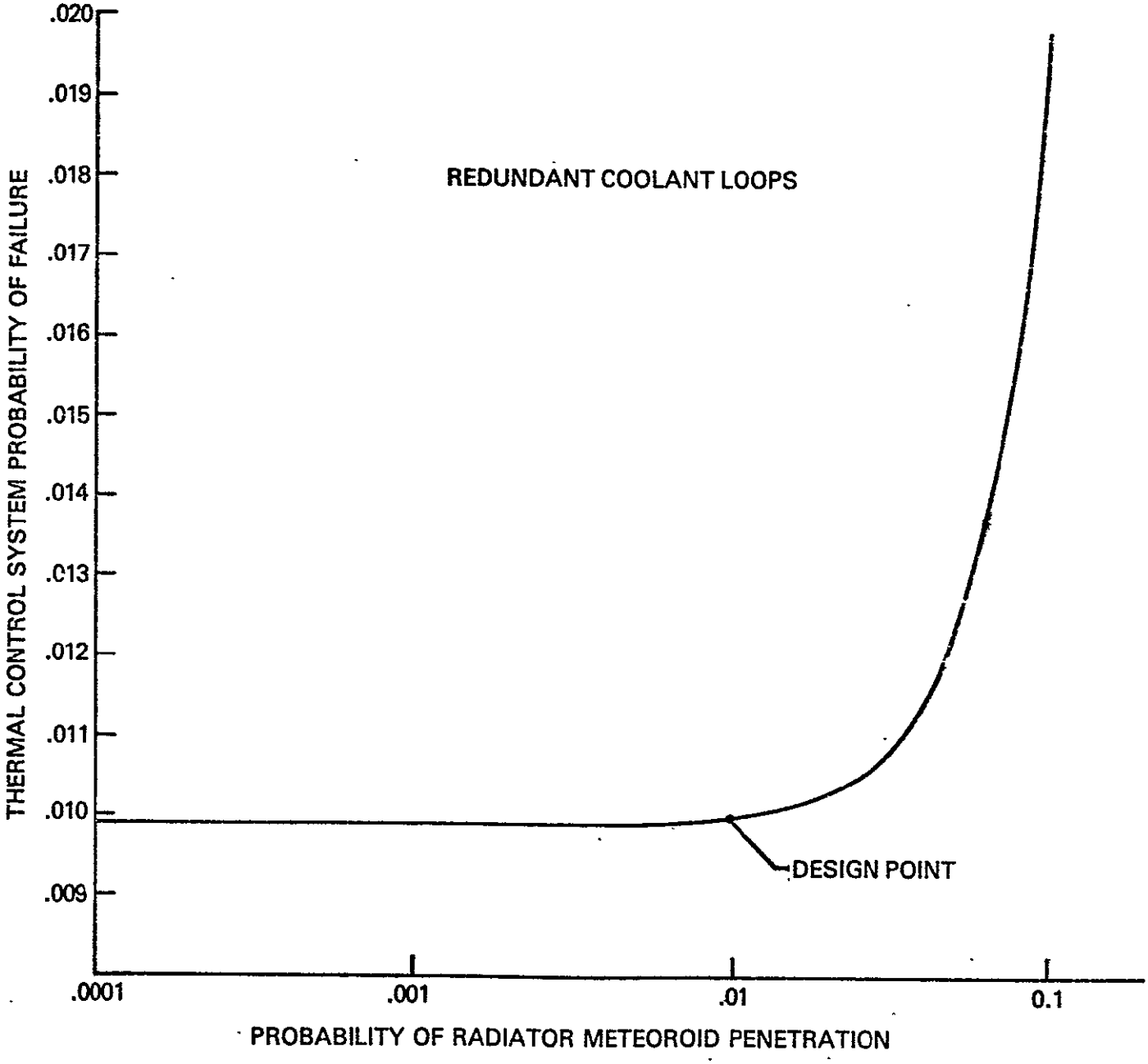

FIGURE 6. EFFECT OF RADIATOR METEOROID RELIABILITY ON THERMAL CONTROL SYSTEM RELIABILITY

VOUGHT

VOUGHT

COOLANT LOOP CONFIGURATION 2
FOR HEAT PIPE/PUMPED FLUID
RADIATOR TRADES

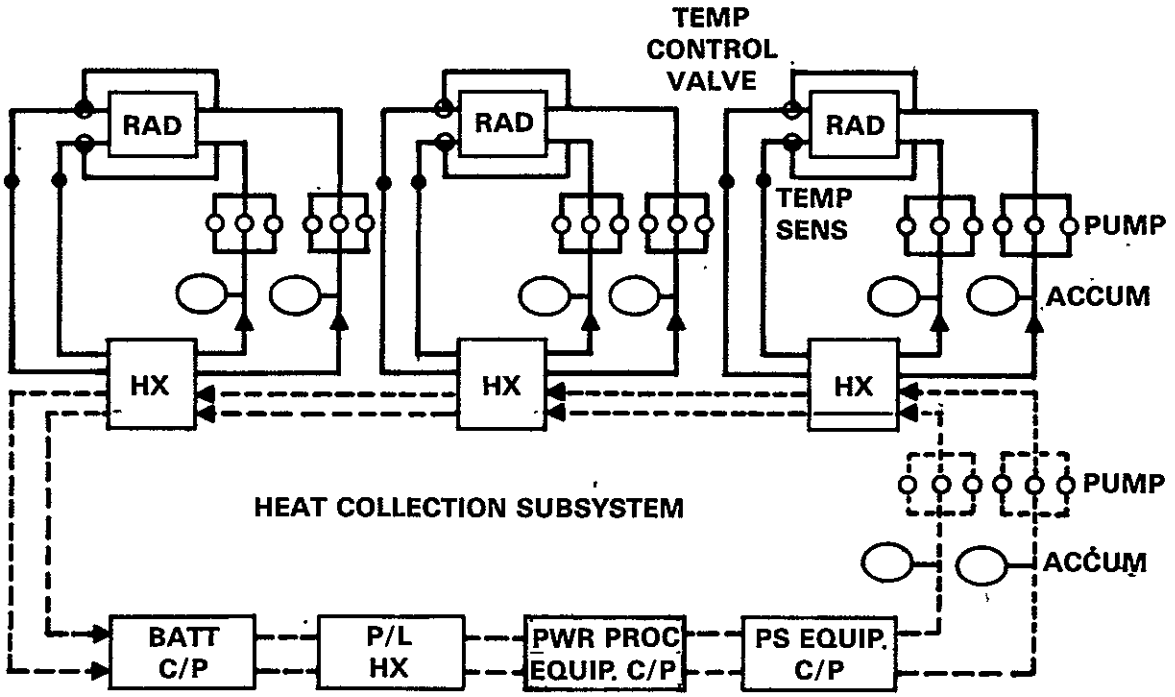

HEAT REJECTION SUBSYSTEM
P_O = 0.9931 -0.9830, OVERSIZED FOR $P_O \geq 0.995$
HEAT COLLECTION SUBSYSTEM P_O = 0.995
TOTAL SYSTEM P_O = 0.99

MULTIPLE SUBSYSTEMS SCHEMATIC

G0-1078-1

FIGURE 7

(a) EXTRUDED BUMPERED TUBE

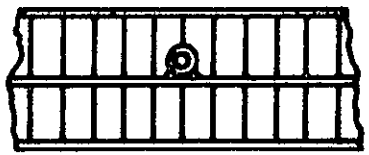

(c) BONDED HONEYCOMB/TUBE WITH BUMPER EFFECT

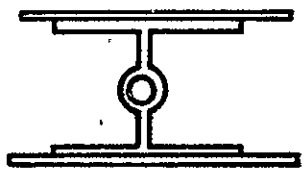

(b) EXTRUDED TUBE/DOUBLE FIN WITH BUMPER EFFECT

(d) EXTRUDED TUBE/BONDED HONEYCOMB WITH BUMPER EFFECT

FIGURE 8

CANDIDATE PUMPED FLUID TUBE/FIN PANEL CROSS-SECTIONS

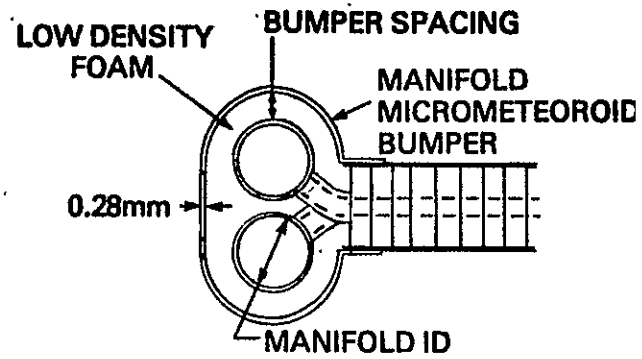

B) A-A, MANIFOLD DETAIL

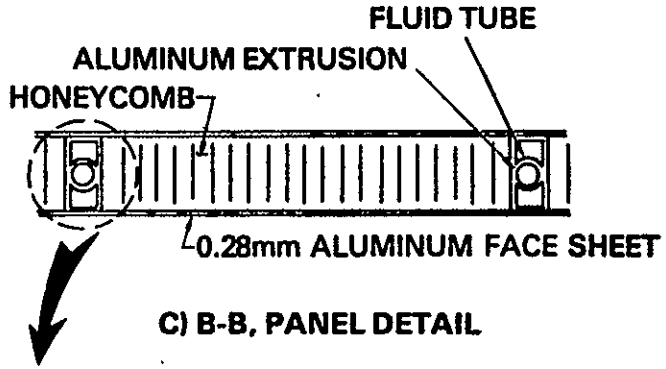

C) B-B, PANEL DETAIL

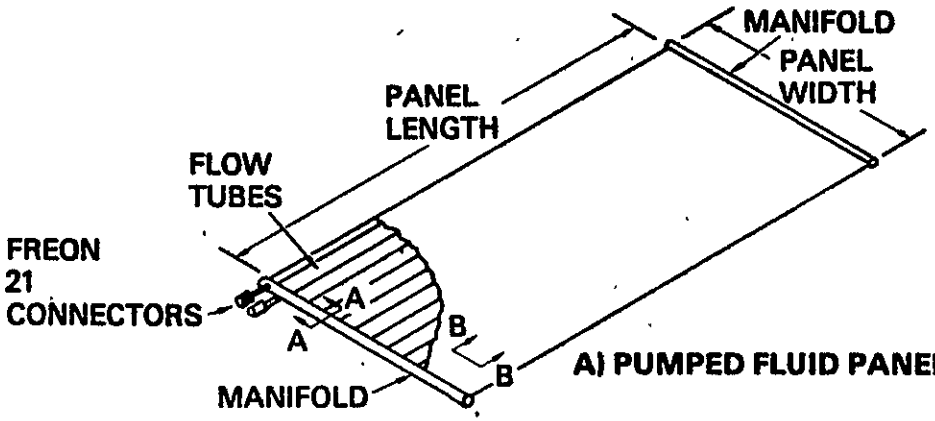

A) PUMPED FLUID PANEL

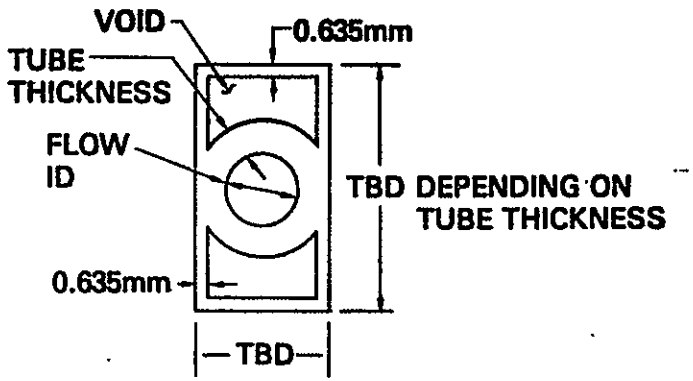

D) EXTRUDED TUBE DETAILS

FIGURE 9

PUMPED FLUID RADIATOR CONCEPT

(a) HEAT PIPE/FORMED SHEET

(b) HEAT PIPE EXTRUSION/FLAT SHEET

(c) HEAT PIPE/BONDED HONEYCOMB

FIGURE 10 CANDIDATE HYBRID PANEL CROSS-SECTIONS

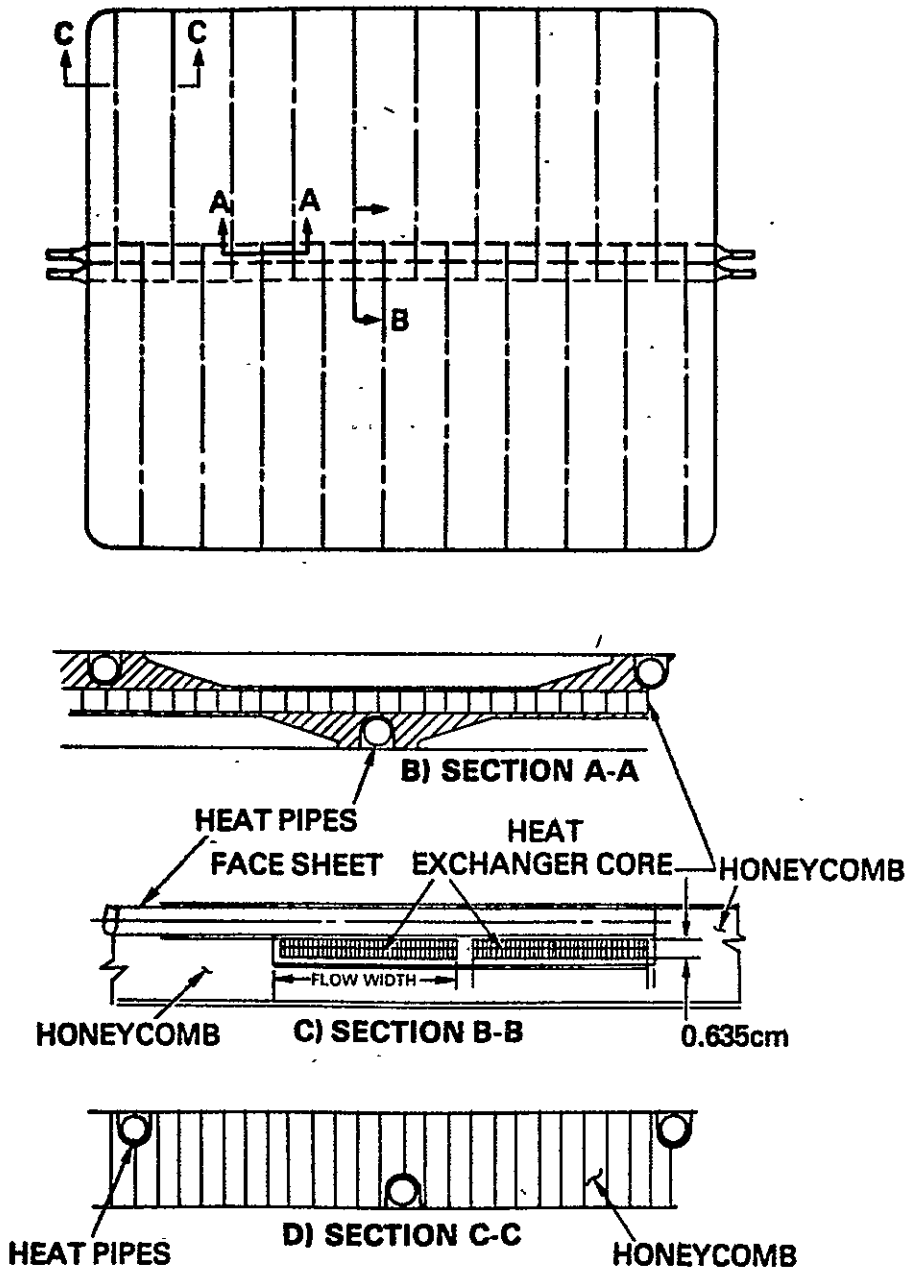

FIGURE 11

LOW COST HYBRID HEAT PIPE CONCEPT

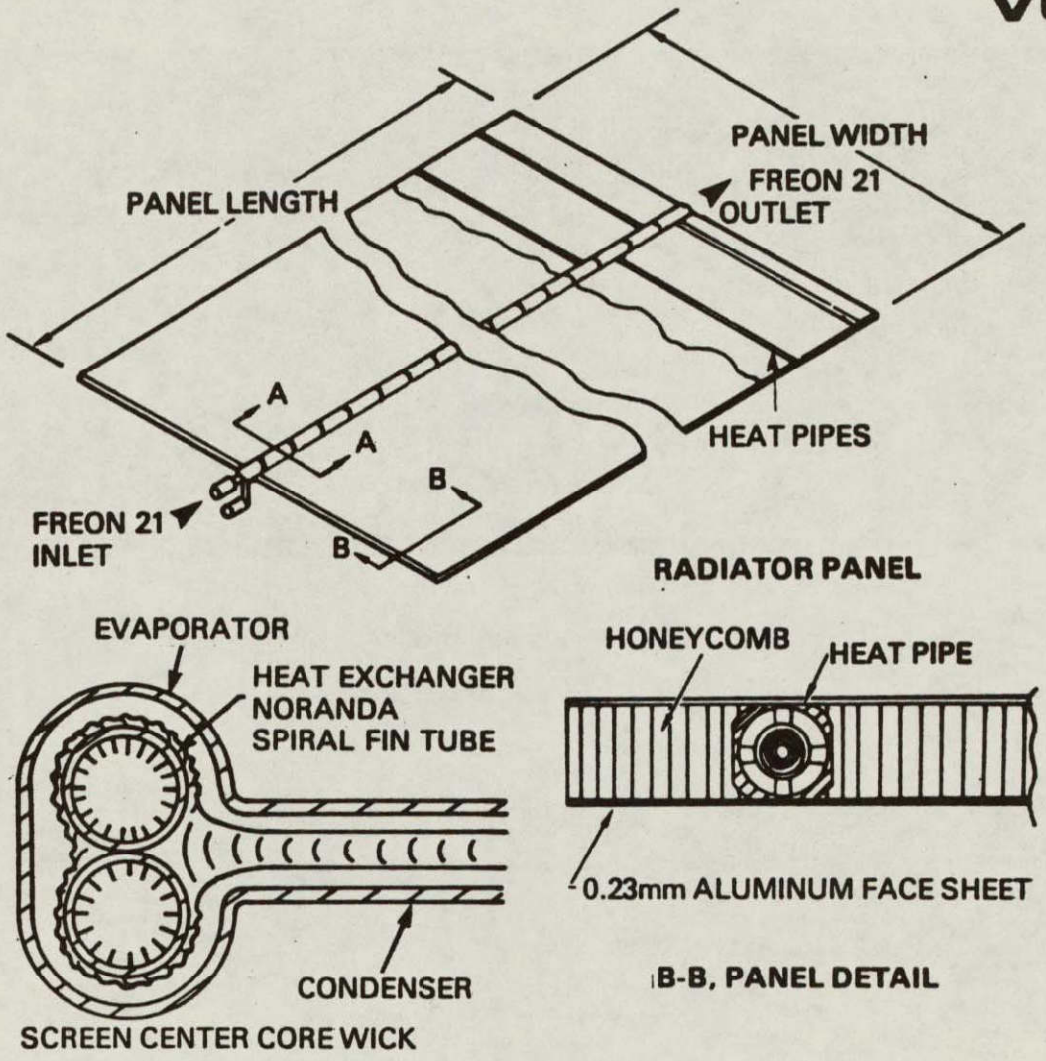

FIGURE 12

INTEGRAL MANIFOLD HEAT PIPE RADIATOR CONCEPT

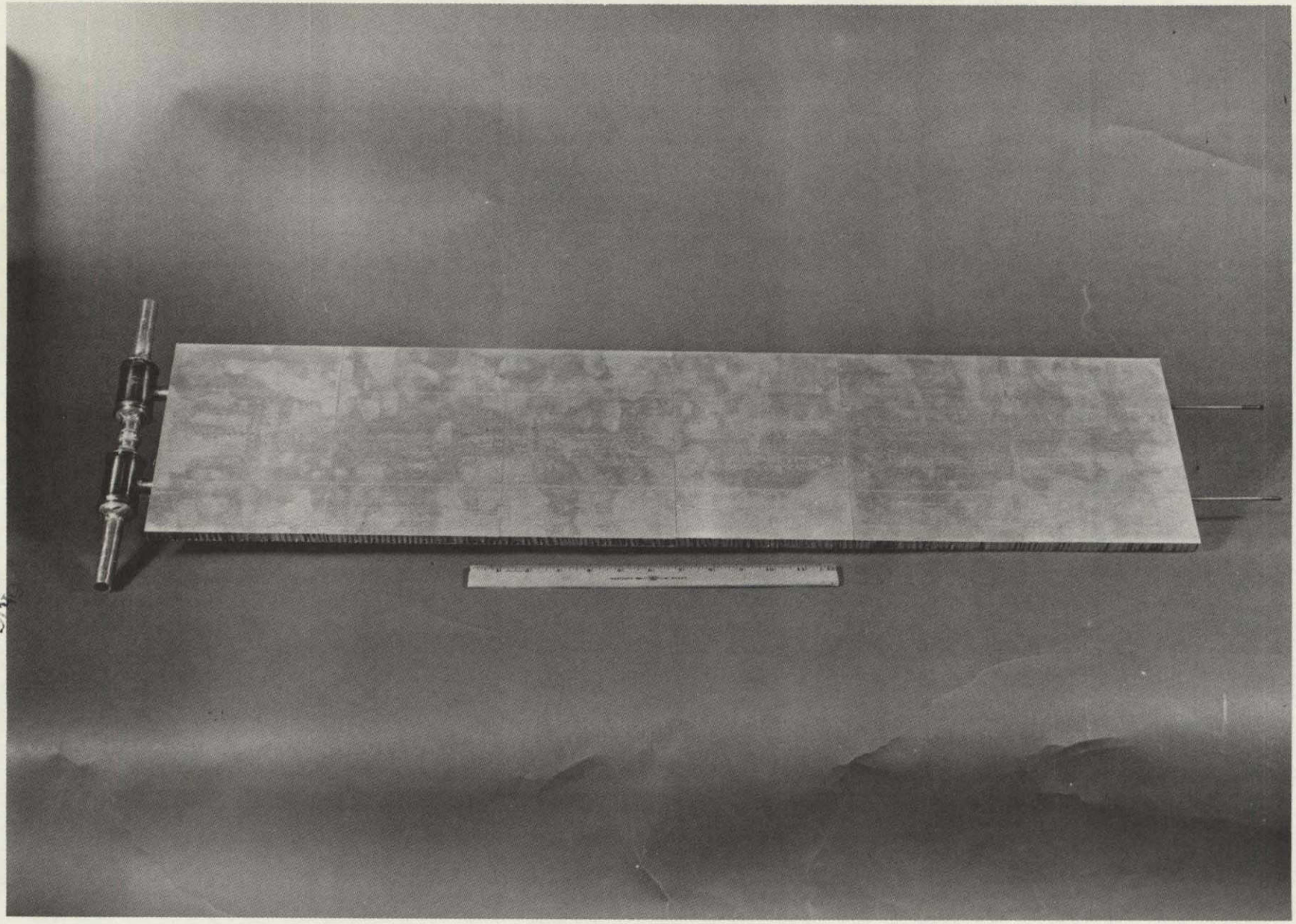

FIGURE 13 INTEGRAL MANIFOLD TEST ELEMENT

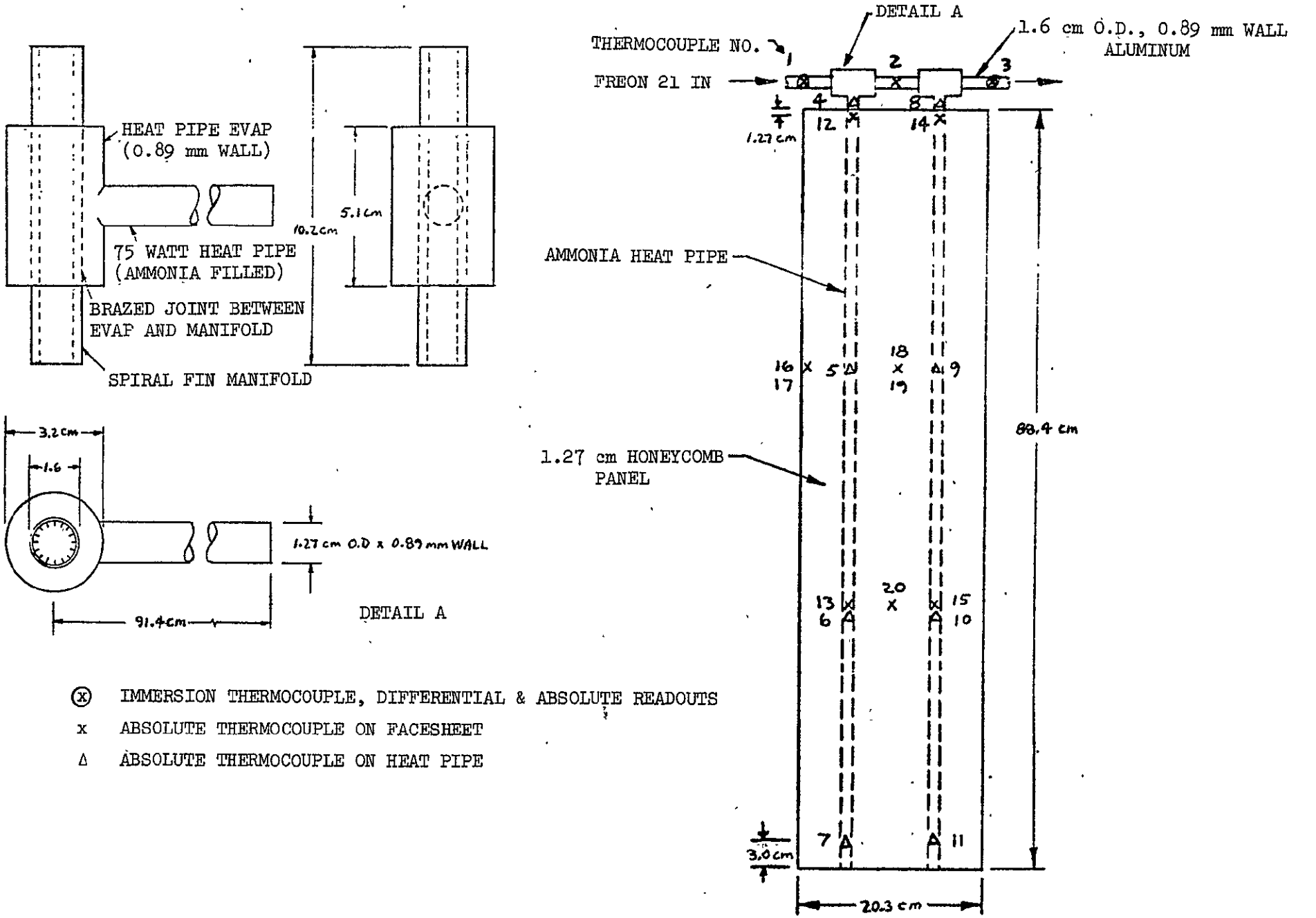

FIGURE 14 HYBRID INTEGRAL MANIFOLD TEST ELEMENT DESIGN

FIGURE 15
EFFECT OF HEAT PIPE DIAMETER
ON RADIATOR WEIGHT

1b kW HEAT LOAD, Tin = 100°F, Tout = 40°F, Ts = -40°F

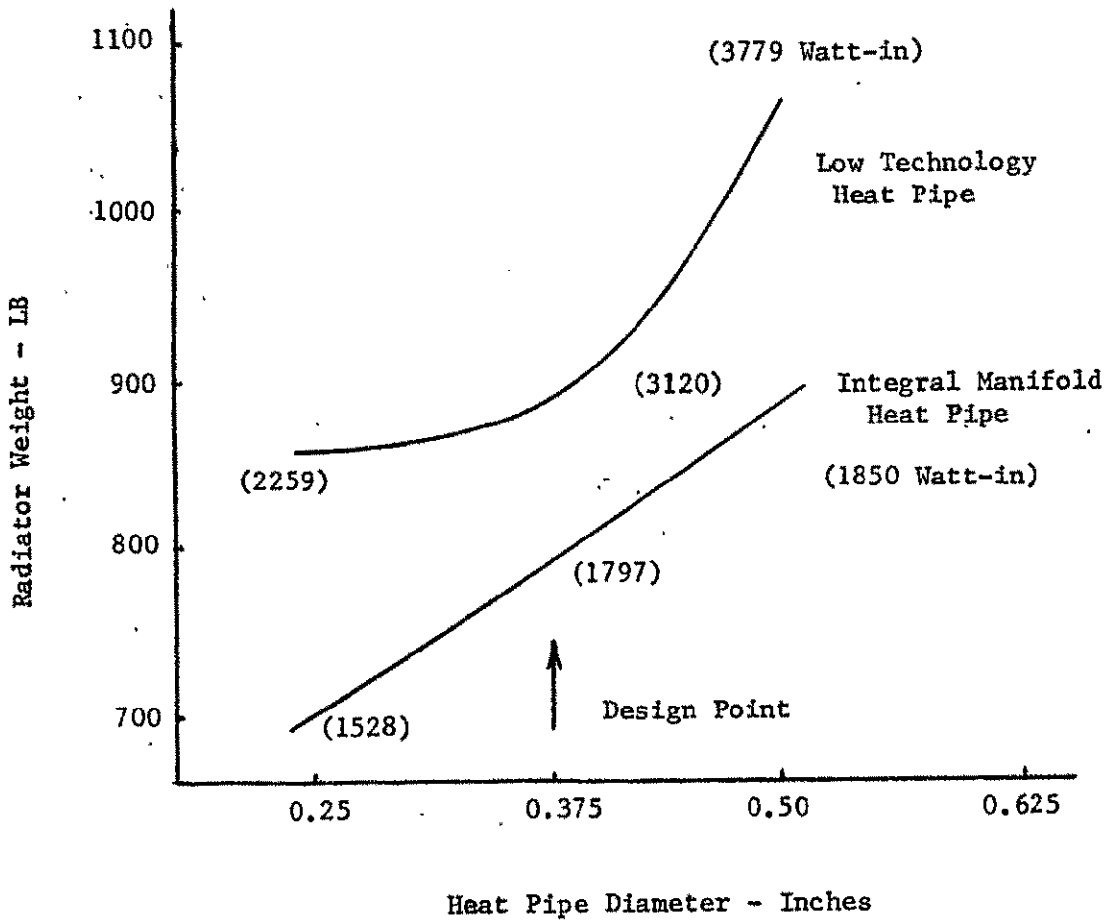

VOUGHT

FIGURE 16

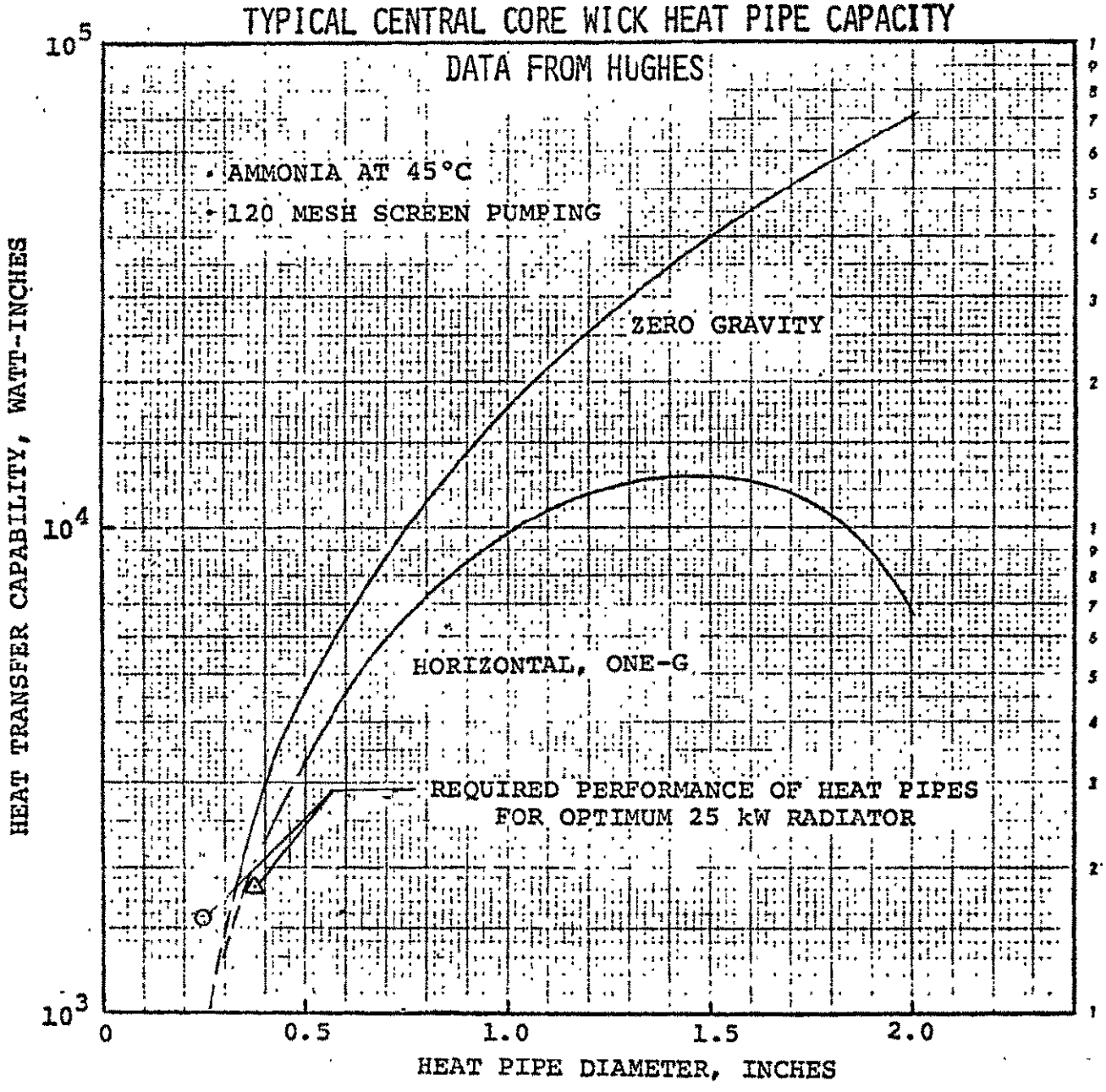
TYPICAL CENTRAL CORE WICK HEAT PIPE CAPACITY
DATA FROM HUGHES
AMMONIA AT 45°C
120 MESH SCREEN PUMPING
ZERO GRAVITY
HORIZONTAL, ONE-G
REQUIRED PERFORMANCE OF HEAT PIPES
FOR OPTIMUM 25 kW RADIATOR
HEAT TRANSFER CAPABILITY, WATT-INCHES
HEAT PIPE DIAMETER, INCHES
10^5
10^4
10^3
0
0.5
1.0
1.5
2.0

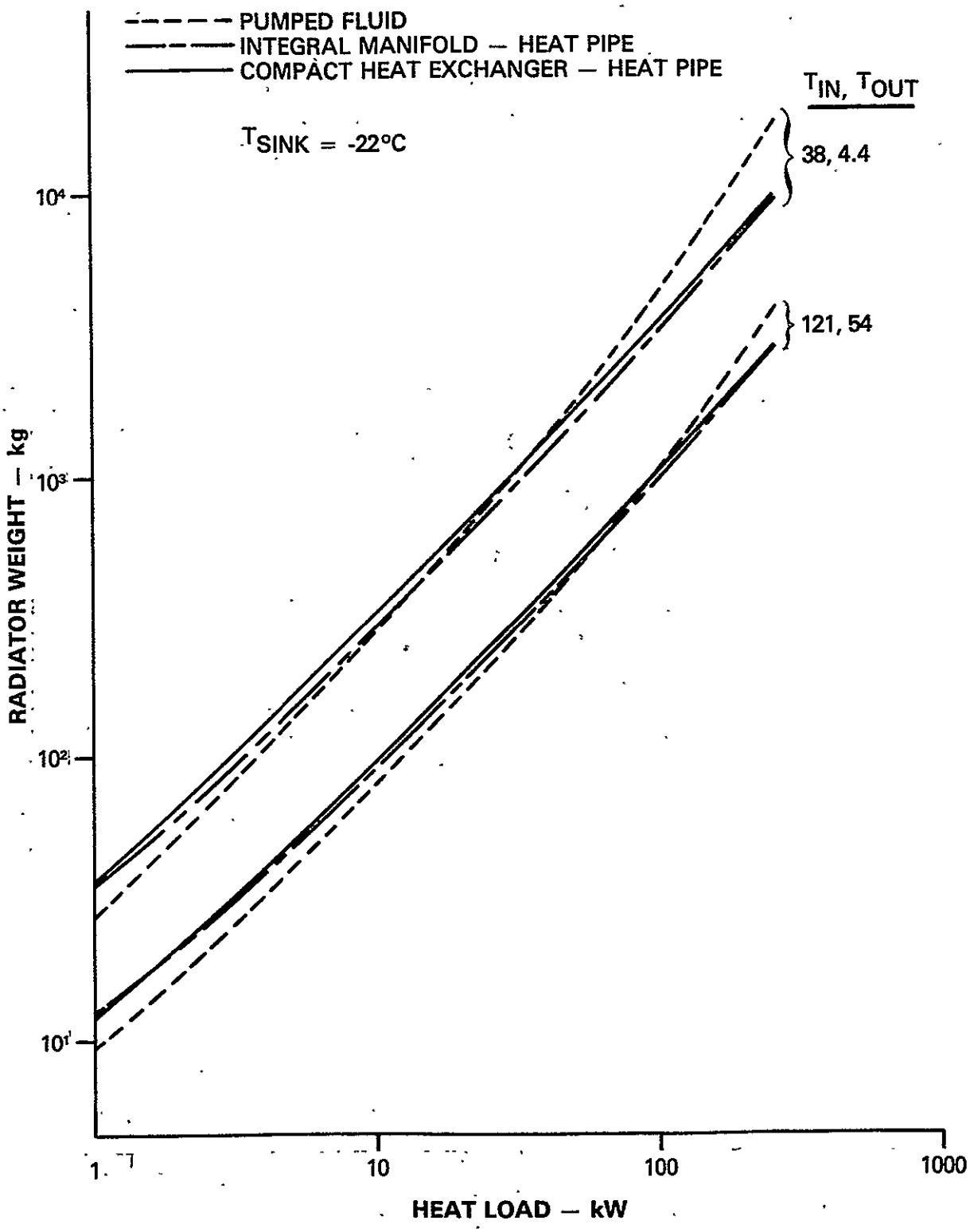

FIGURE 17 RADIATOR WEIGHT OPTIMIZATION, T_{SINK} = -22°C

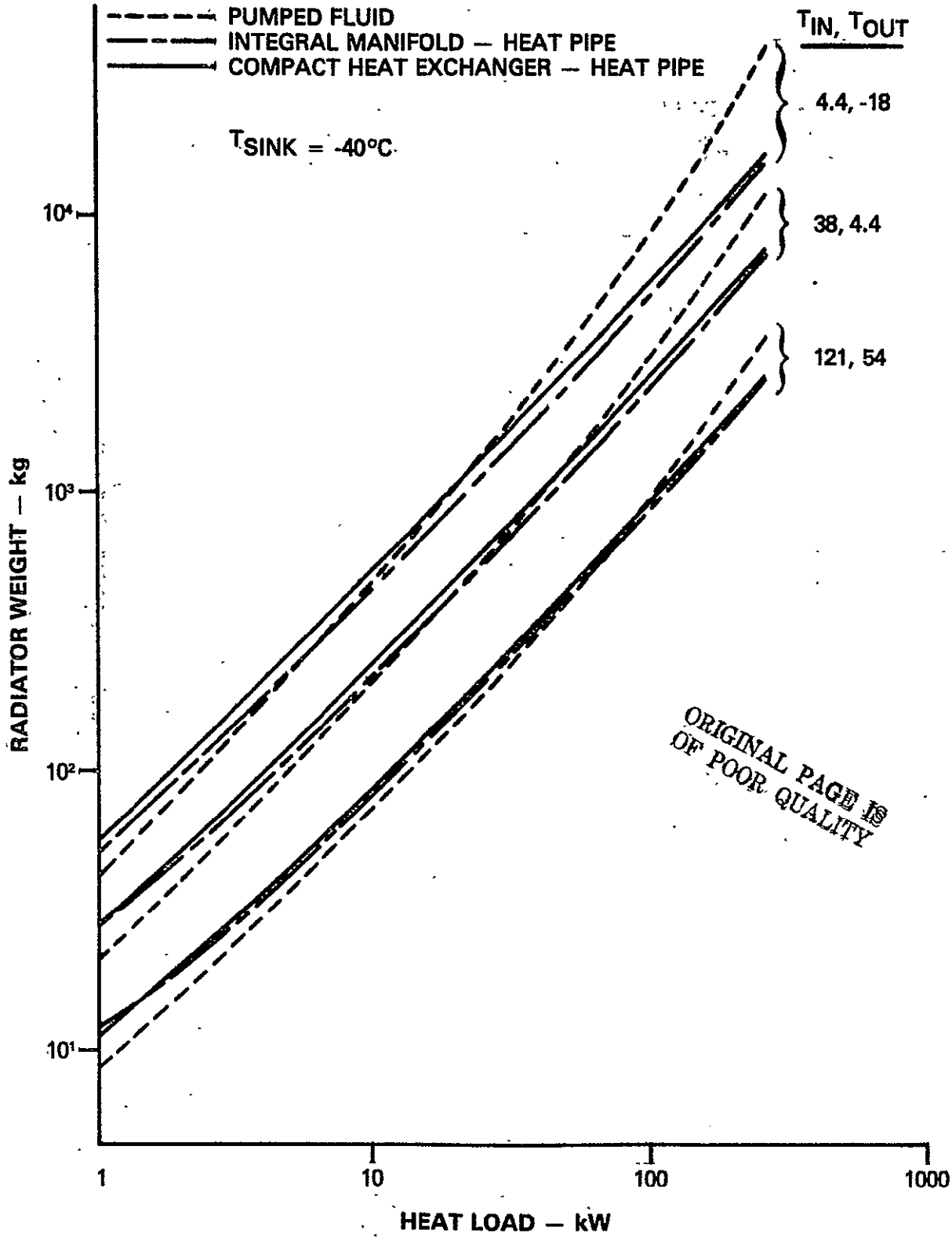

FIGURE 18 RADIATOR WEIGHT OPTIMIZATION, T_{SINK} = -40°C

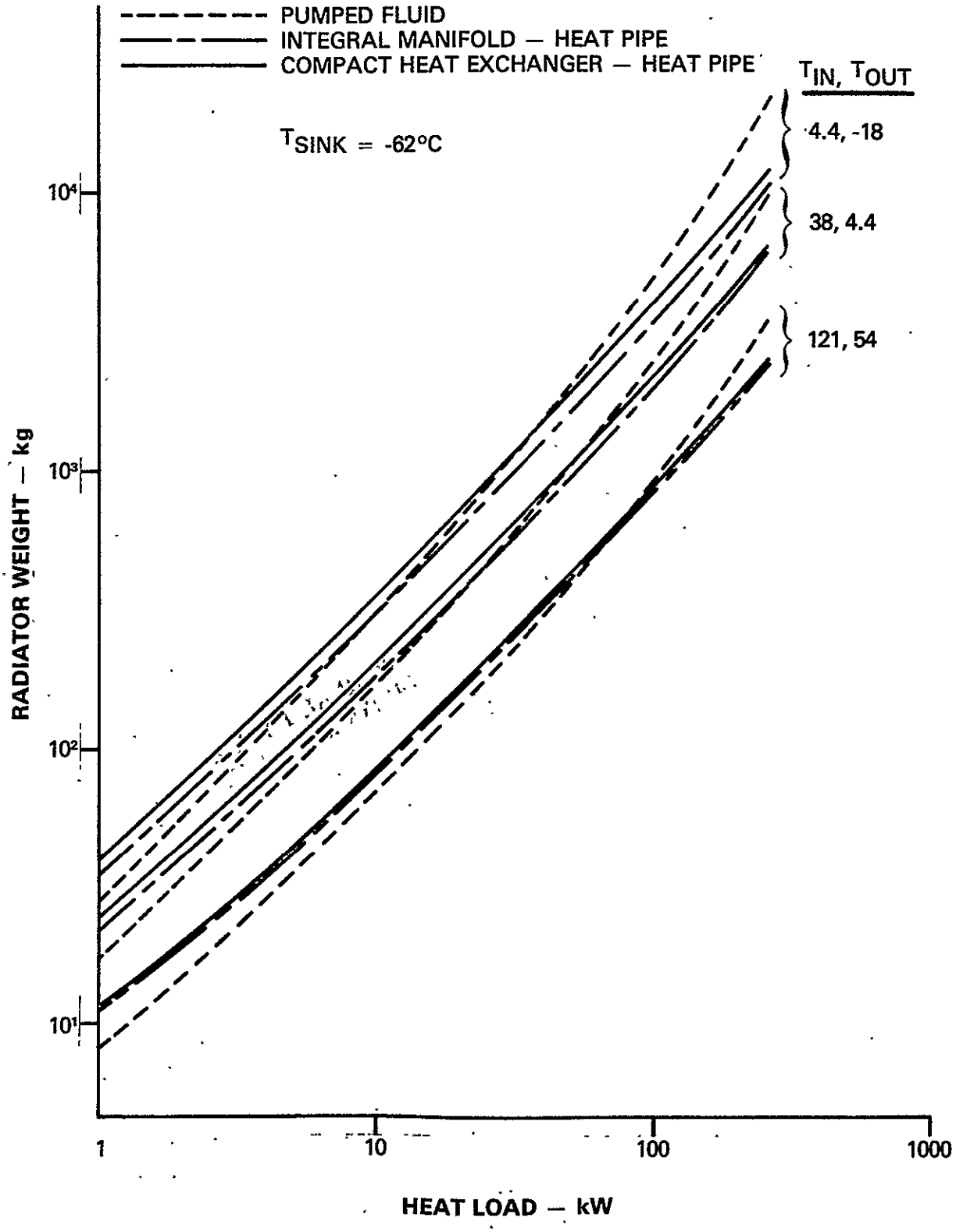

FIGURE 18a RADIATOR WEIGHT OPTIMIZATION, T_{SINK} = -62°C

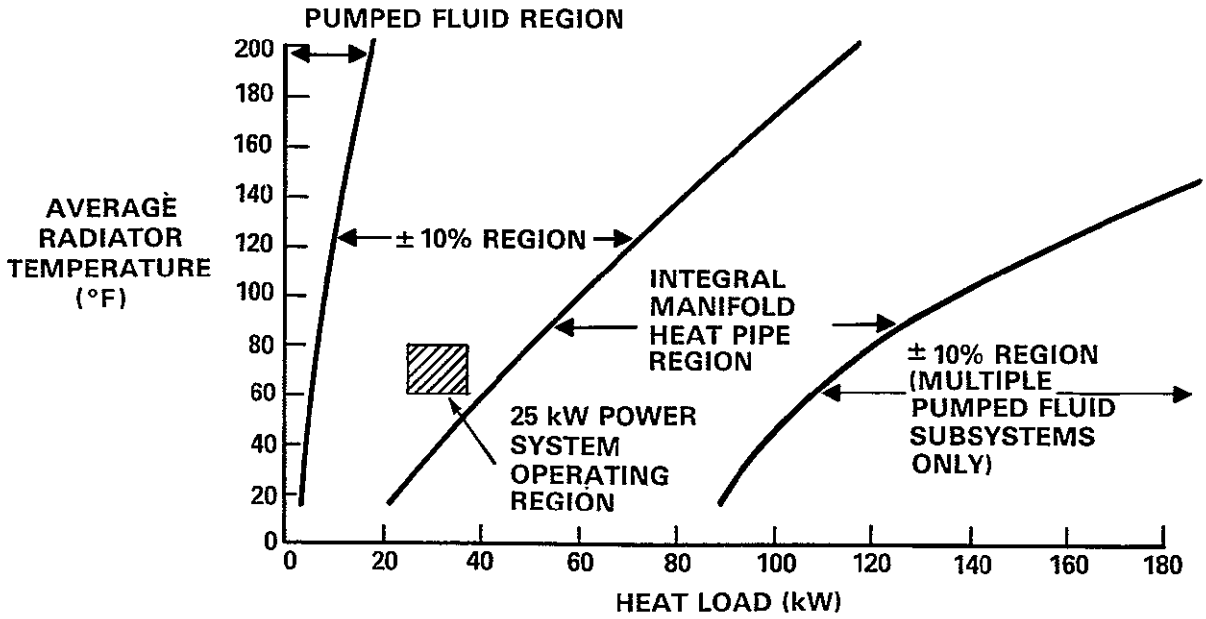

FIGURE 19
HEAT PIPE/PUMPED FLUID RADIATOR
WEIGHT OPTIMUM OPERATING REGIONS

G0-1078-14

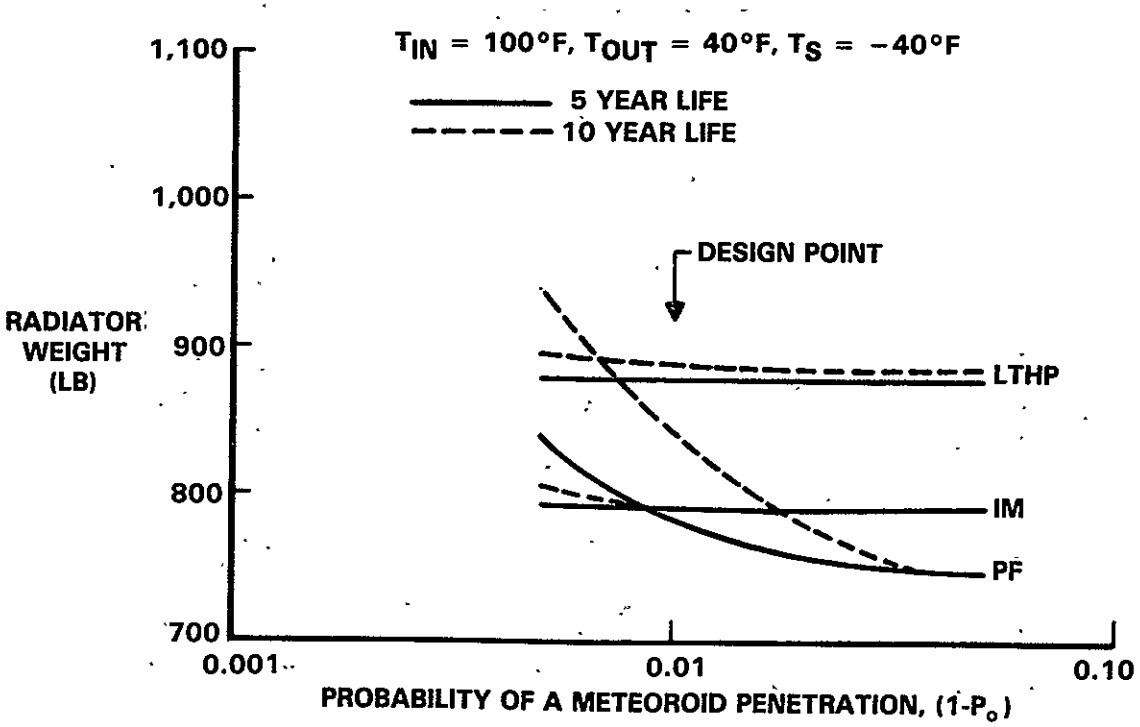

FIGURE 20
EFFECT OF METEROID PROBABILITY ON RADIATOR WEIGHT 16 kW HEAT LOAD

VOUGHT

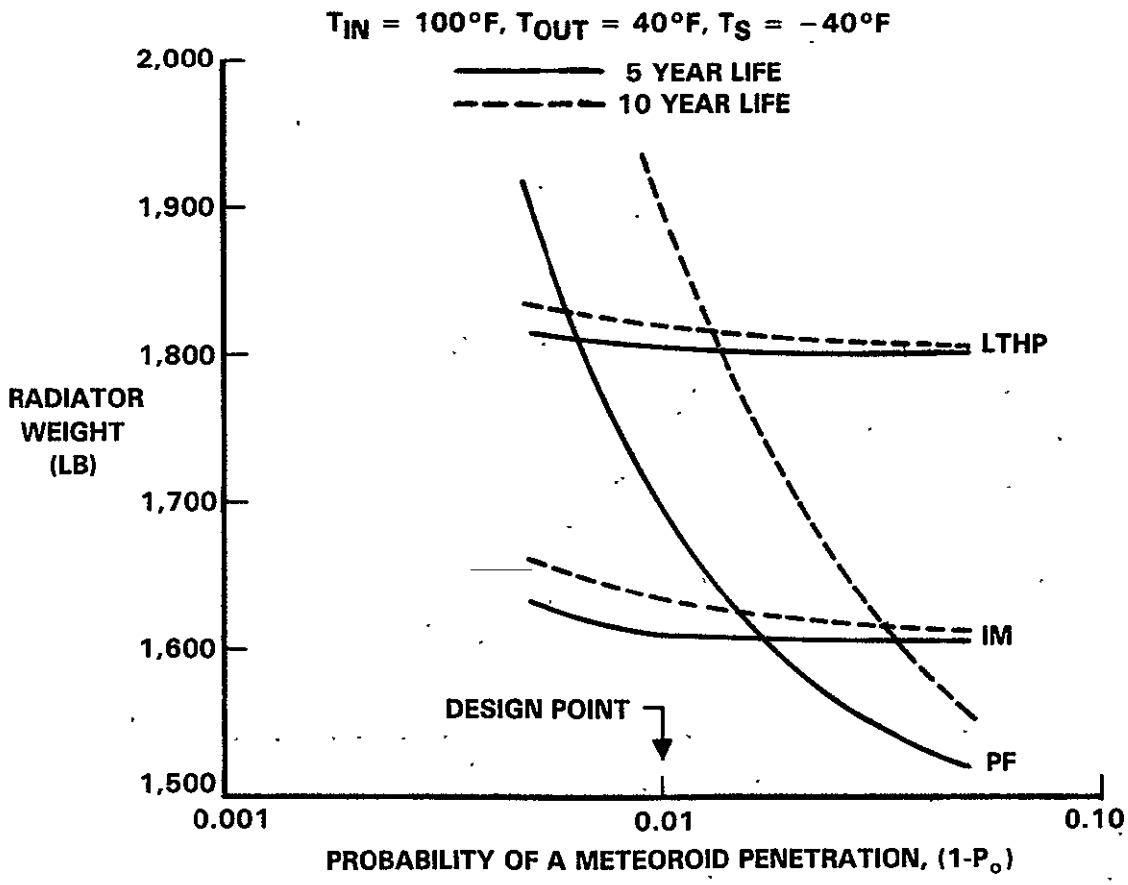

FIGURE 21
EFFECT OF METEOROID PROBABILITY ON RADIATOR WEIGHT
32kW HEAT LOAD

G0-1078-22

VOUGHT

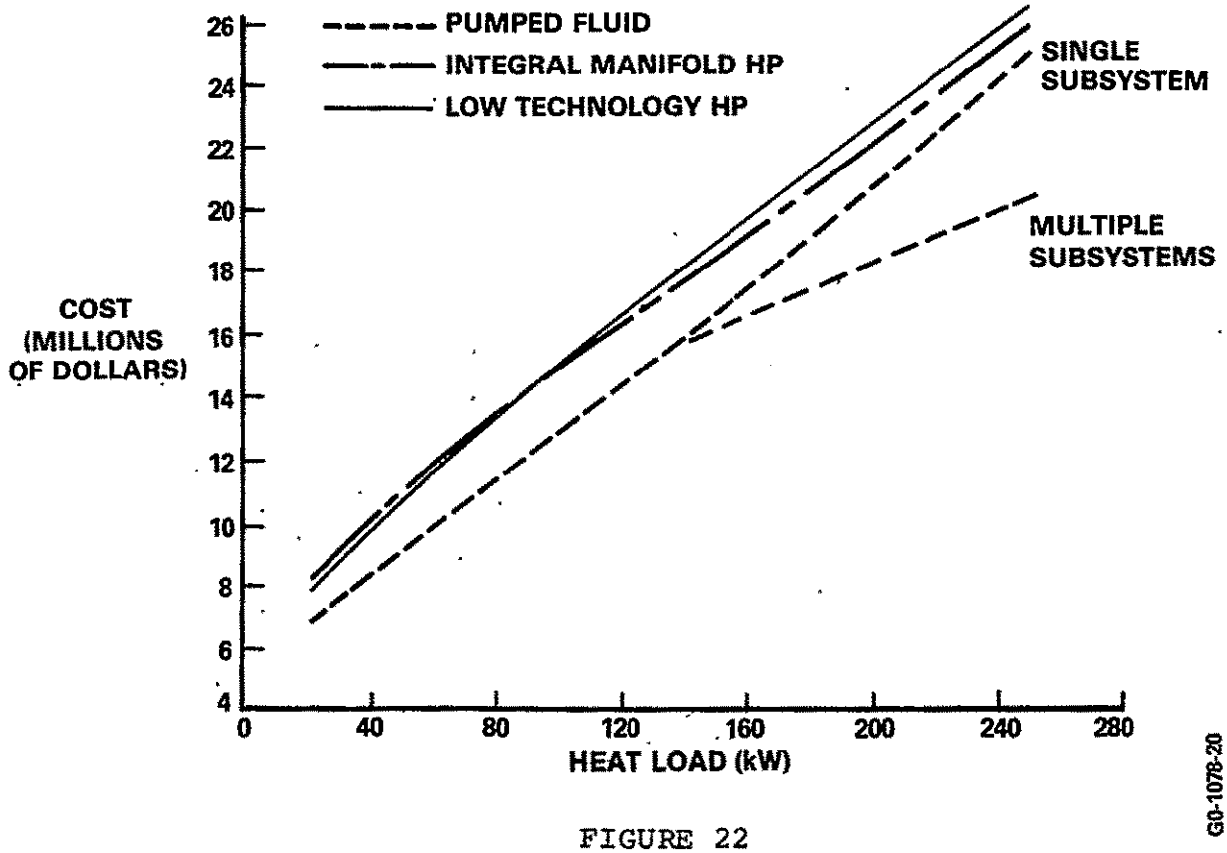

FIGURE 22

HEAT PIPE/PUMPED FLUID TCS
COST COMPARISON

FIGURE 23

EFFECT OF BODY MOUNTED HEAT PIPE TCS ON FLUID LOOP

VOUGHT

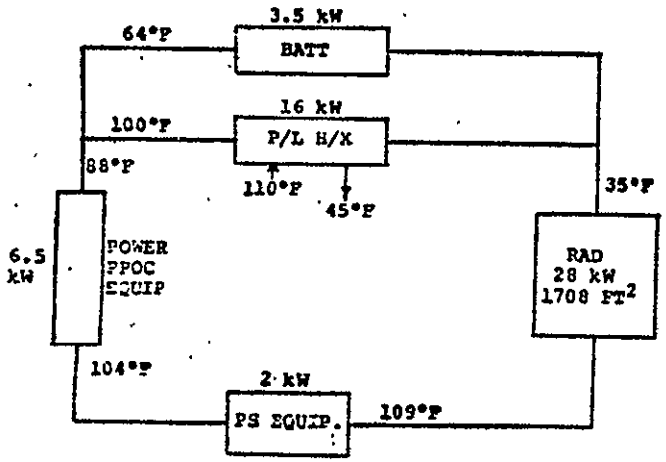

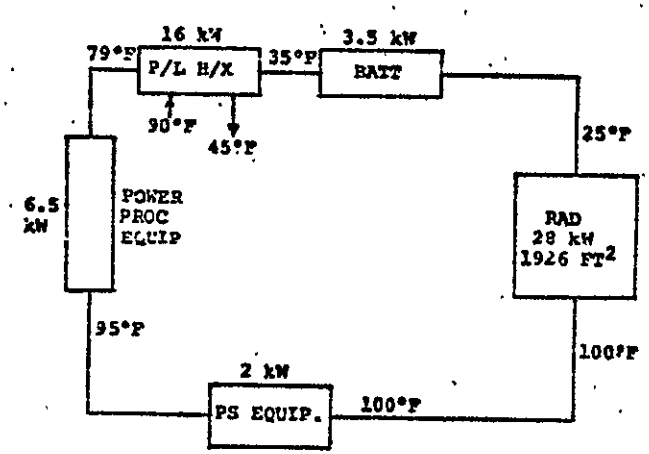

BASELINE CANDIDATES

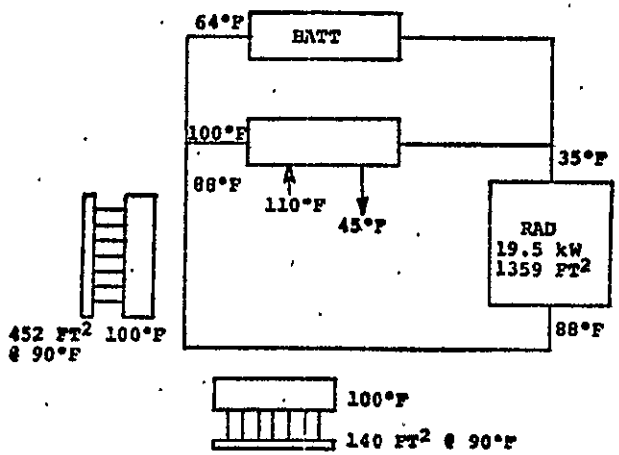

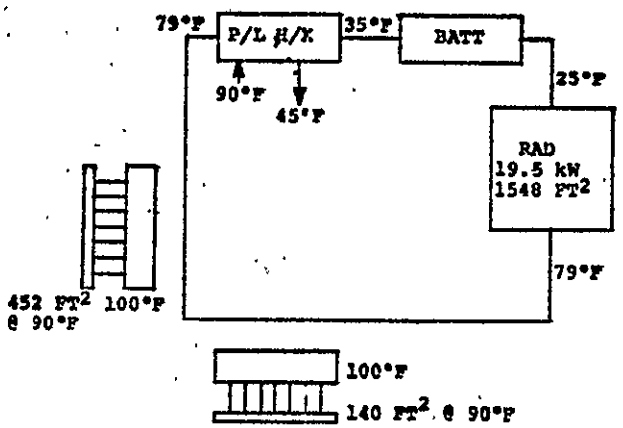

BODY MOUNTED HP RAD FOR POWER PROCESSING AND PS EQUIP

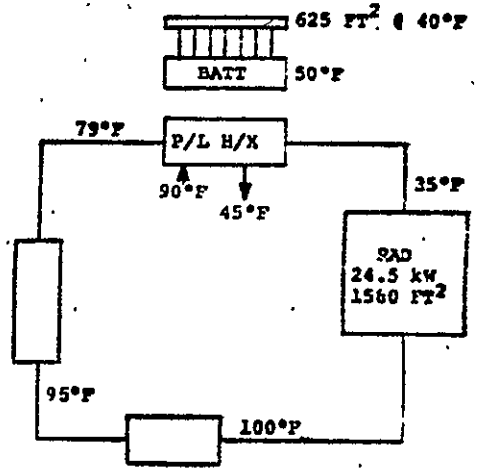

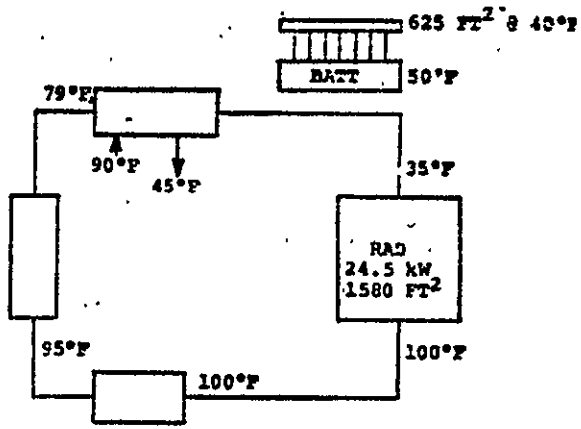

BODY MOUNTED HP RAD FOR BATTERIES

FIGURE 24

BODY MOUNTED ALL HEAT PIPE TCS CONCEPT

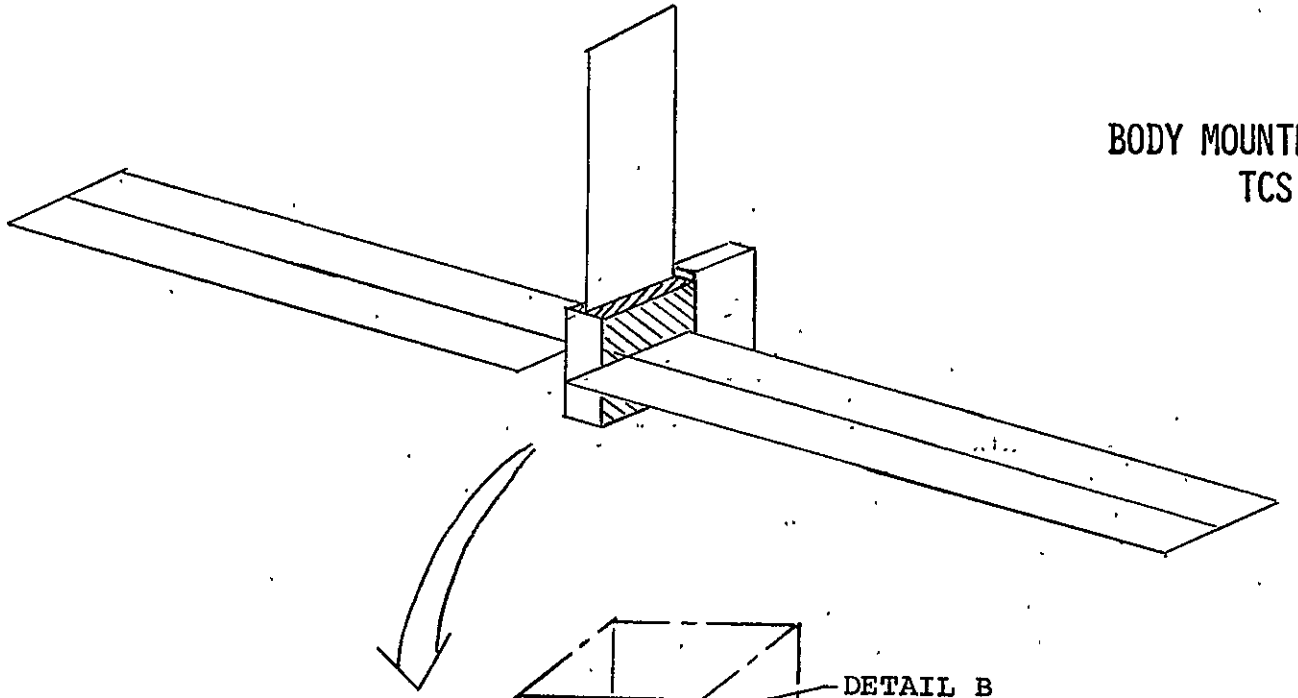

DETAIL B
PERIMETER HEAT PIPE

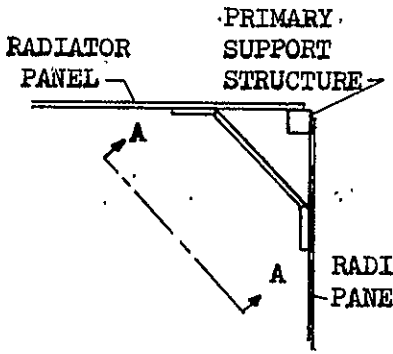

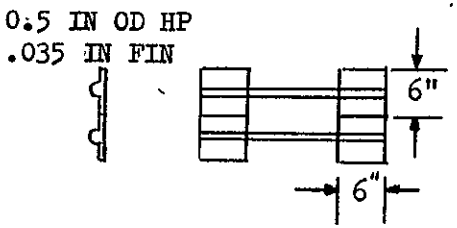

VIEW A-A

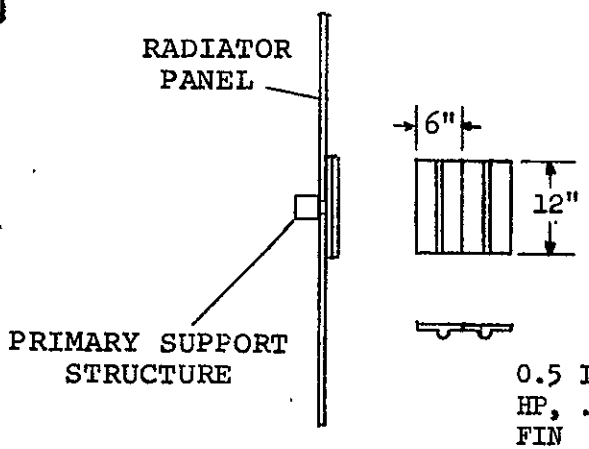

DETAIL A

VOUGHT

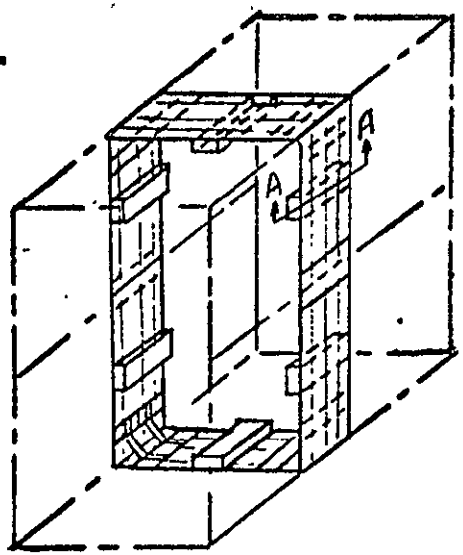

FIGURE 25
EQUIPMENT MOUNTING CONCEPT FOR
ALL HEAT PIPE TCS

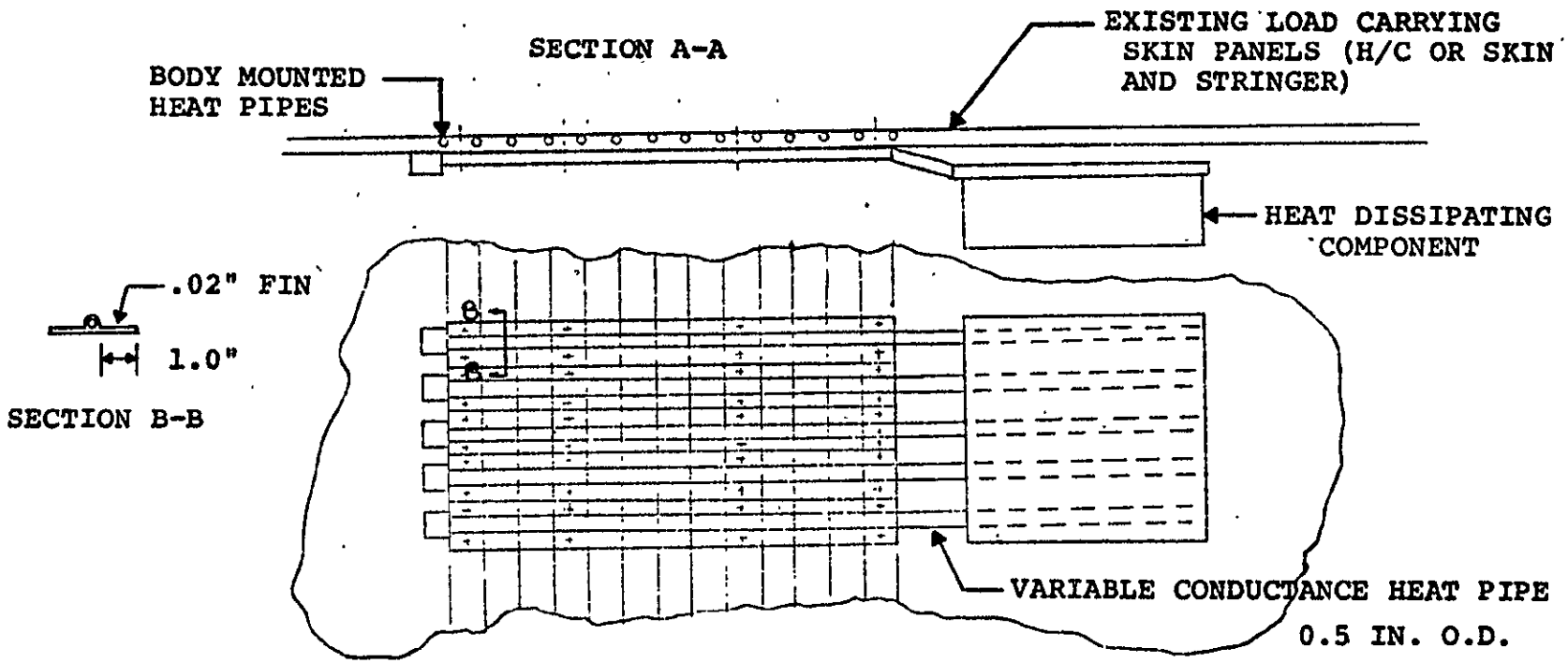

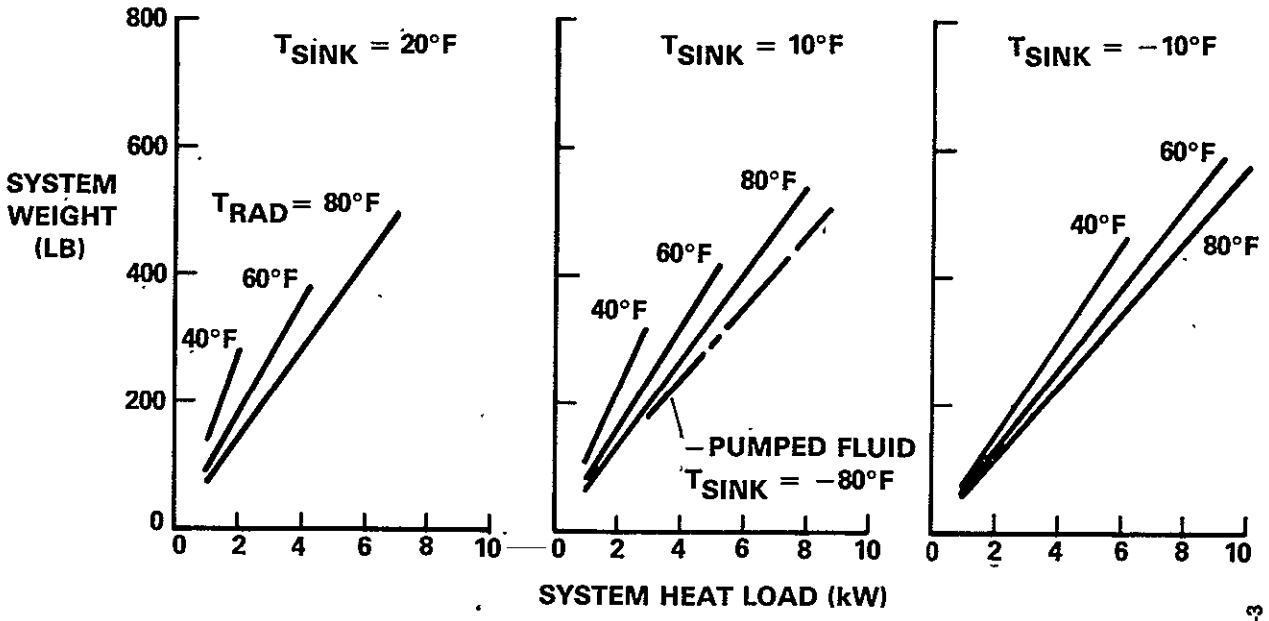

FIGURE 26
BODY MOUNTED - ALL HEAT PIPE TCS WEIGHT

VOUGHT

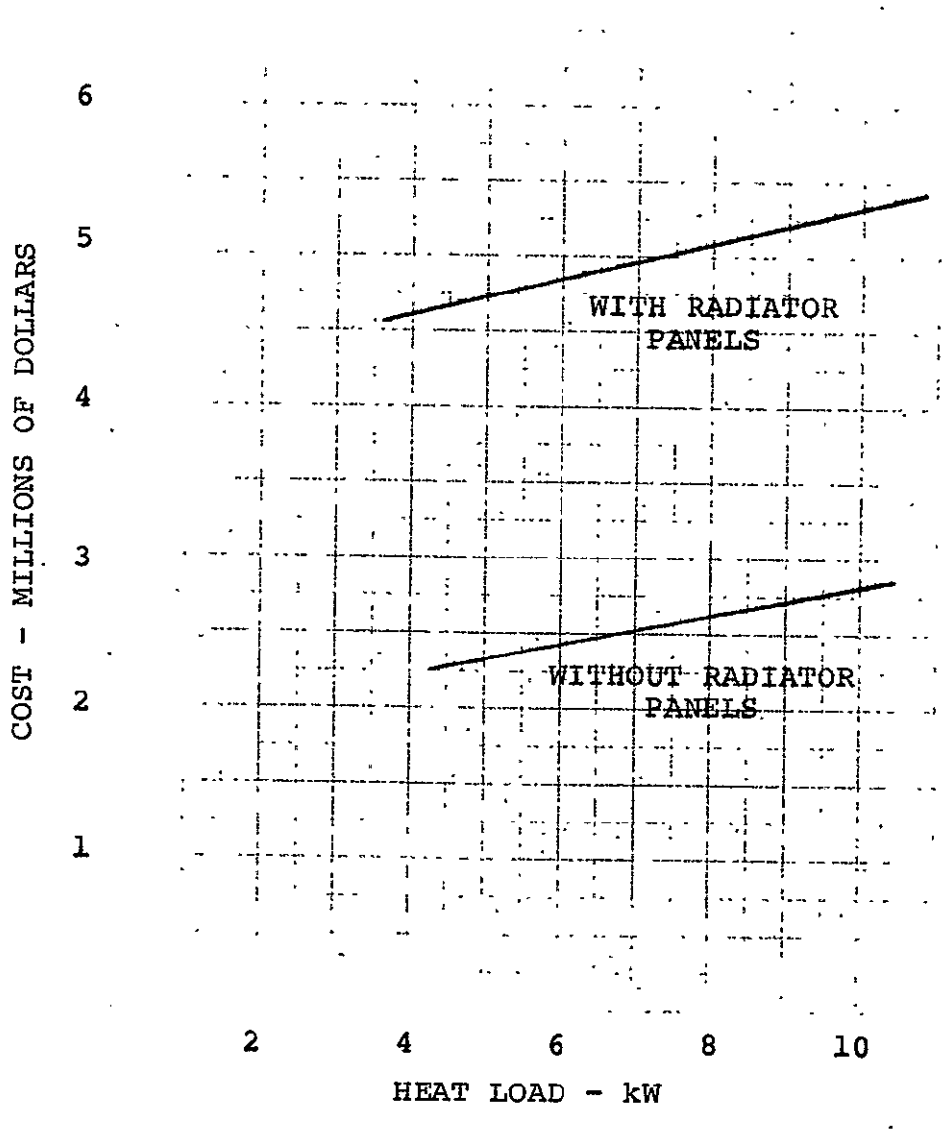

FIGURE 27 BODY MOUNTED HEAT PIPE RADIATOR COST

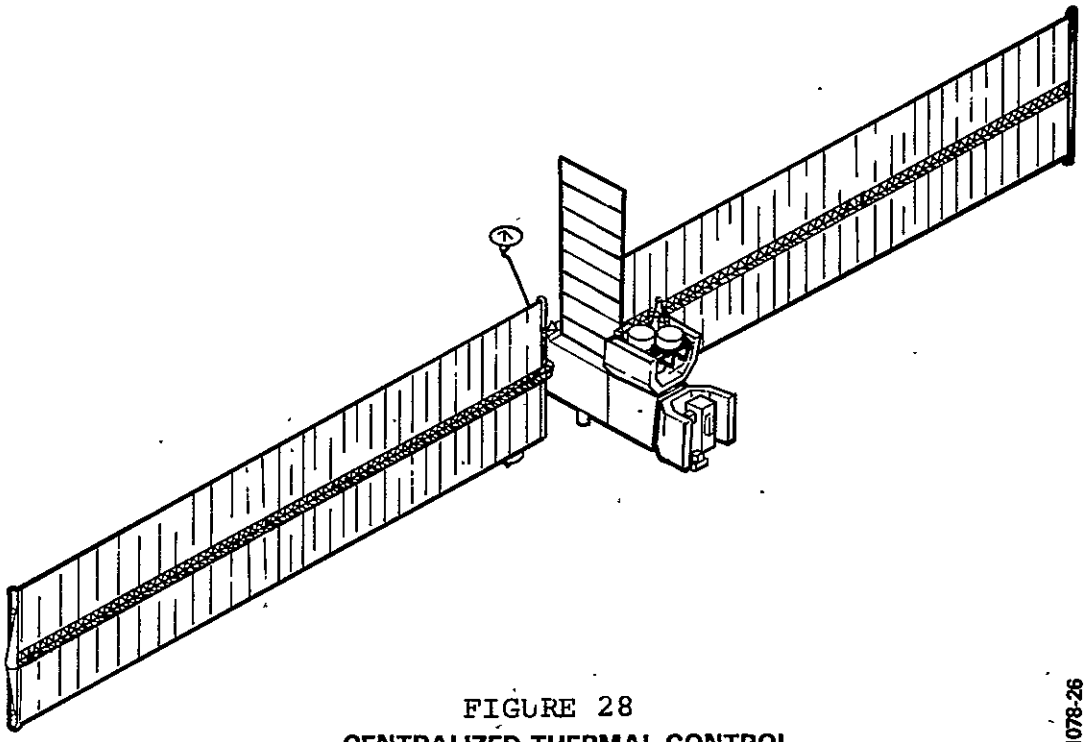

FIGURE 28
CENTRALIZED THERMAL CONTROL
SYSTEM CONCEPT

G0-1078-26

VOUGHT

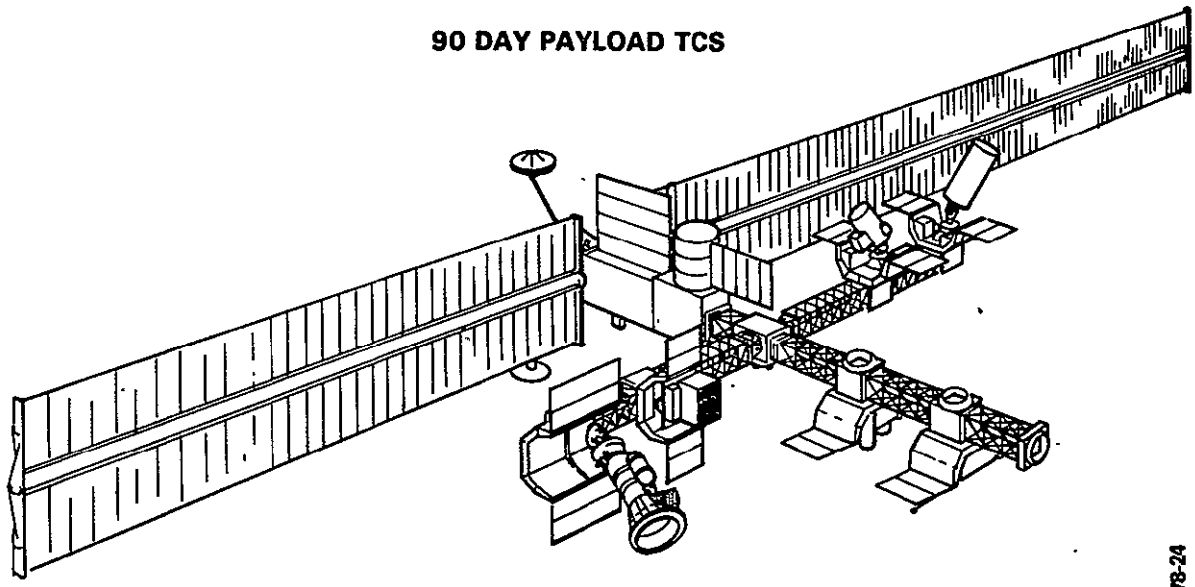

G0-1078-24

FIGURE 29
DISTRIBUTED THERMAL CONTROL SYSTEM CONCEPT

VOUGHT

5 YEAR PAYLOAD TCS

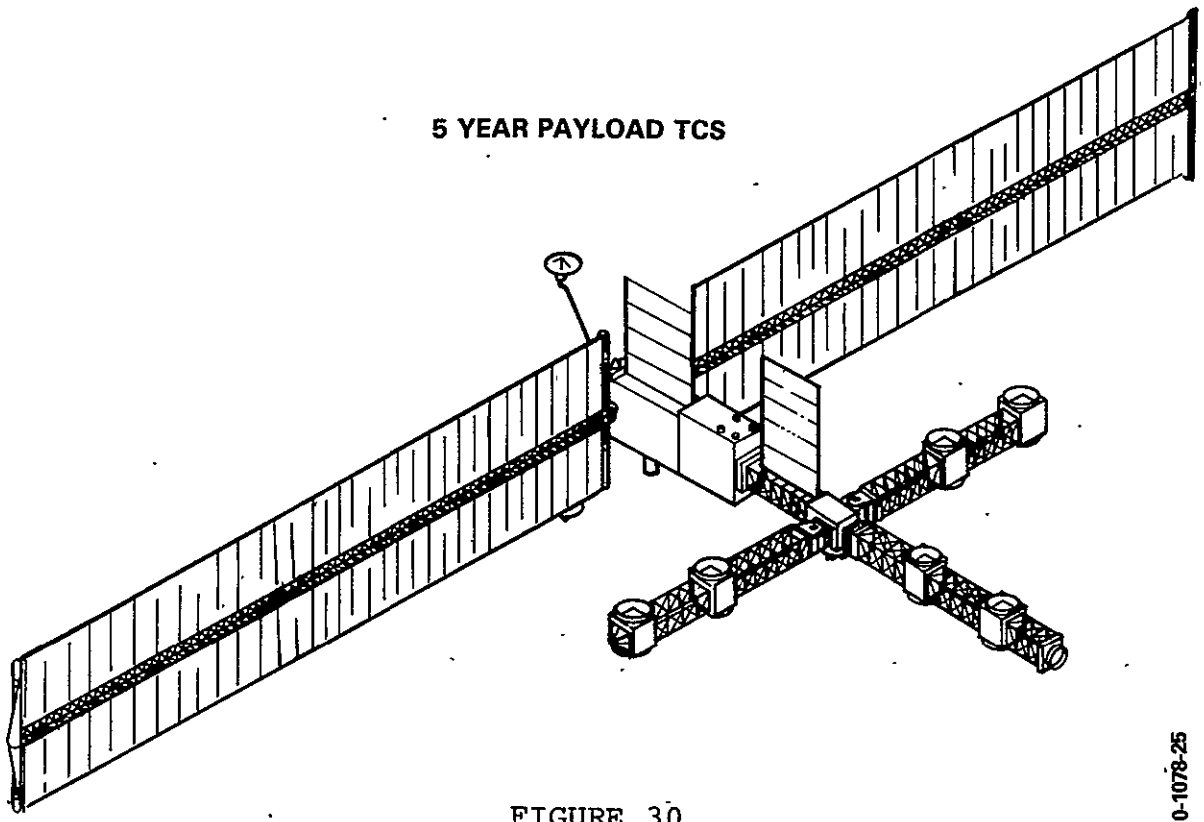

G0-1078-25

FIGURE 30
DISTRIBUTED THERMAL CONTROL SYSTEM CONCEPT

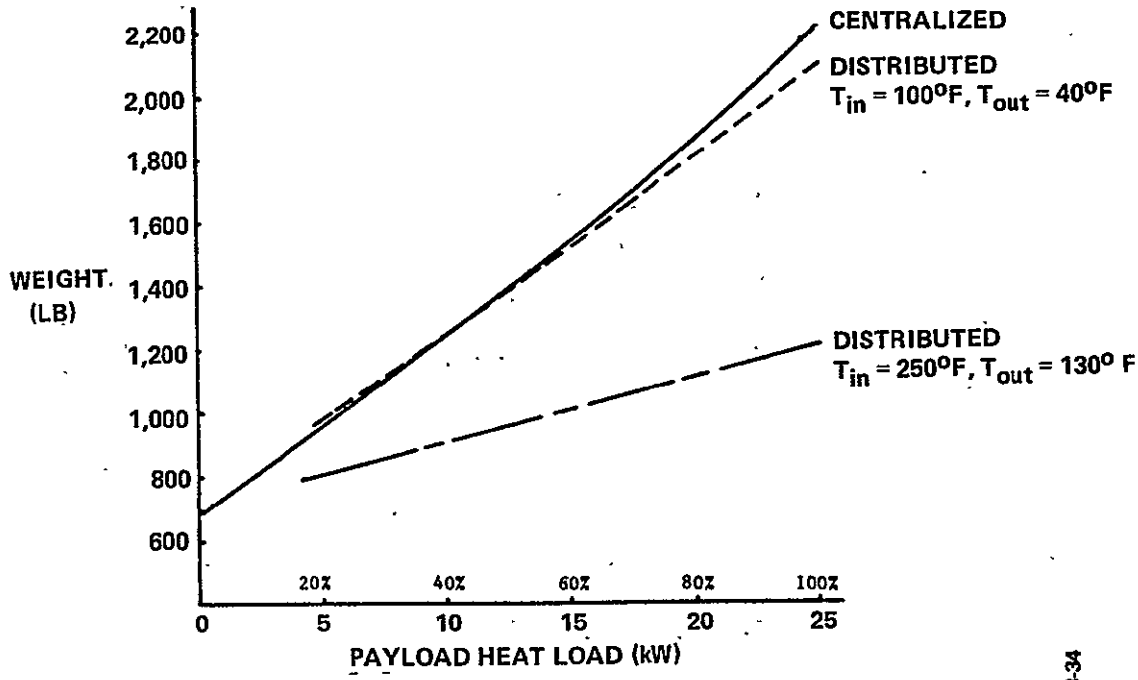

FIGURE 31
CENTRALIZED AND DISTRIBUTED TCS WEIGHT COMPARISON

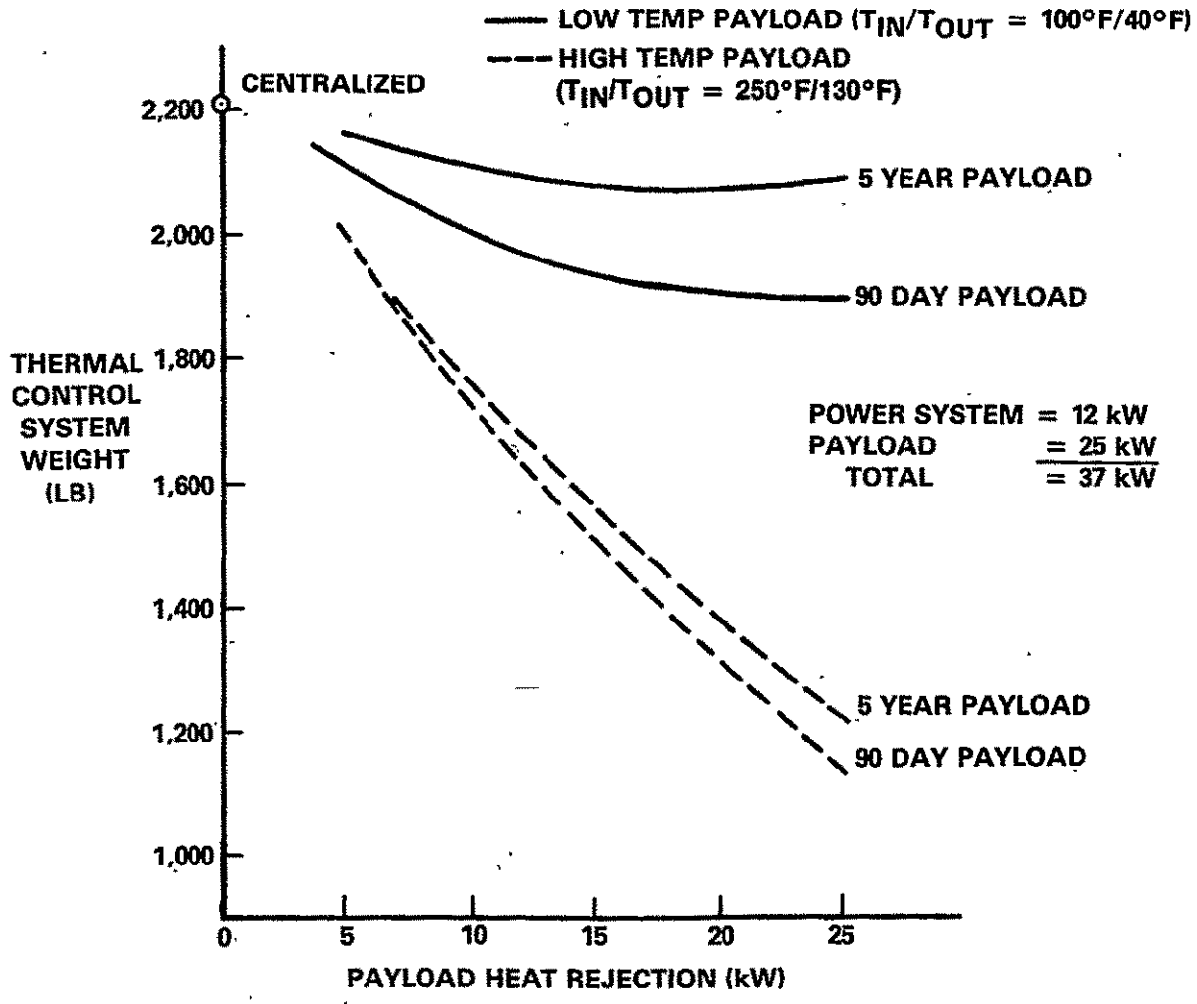

FIGURE 32
POWER SYSTEM/PAYLOAD
THERMAL CONTROL SYSTEM WEIGHT

G0-1078-5

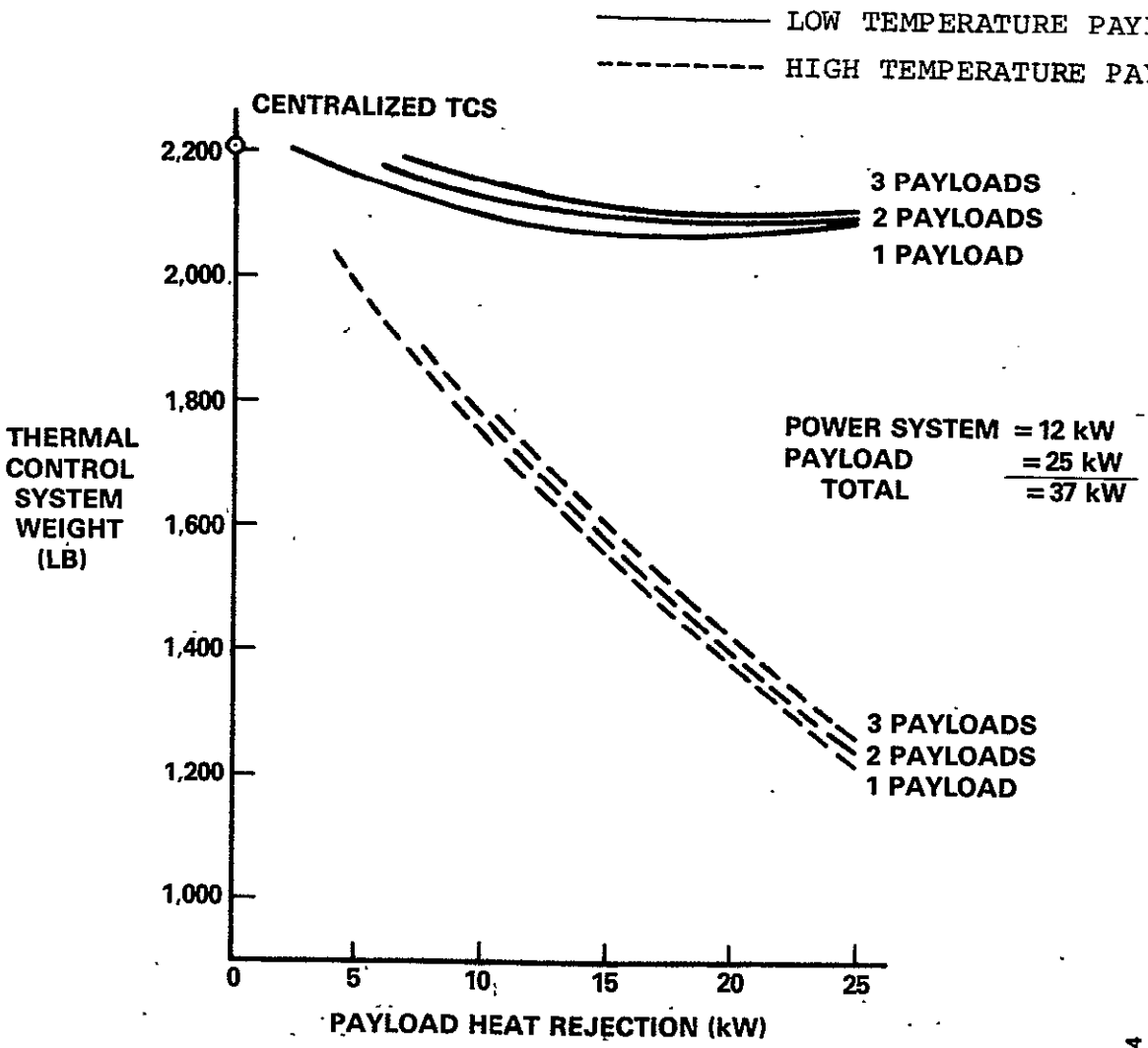

FIGURE 33
POWER SYSTEM/PAYLOAD THERMAL CONTROL SYSTEM WEIGHT

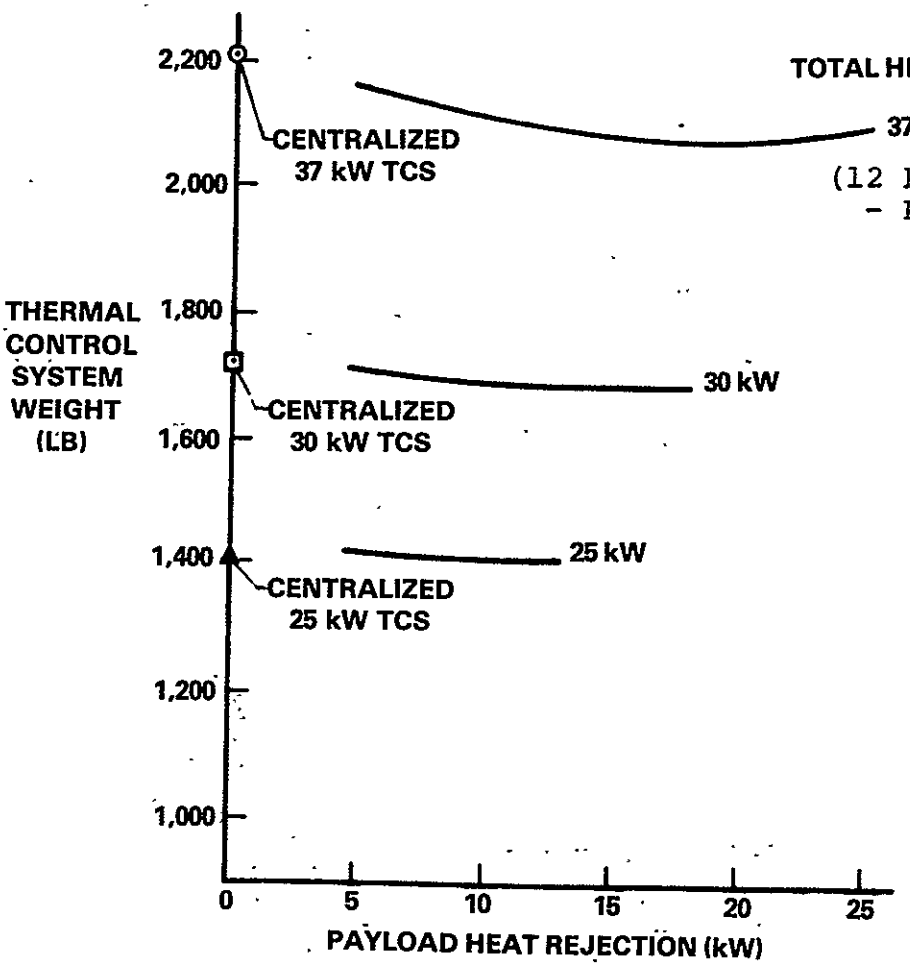

FIGURE 34
POWER SYSTEM/PAYLOAD
THERMAL CONTROL SYSTEM WEIGHT

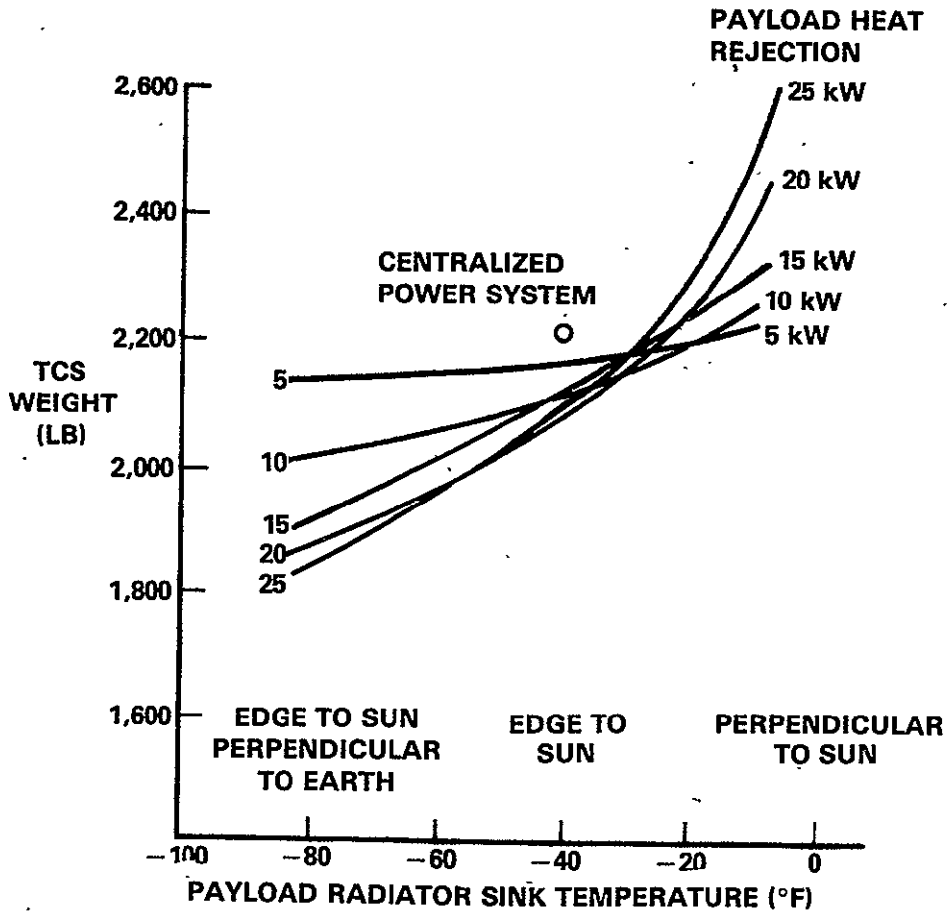

FIGURE 35
EFFECT OF PAYLOAD SINK TEMPERATURE ON TCS WEIGHT

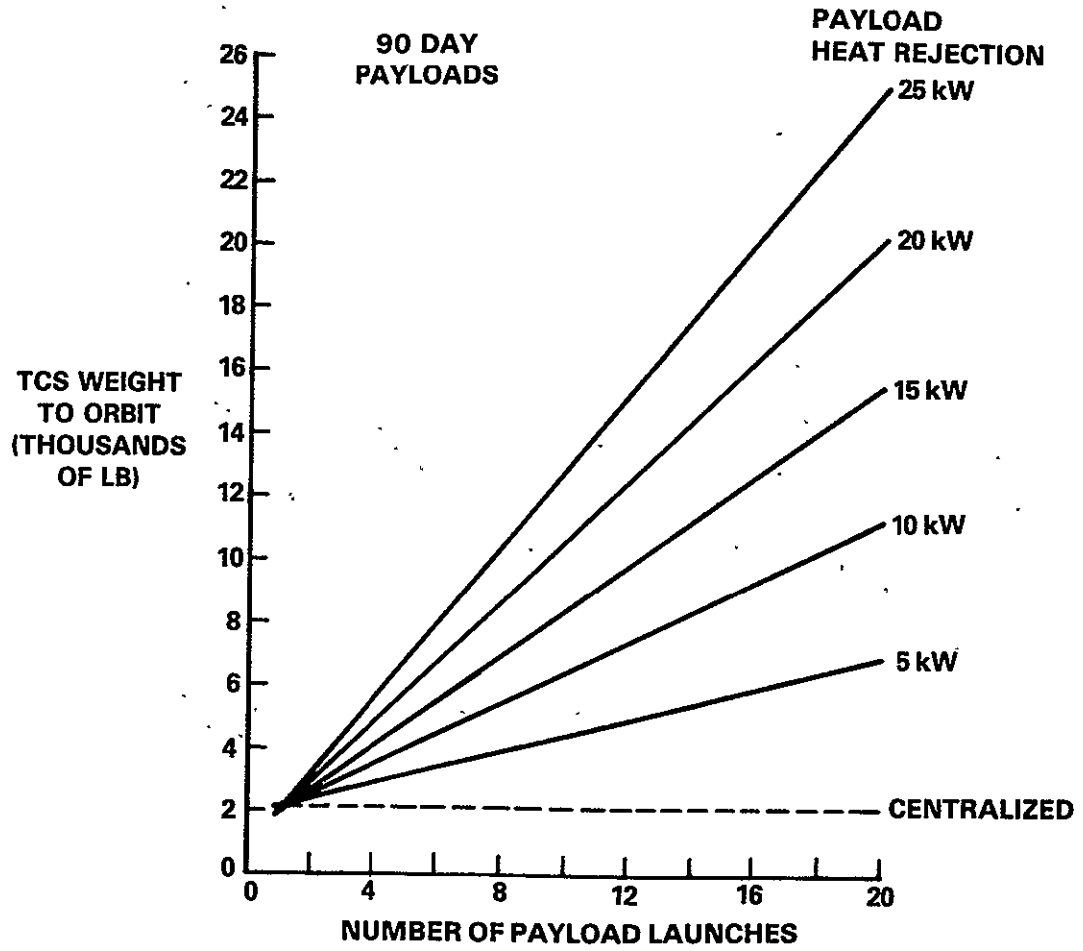

FIGURE 36
POWER SYSTEM/PAYLOAD
THERMAL CONTROL SYSTEM WEIGHT

G0-1078-7

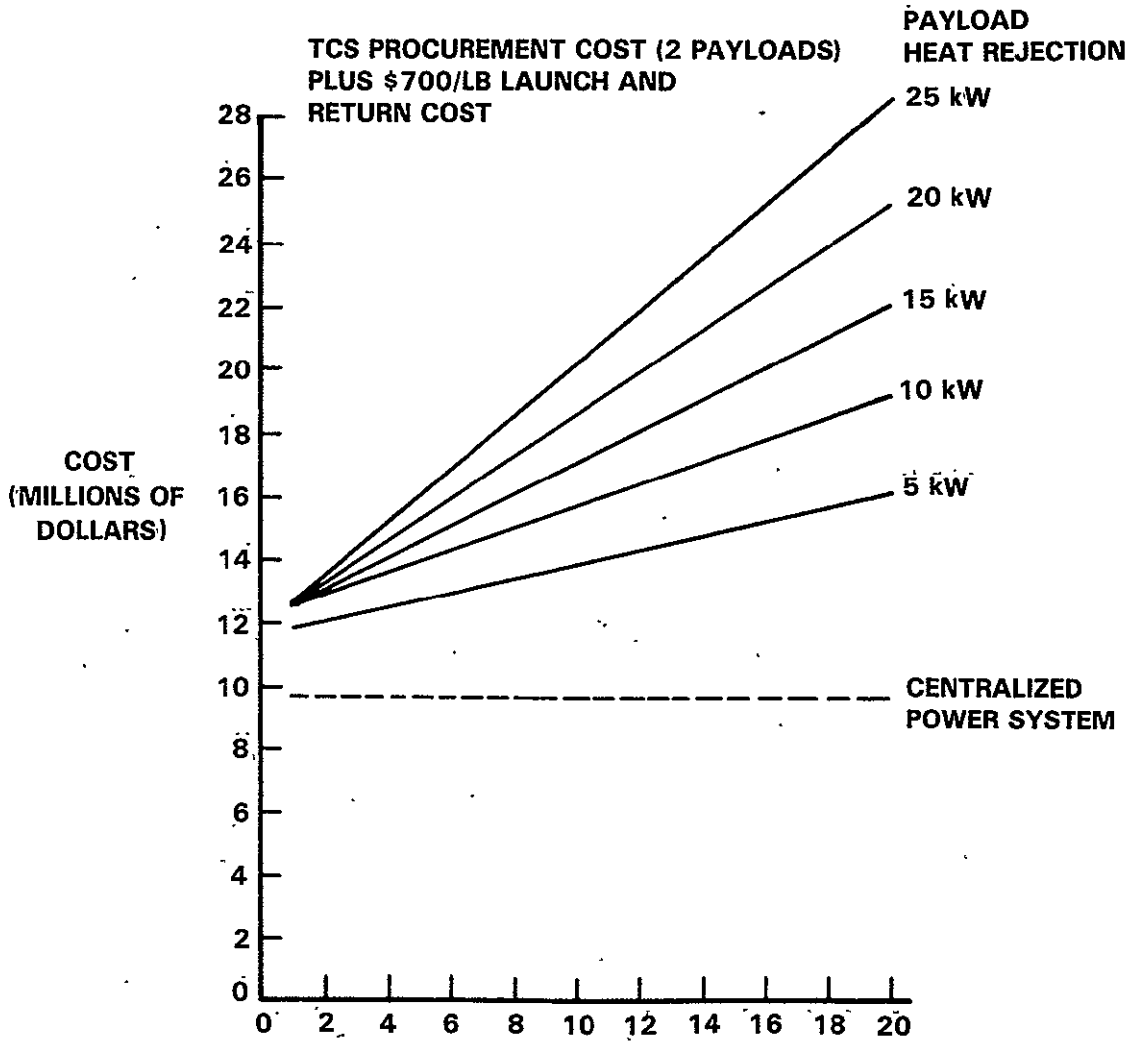

FIGURE 37
POWER SYSTEM/PAYLOAD TCS COST COMPARISON

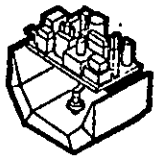

- PASSIVE HEAT REJECTION:
  - EXPECT 20%-40% MANY PAYLOADS
  - NEEDS STUDY

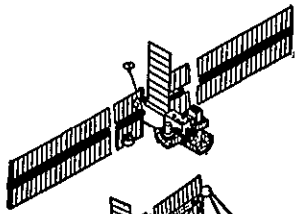

- SCIENCE PAYLOADS:
  - PAYLOAD GIMBALLING DESIRED (SASP STUDIES)
  - GIMBAL HEAT TRANSPORT TECHNOLOGY READINESS QUESTIONABLE
  - EARLY PAYLOADS HAVE MODEST POWER REQUIREMENTS
    - UP TO 15 kW (25 kW POWER MODULE EVOLUTION STUDY)
    - CANDIDATES FOR DIRECT PALLET MOUNTING TO POWER SYSTEM (NO GIMBAL)

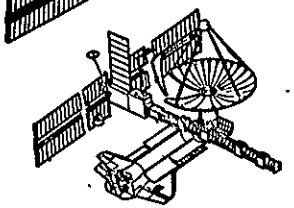

- SPACE CONSTRUCTION:
  - PUBLIC SERVICES PLATFORM ASSEMBLY AND TEST UP TO 15 kW (25 kW PM EVOL STUDY)
  - HIGH PASSIVE HEAT REJECTION POTENTIAL

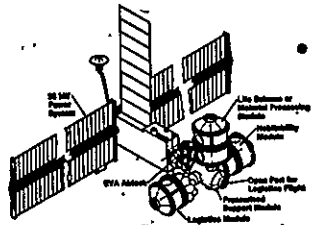

- MANNED MODULES:
  - 7 kW TO 27 kW HEAT REJ NEEDED USING 25 kW PS, 40 kW GROWTH (SASP CONCEPTUAL DES STUDY)
  - 45°F HUMIDITY CONTROL
  - CANDIDATE FOR CENTRALIZED HEAT REJ; ALSO CONTROLLED STR HEAT LEAK

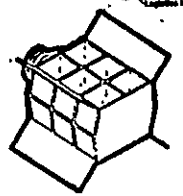

- MATERIALS PROCESSING:
  - 10 kW TO 65 kW HEAT REJ NEEDED USING 25 kW PS, 100 kW GROWTH (MEC AND SASP STUDIES)
  - TEMPERATURES UP TO 300°F
  - CANDIDATE FOR SPECIALIZED HEAT REJECTION

CONCLUSION: 10-16 kW CENTRALIZED POWER SYSTEM HEAT REJECTION TO PAYLOADS PROVIDED BY MSFC REFERENCE CONCEPT CAN BE EFFECTIVELY USED AND SHOULD SATISFY ESSENTIALLY ALL EARLY MISSION REQUIREMENTS.

FIGURE 38 PAYLOAD CONSIDERATIONS FOR CENTRALIZED/DECENTRALIZED TRADES

- DEVELOP FOR USE WITH EARLY PAYLOADS
- PANELS DESIGNED TO INTERFACE SPACELAB PALLET AND PLATFORM NONDEPLOYABLE TRUSS
- INSTALLED ON GROUND AS KIT
- PALLET AREAS AVAILABLE INCLUDE MOUNTING CLEARANCE IN SHUTTLE

VOUGHT

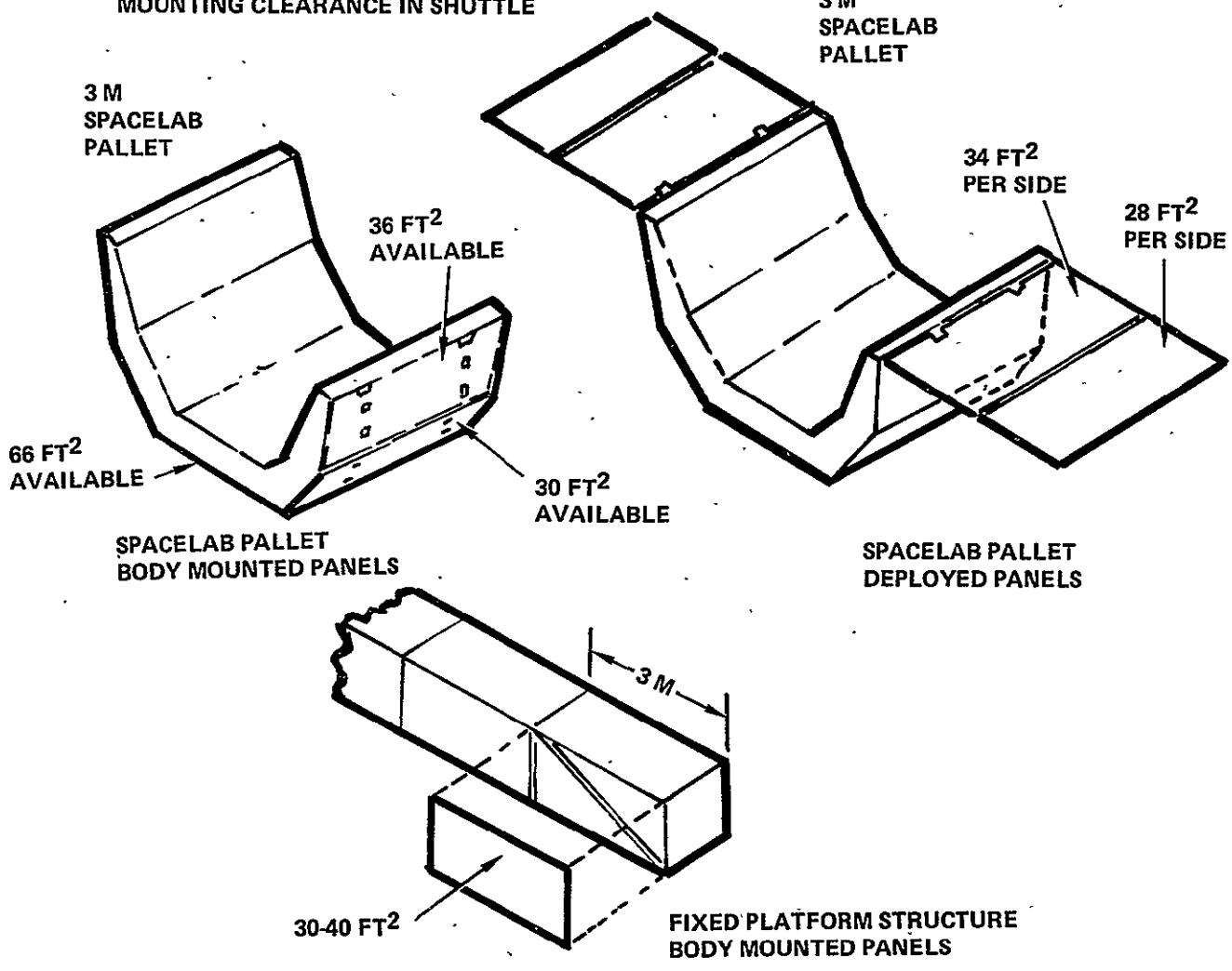

FIGURE 39

PAYLOAD KIT RADIATOR

G0-1078-32

VOUGHT

- EVALUATE FOR USE AS PAYLOAD REQUIREMENTS EMERGE
- ACCOMMODATE PAYLOAD HEAT REJECTION NOT SUITABLE FOR CENTRALIZATION
- AVOID REPEATED DEV/PROD./LAUNCH COSTS

CONCEPT 1

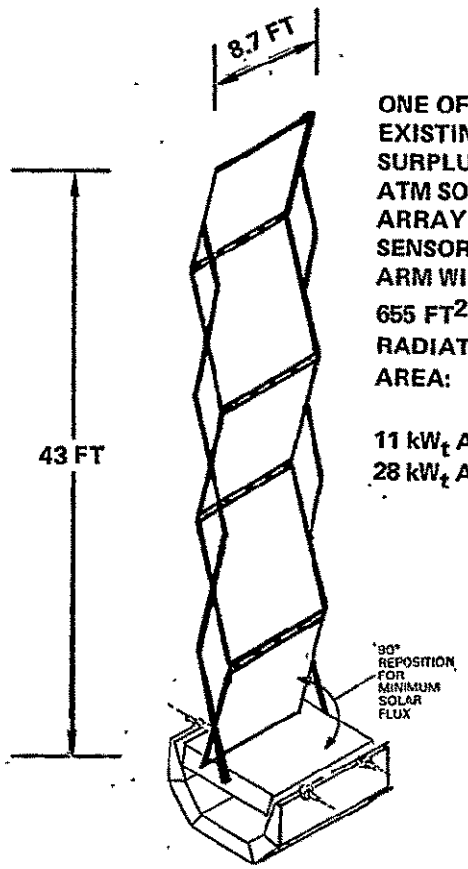

ONE OF 4 EXISTING SURPLUS ATM SOLAR ARRAY SENSORS ARM WINGS – 655 FT^2 RADIATING AREA:

11 kW_t AT 100° F/ 40° F
28 kW_t AT 250° F/ 70° F

RELOCATABLE HEAT REJECTION MODULE CONCEPT USING ESA PALLET AND ATM DEPLOYMENT STRUCTURE (ALSO 4 PALLET TRAIN)

CONCEPT 2

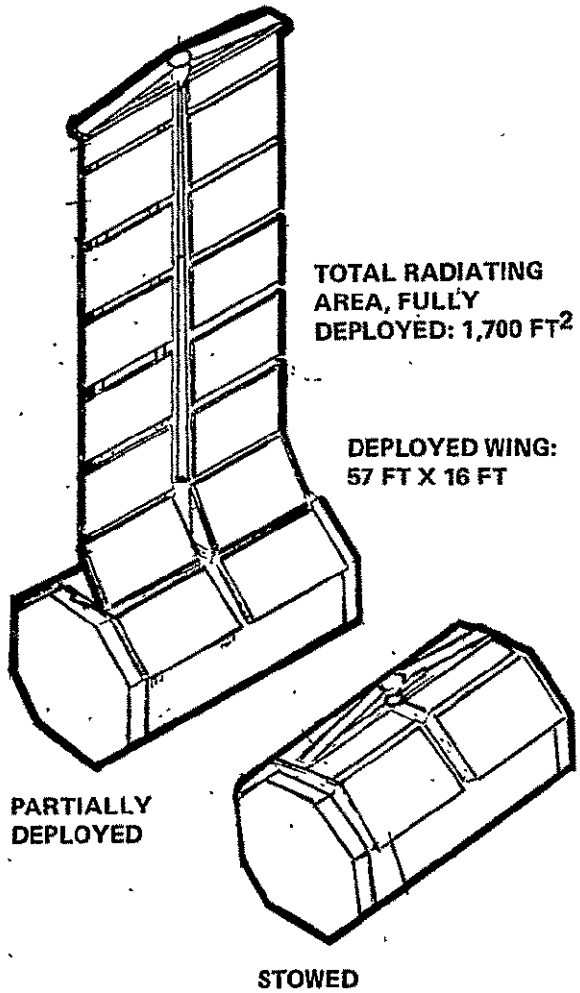

TOTAL RADIATING AREA, FULLY DEPLOYED: 1,700 FT^2

DEPLOYED WING: 57 FT X 16 FT

PARTIALLY DEPLOYED

STOWED

G0-1078-33

FIGURE 40
TYPICAL RELOCATABLE HEAT REJECTION MODULE CONCEPTS

VOUGHT

INITIAL 25 kW PS	INTERMEDIATE GROWTH	LONG-TERM GROWTH
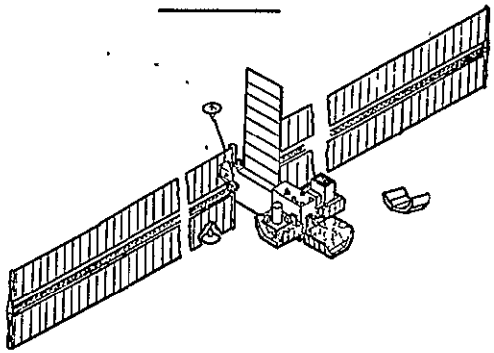	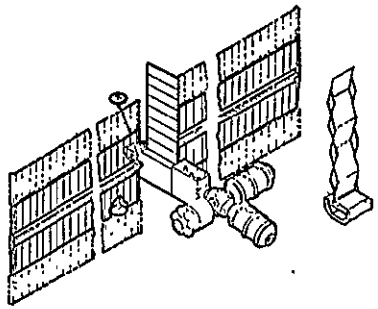	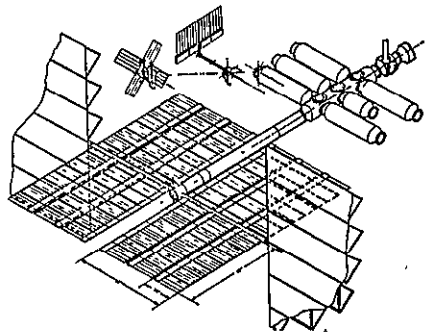
• CENTRALIZED AS MUCH AS EFFECTIVE – APPROX 10-16 kW FOR PAYLOADS • PASSIVE WHERE CAN • KIT P/L RADIATORS WHERE CANNOT CENTRALIZE OR PASSIVE	• INCREASED CENTRALIZATION • CONTINUED EFFECTIVE USE OF PASSIVE • RELOCATABLE MODULE AS REQUIREMENTS EMERGE	• HIGHLY CENTRALIZED • EFFECTIVE USE OF PASSIVE AND CONTROLLED STRUCTURAL HEAT LEAK • LARGE SCALE THERMAL MANAGEMENT
PAYLOAD STUDIES AND DEVELOPMENT →	PAYLOAD NEEDS →	PAYLOAD NEEDS →
	– INITIAL MANNED MODULES – GROWTH OF SCIENCE AND SPACE PROCESSING	– FURTHER MANNED OPERATIONS – LARGE SCALE PLATFORM
TECHNOLOGY DEVELOPMENT →	→	→
	– SWIVELS – DISCONNECTS – CONTACT HX	– THERMAL UMBILICAL – CONSTRUCTABLE RADIATORS

G0-1078-31

FIGURE 41 TYPICAL EVOLUTIONARY PATH

FIGURE 42
POWER SYSTEM/PAYLOAD THERMAL INTERFACE CONCEPT
CONTACT HEAT EXCHANGER

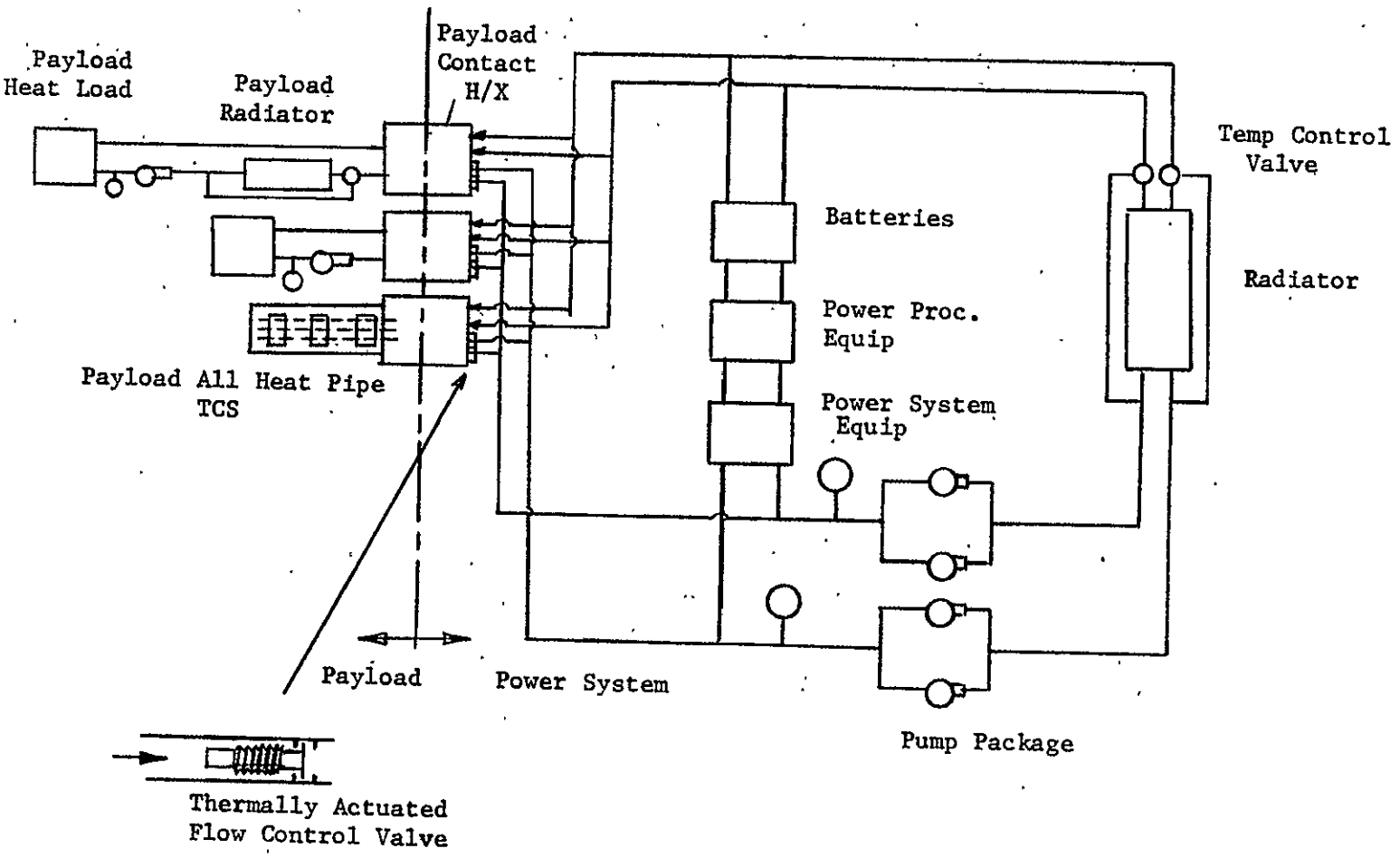

VOUGHT

FIGURE 43

POWER SYSTEM/PAYLOAD THERMAL INTERFACE CONCEPT

FLUID HEAT EXCHANGER

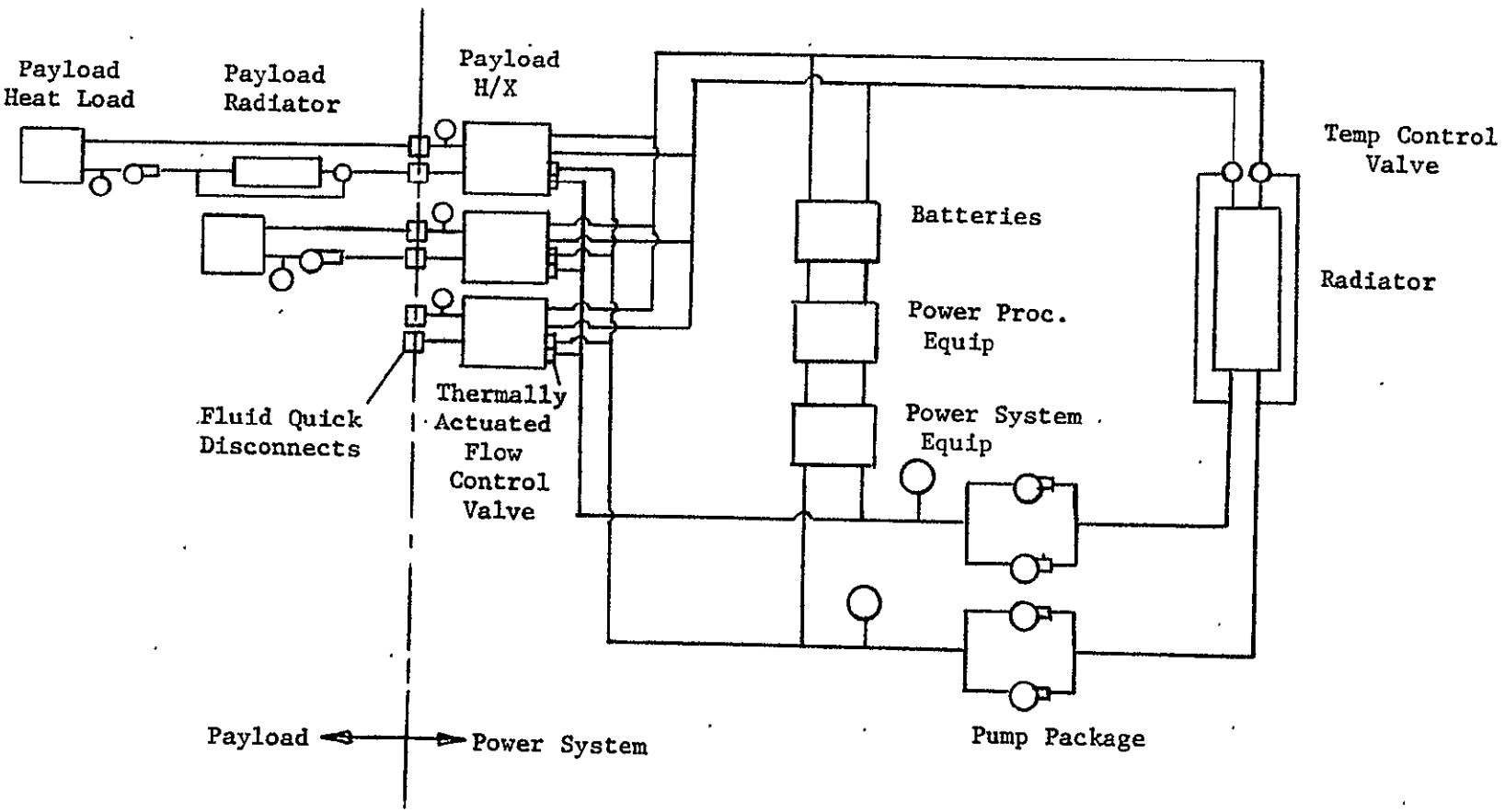

VOUGHT

FIGURE 44

POWER SYSTEM/PAYLOAD THERMAL INTERFACE CONCEPT

DIRECT FLUID COUPLING

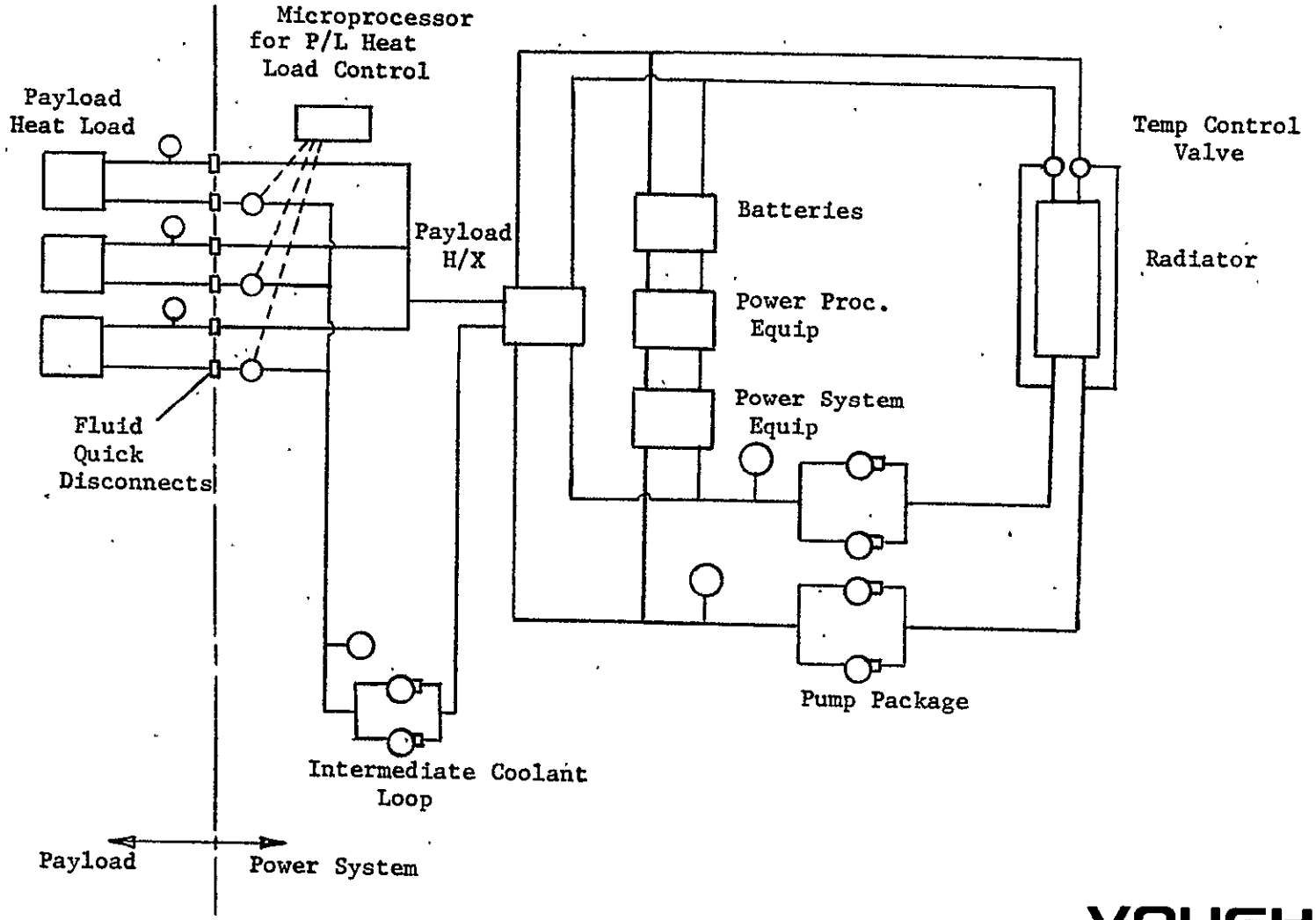

VOUGHT

FIGURE 45

POWER SYSTEM/PAYLOAD INTERFACE
HEAT EXCHANGER WEIGHT

16 kW

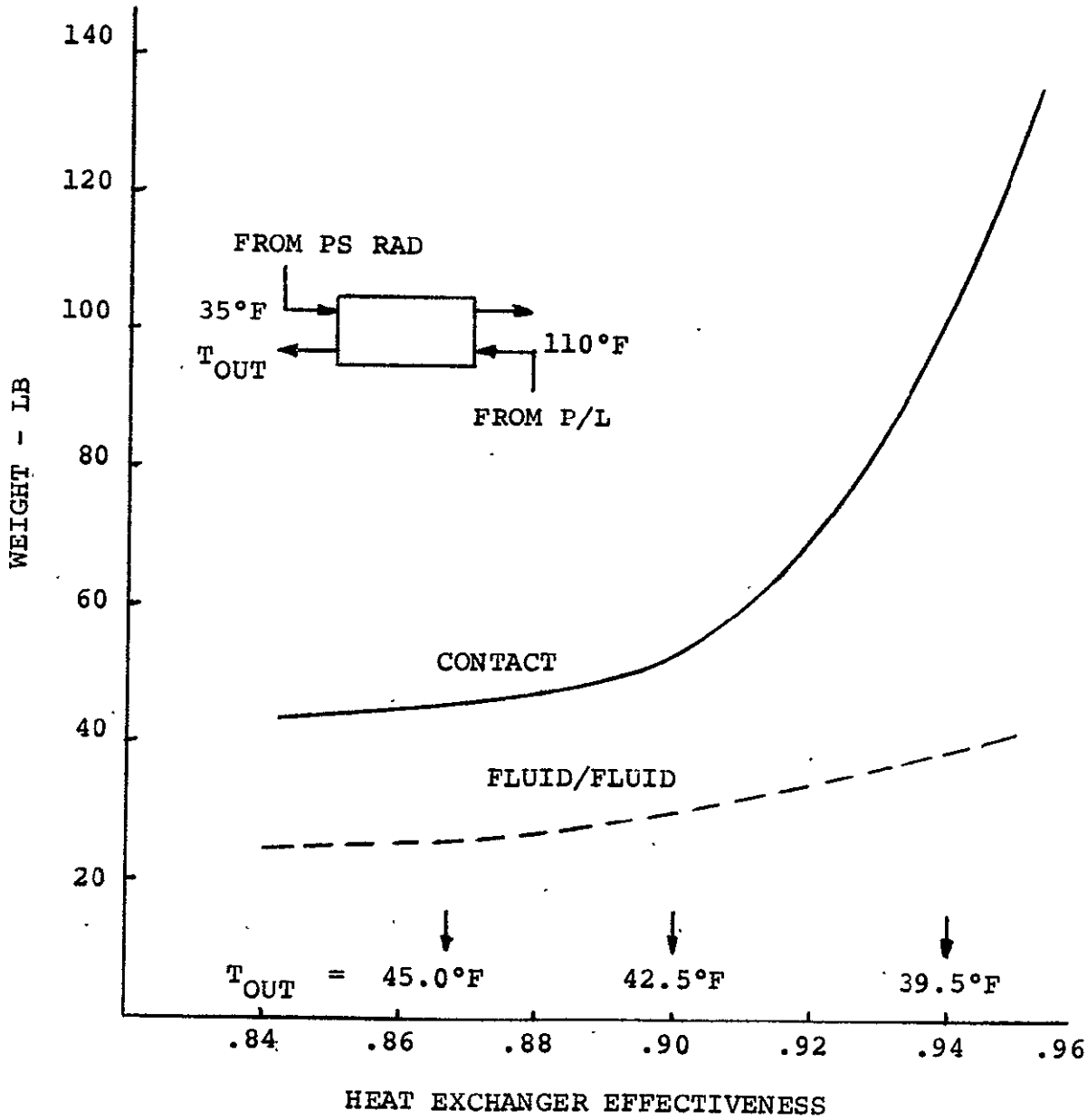

VOUGHT CORPORATION

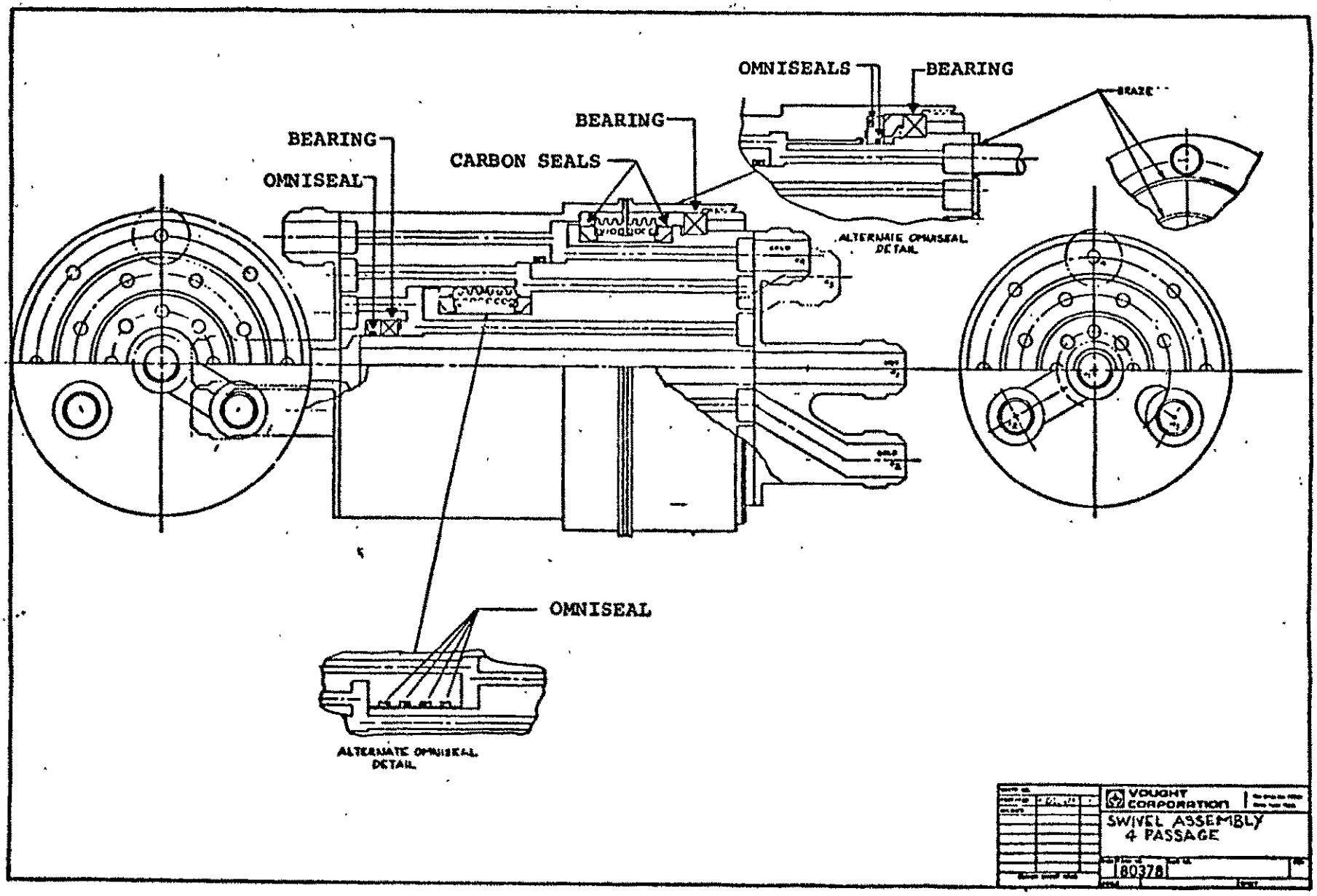

FIGURE 46 FOUR PASS FLUID SWIVEL

SCALE: 1/4" = 1"

FIGURE 47

FLEX HOSE/REEL ROTATING JOINT CONCEPT

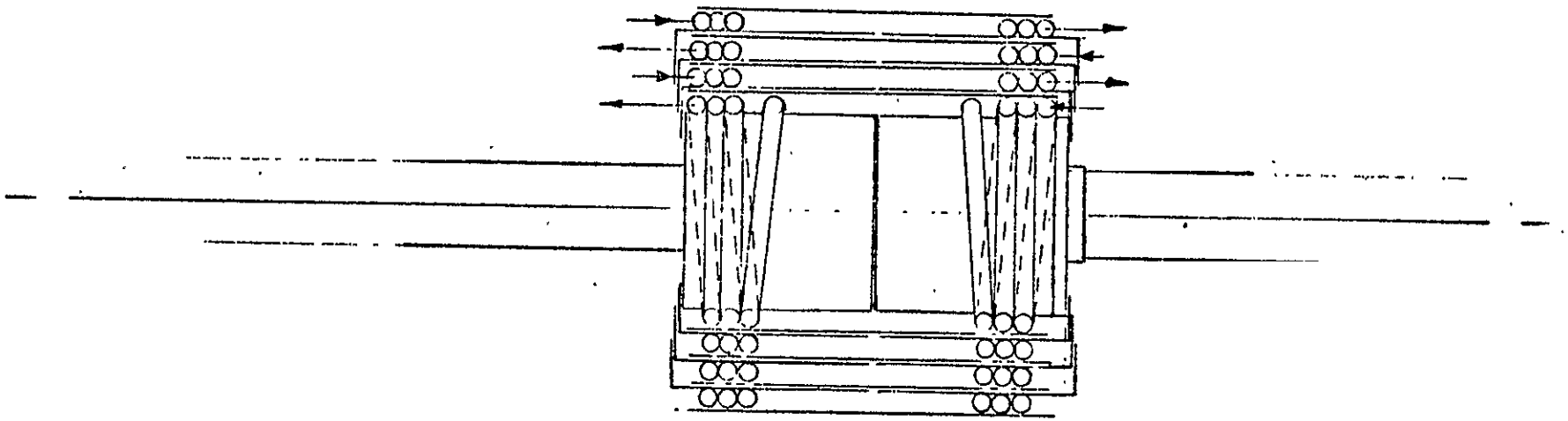

VOUGHT CORPORATION

FIGURE 48

FLEXHOSE/REEL WEIGHT

INCLUDES F-21 WEIGHT

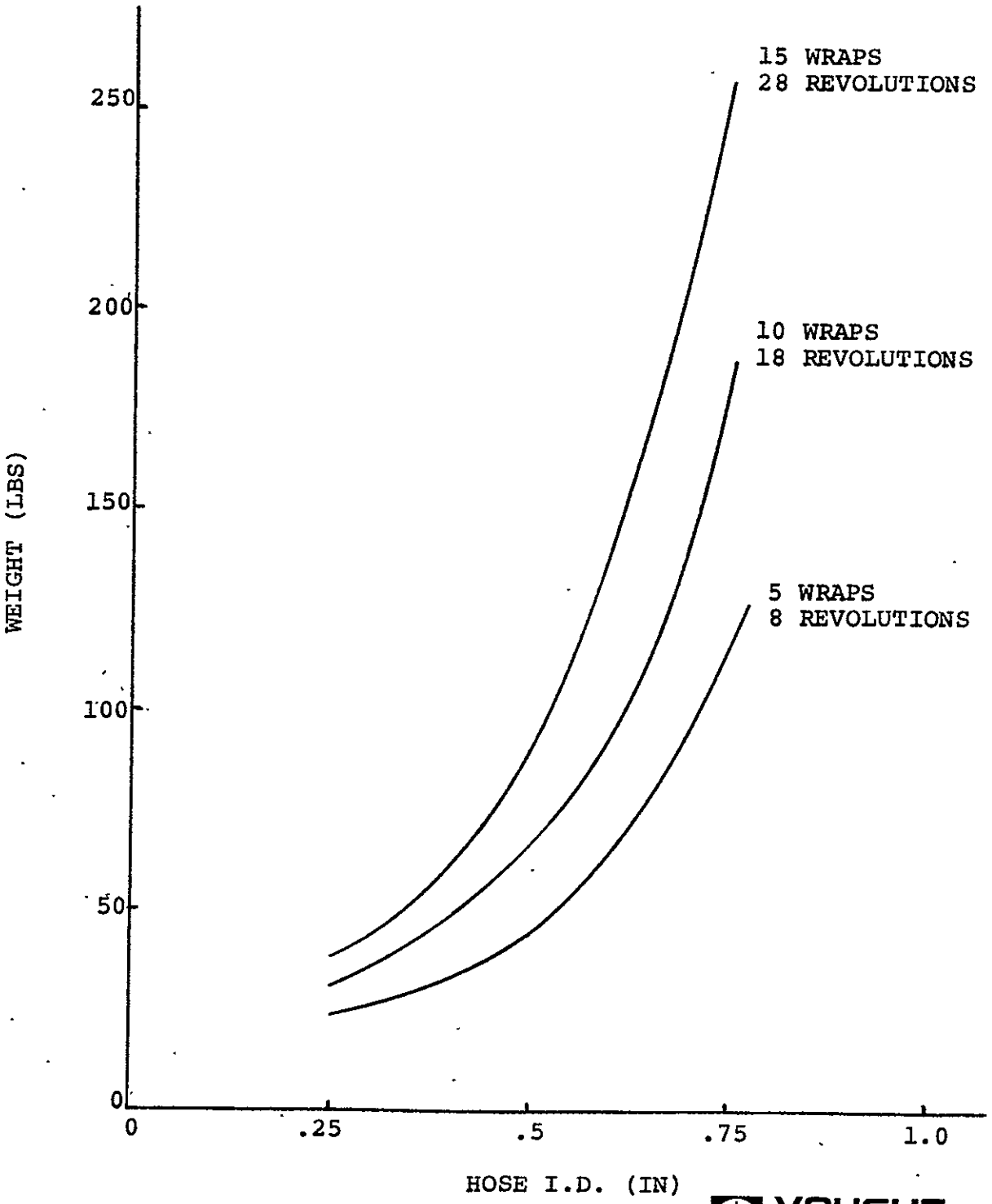

VOUGHT CORPORATION

FIGURE 49

FLEXHOSE/REEL VOLUME

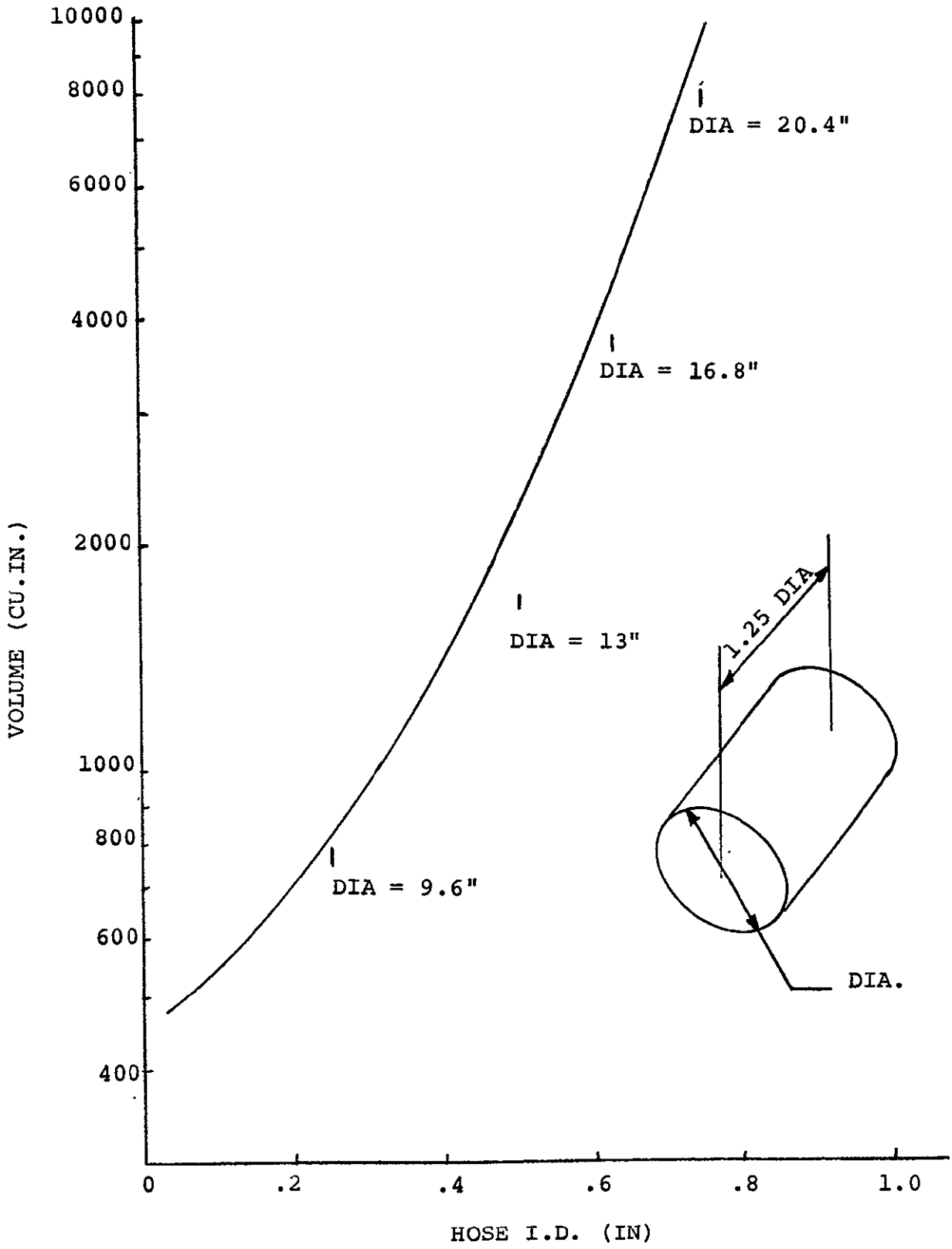

VOUGHT CORPORATION

FIGURE 50

FLEX HOSE/REEL PRESSURE DROP

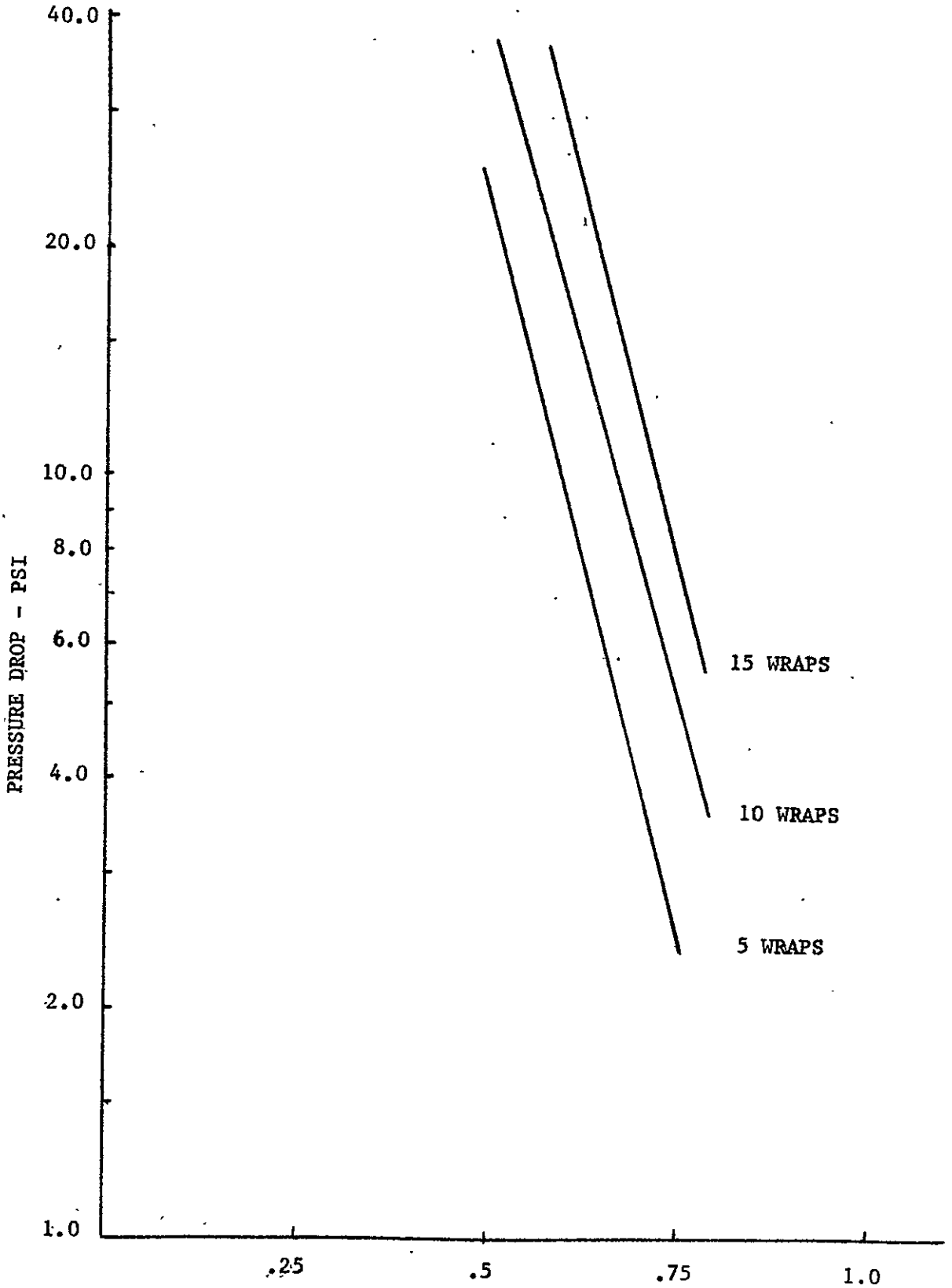

VOUGHT CORPORATION

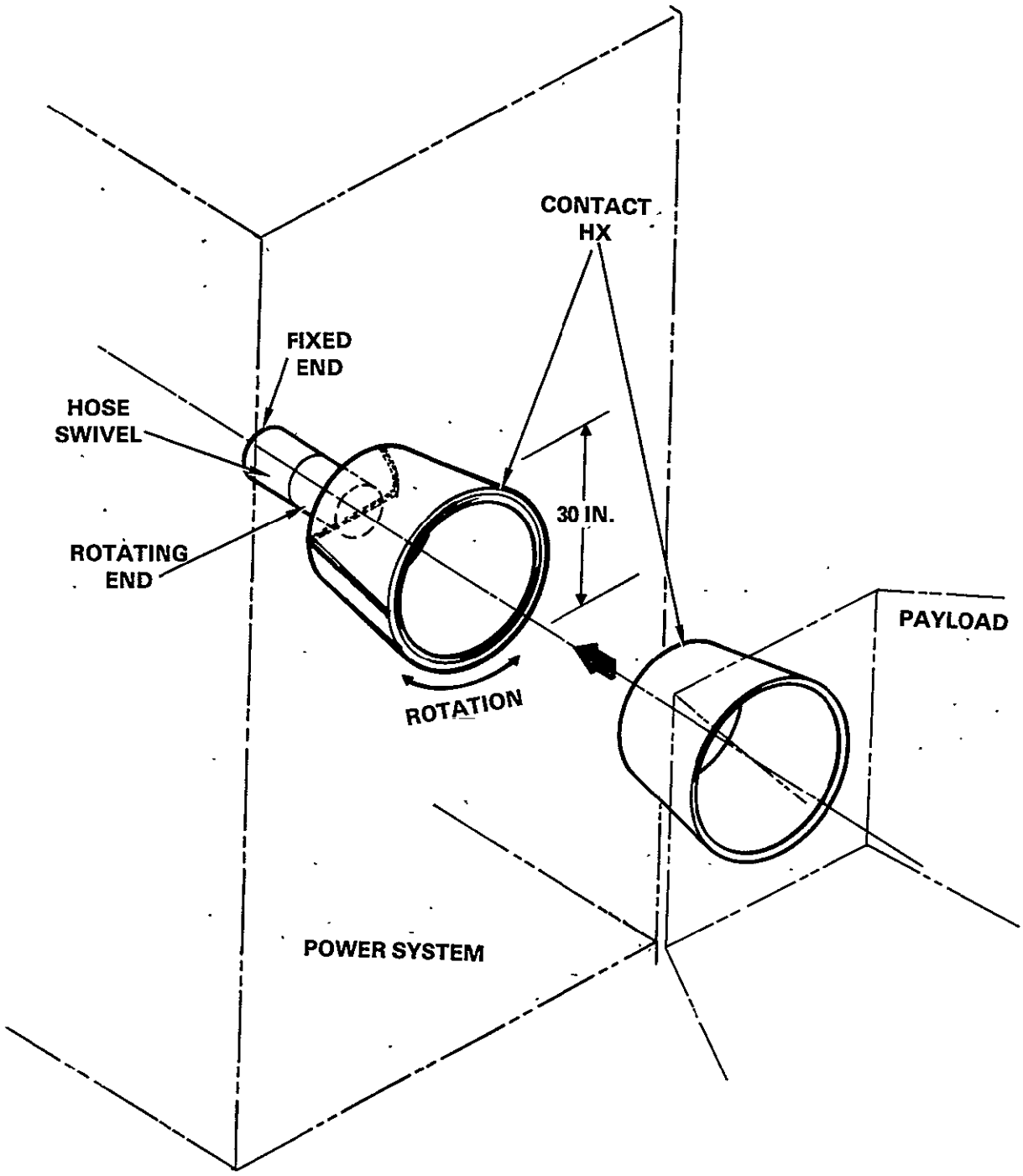

FIGURE 51
POWER SYSTEM/PAYLOAD
THERMAL INTERFACE CONCEPT

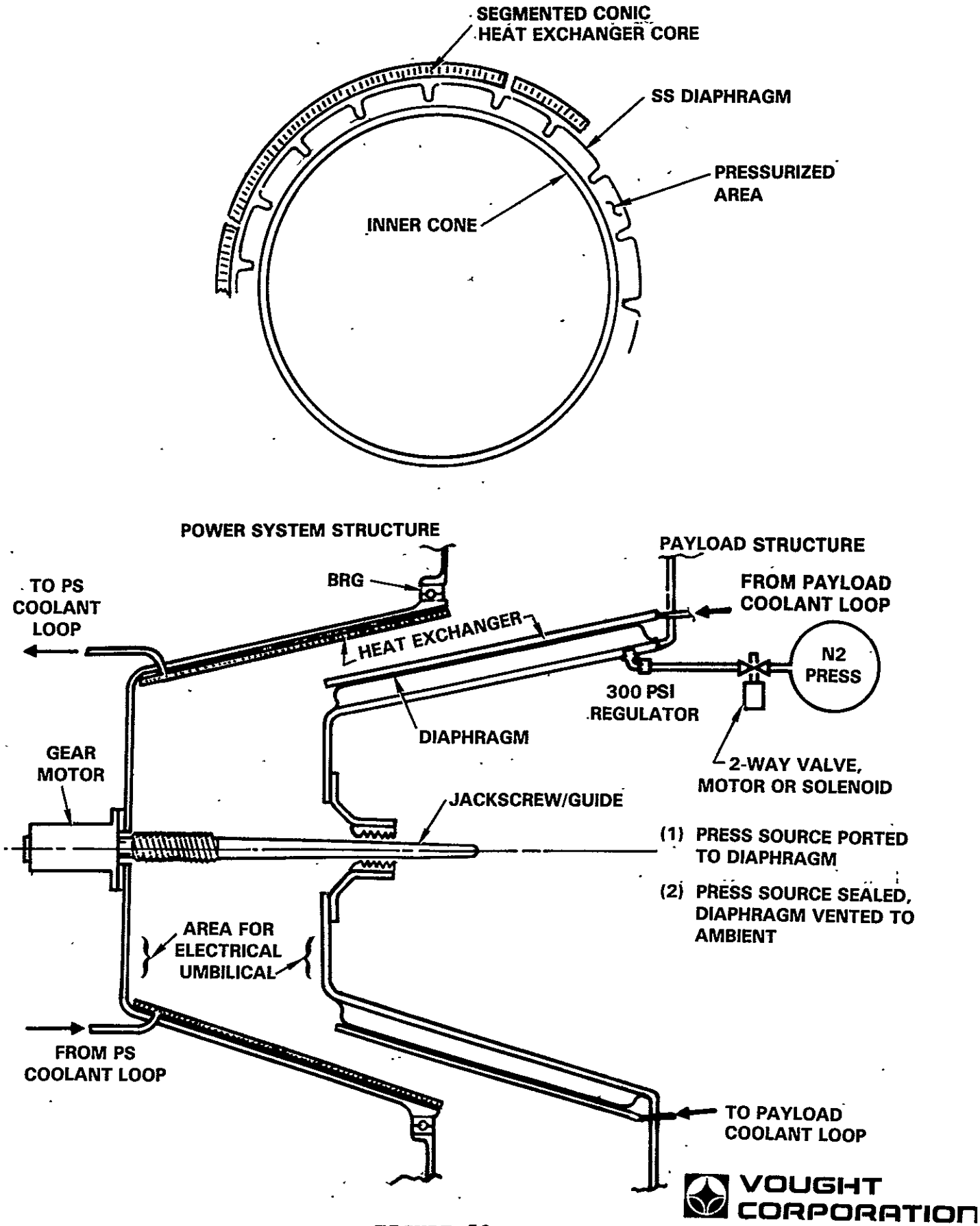

FIGURE 52
CONICAL CONTACT HEAT EXCHANGER CONCEPT

FIGURE 53
POWER SYSTEM TCS SCHEMATIC

VOUGHT

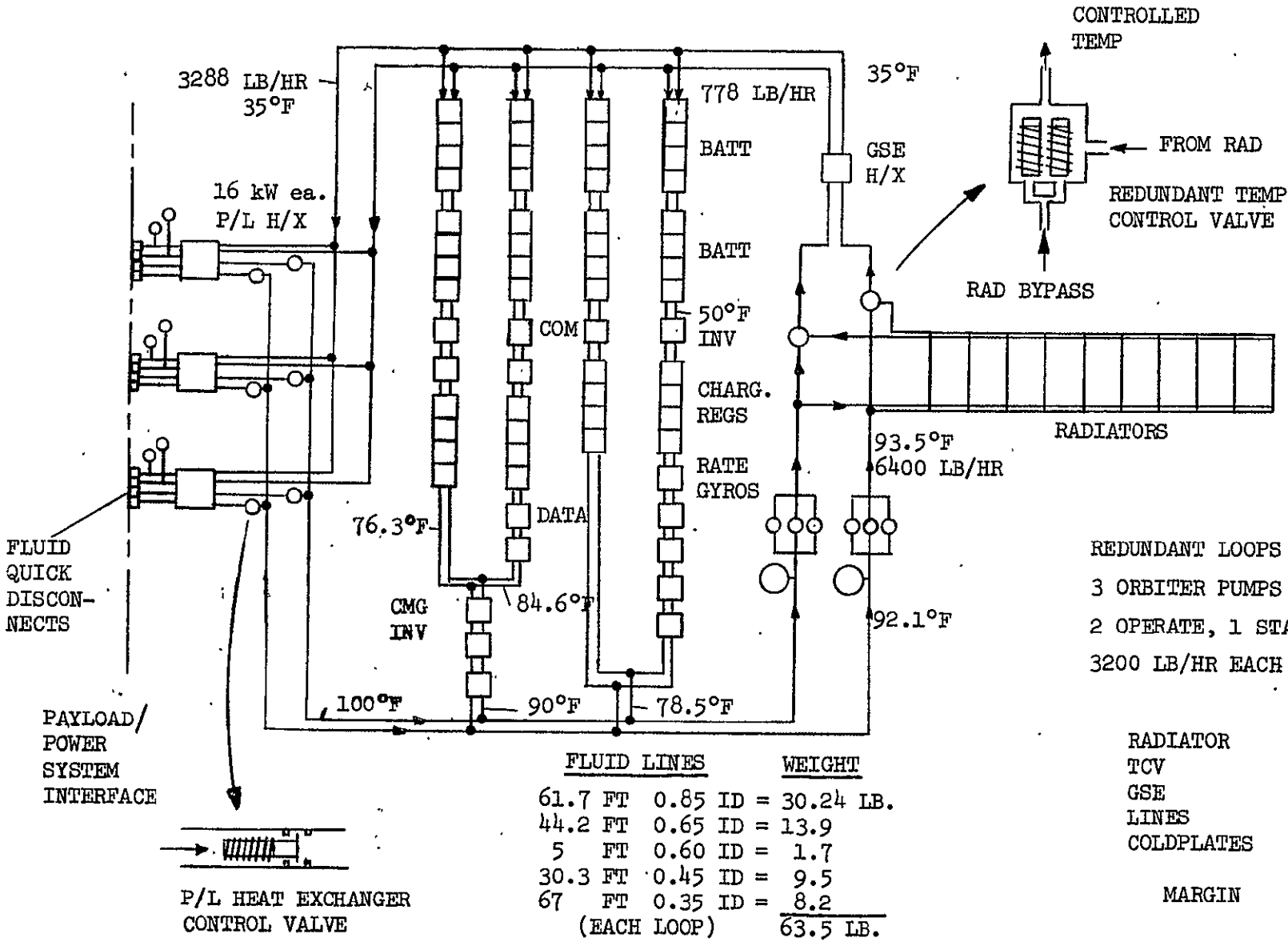

FLUID LINES				WEIGHT
61.7 FT	0.85 ID	=		30.24 LB.
44.2 FT	0.65 ID	=		13.9
5 FT	0.60 ID	=		1.7
30.3 FT	0.45 ID	=		9.5
67 FT	0.35 ID	=		8.2
(EACH LOOP)				63.5 LB.

REDUNDANT LOOPS (ONE STANDBY)

3 ORBITER PUMPS EACH LOOP

2 OPERATE, 1 STANDBY

3200 LB/HR EACH AT 64 PSI

	ΔP
RADIATOR	30.0
TCV	6.0
GSE	3.0
LINES	8.8
COLDPLATES	3.0
	50.8 PSI
MARGIN	13.2
	64

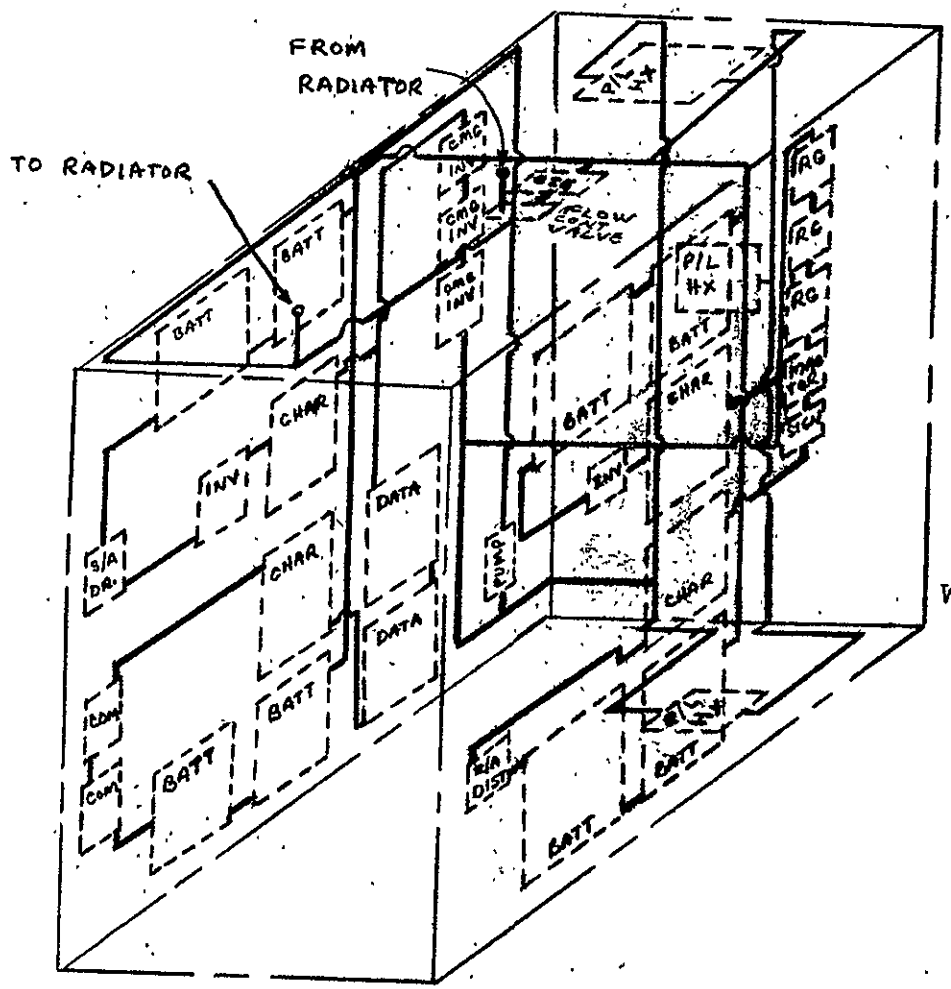

WEIGHT OPTIMIZED PLUMBING - POWER PENALTY = 350 LB/kW

FLUID LINES				WEIGHT
61.7 FT	0.85 ID	=	30.24 LB
44.2 FT	0.65 ID	=	13.9
5 FT	0.60 ID	=	1.7
30.3 FT	0.45 ID	=	9.5
67 FT	0.35 ID	=	8.2
(EACH LOOP)			63.5 LB

FIGURE 54 FLUID LINES ROUTING 25 kW POWER SYSTEM REFERENCE CONCEPT

FIGURE 55 SPACELAB COLDPLATE PRESSURE DROP DATA

THERMAL CONTROL SUBSYSTEM - PRELIMINARY DESIGN REVIEW

6.1 ANALYSIS - COLD PLATE/WATER & FREON PRESS. DROP VS MASS FLOW

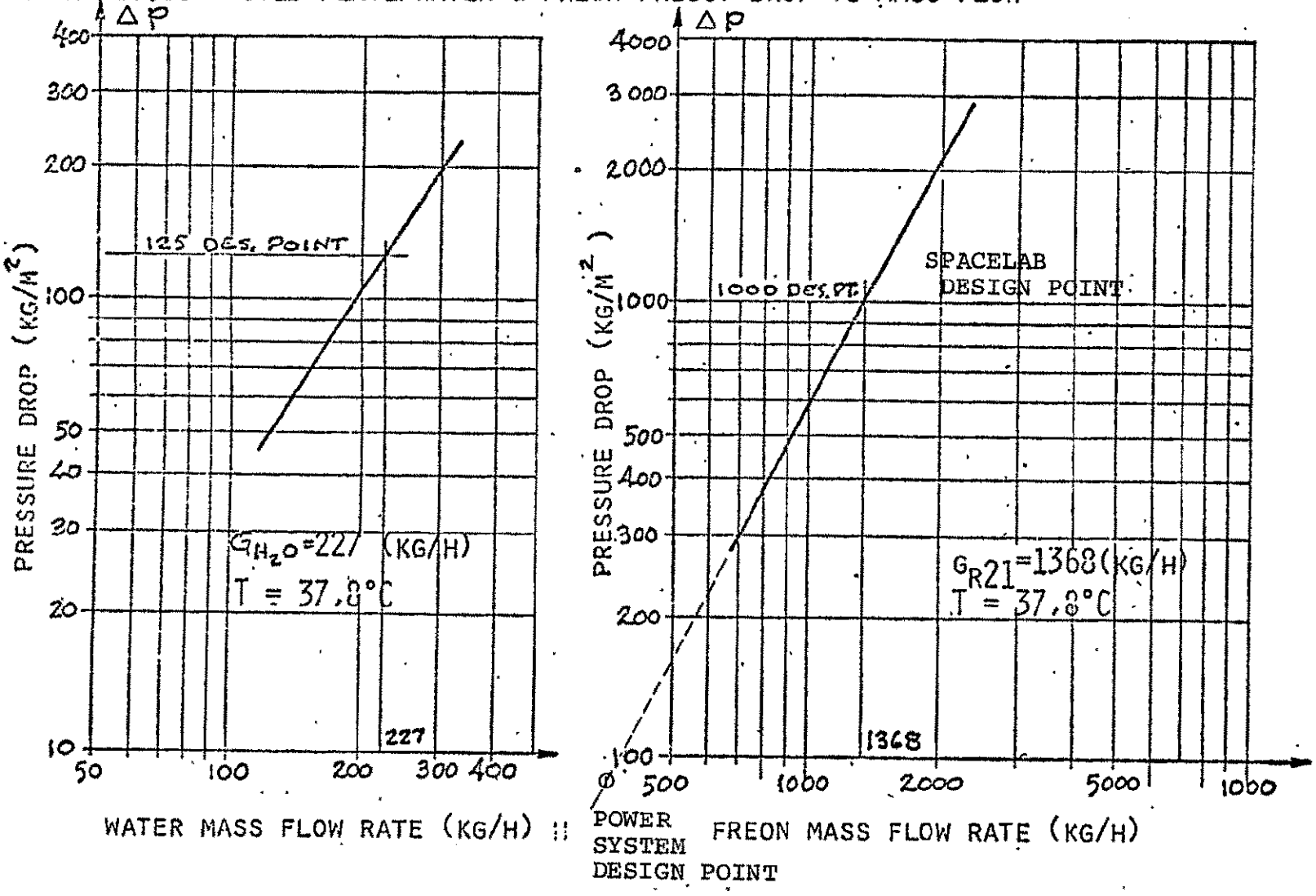

FIGURE 56 SPACELAB COLDPLATE THERMAL PERFORMANCE

THERMAL CONTROL SUBSYSTEM - PRELIMINARY DESIGN REVIEW

6.1 ANALYSIS - COLD PLATE PERFORMANCE/FREON

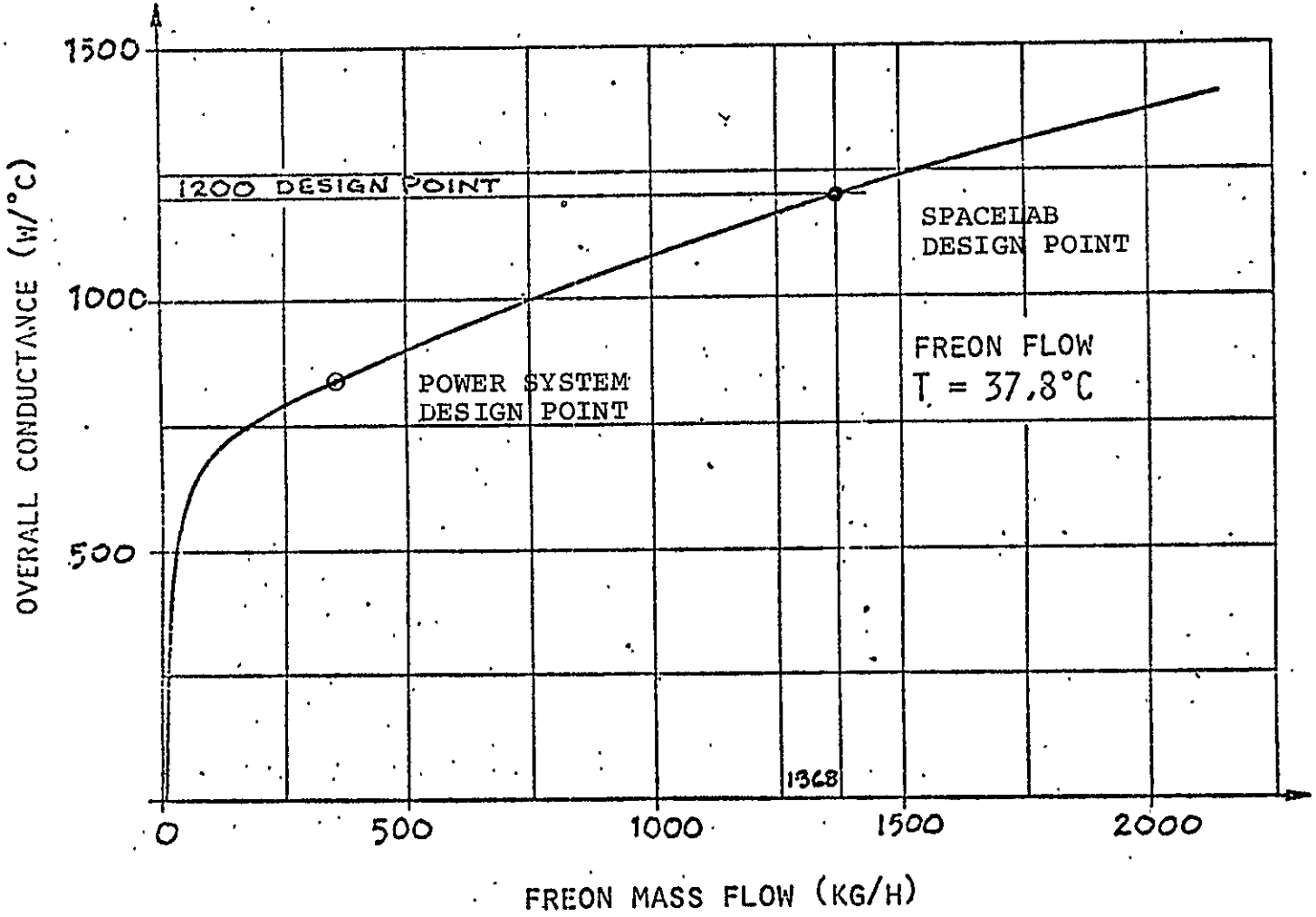

FIGURE 57

SPACE SHUTTLE FREON 21 PUMP PERFORMANCE

MODEL 145660-200

FLUID TEMP:	DEMONSTRATED -65°F TO +120°F CAPABILITY -200°F TO +300°F
FLUID PRESSURE:	DEMONSTRATED 570 PSI PROOF
LEAKAGE:	$< 6.8 \times 10^{-4}$ SCC/SEC HELIUM @ 380 PSI

MATERIALS IN CONTACT WITH FLUID

- STAINLESS STEEL (PASSIVATED)
- ALUMINUM (ANODIZED)
- CARBON - GRAPHITE
- CHROME
- TEFLON SEALS

LIFE:	28000 HRS. DEMONSTRATED AND STILL RUNNING (DECEMBER 1980)
WEIGHT:	3.9 LBS.
VOLUME:	7.9" L x 3.5" DIA.

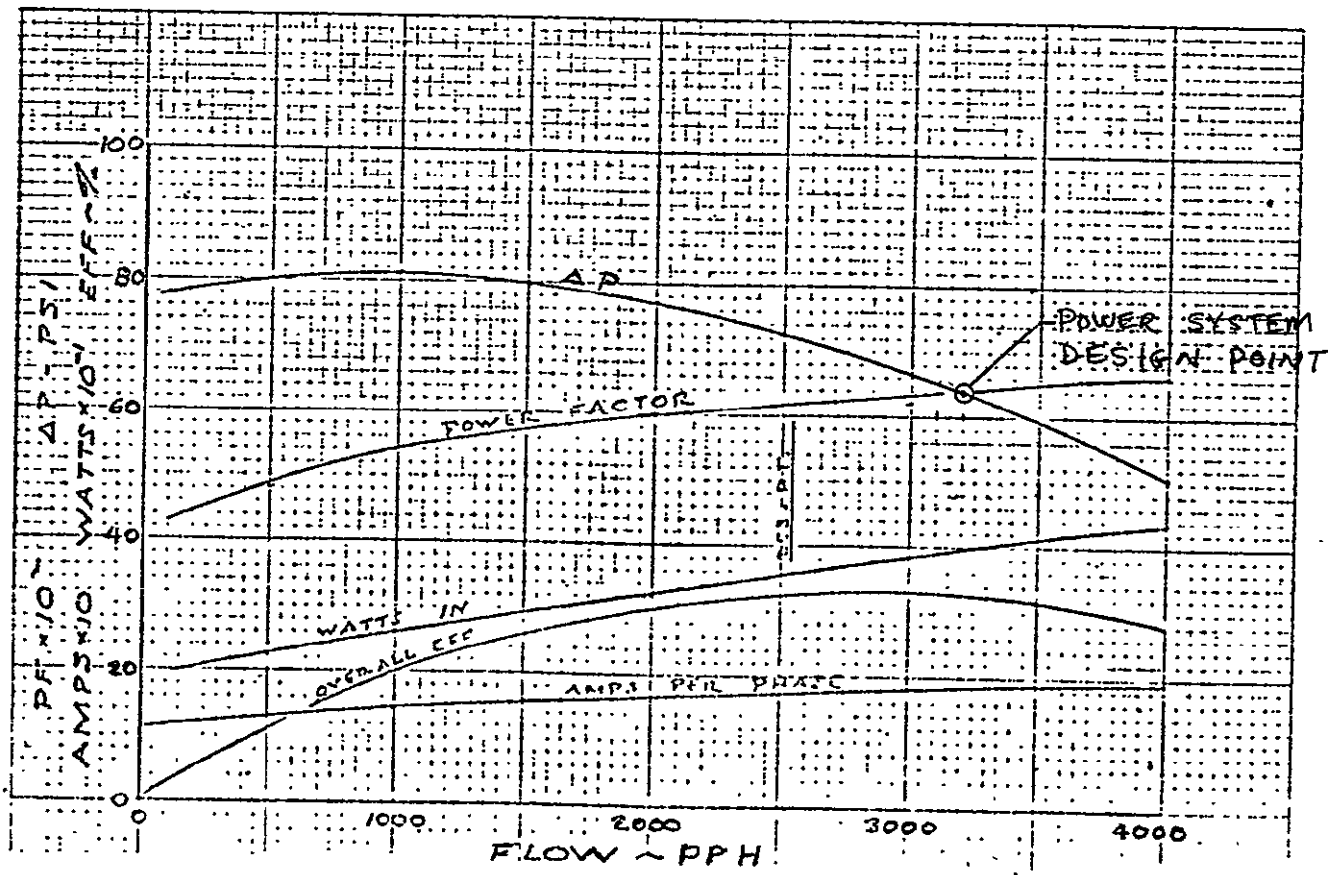

FIGURE 58 POWER SYSTEM/ORBITER ENVIRONMENT MODEL

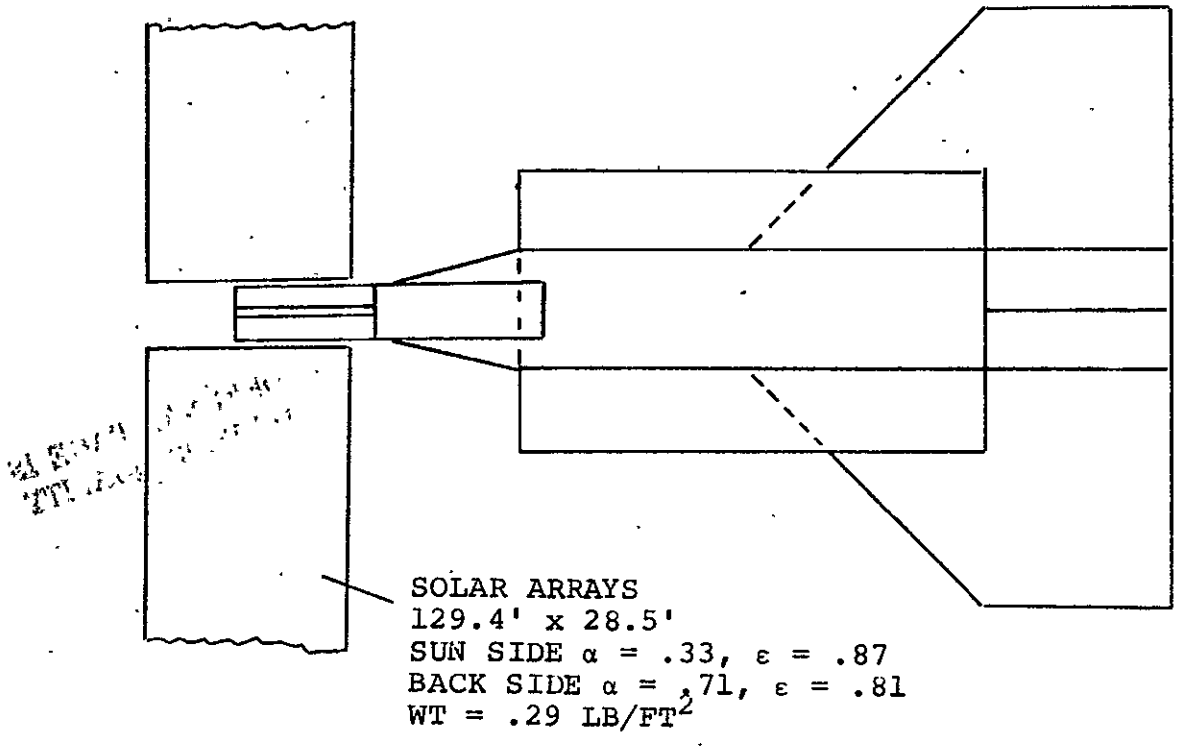

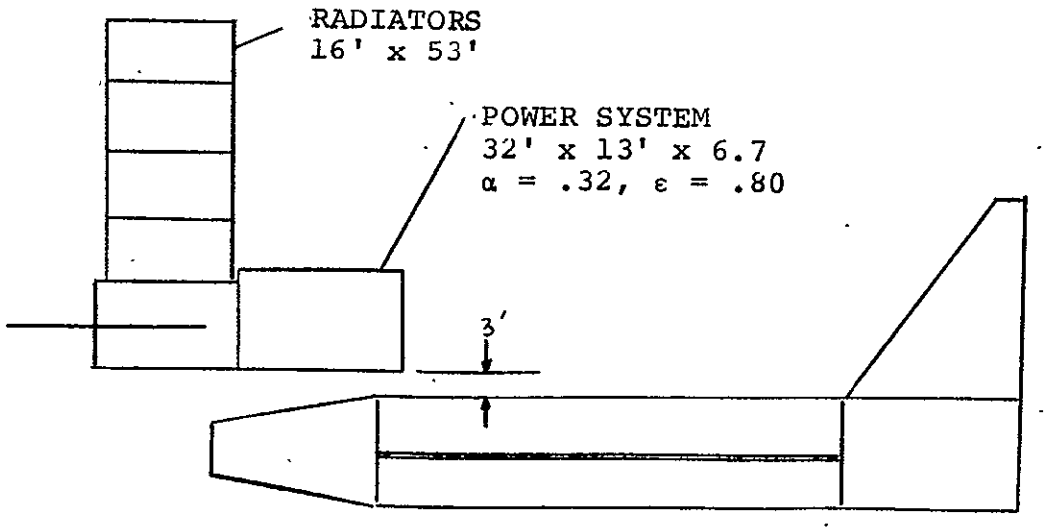

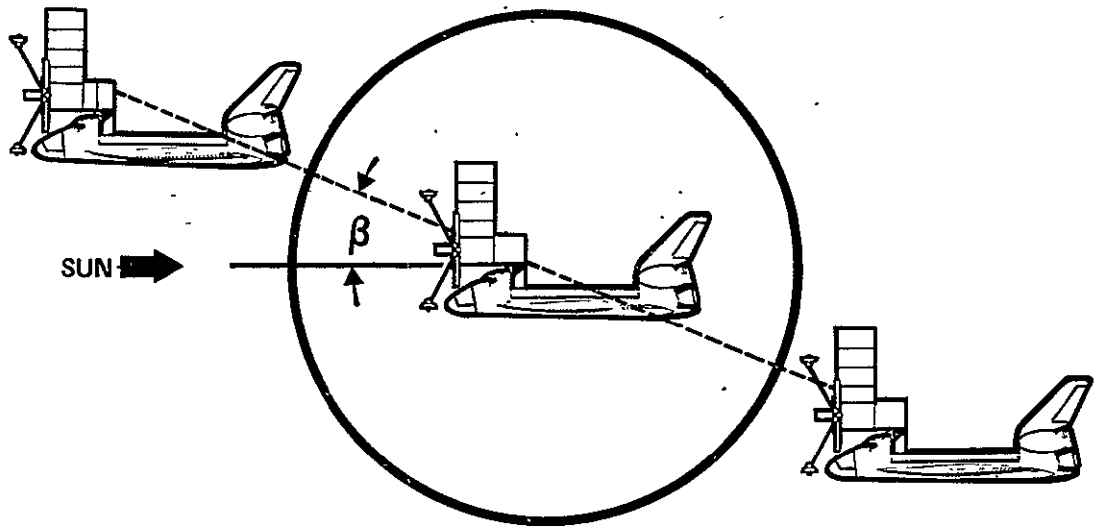

X AXIS PARALLEL TO SUN LINE (PSL)

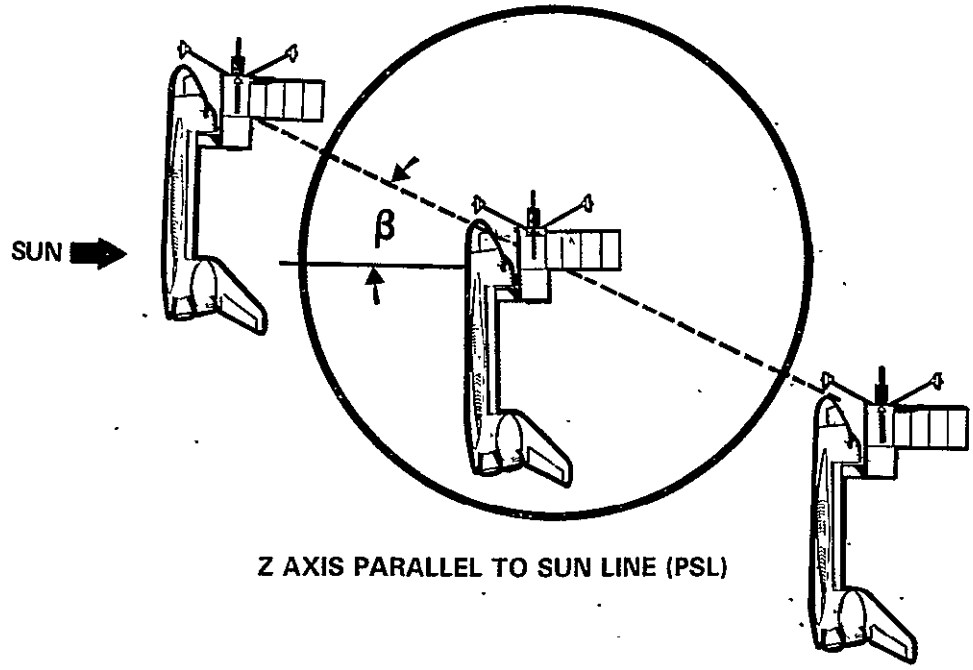

Z AXIS PARALLEL TO SUN LINE (PSL)

T_{SINK} – °F

	Z-PSL				X-PSL			
	α				α			
β	0.11	0.20	0.30	0.50	0.11	0.20	0.30	0.50
0	–57	–49	–41	–26	–87	–79	–69	–53
28.5	–60				–90			
57	–63				–93			
90	–66				–96			

DESIGN CONDITION IS Z-PSL, $\beta = 0°$

G0-1078-17

FIGURE 59 **RADIATOR THERMAL ENVIRONMENT STUDY RESULTS**

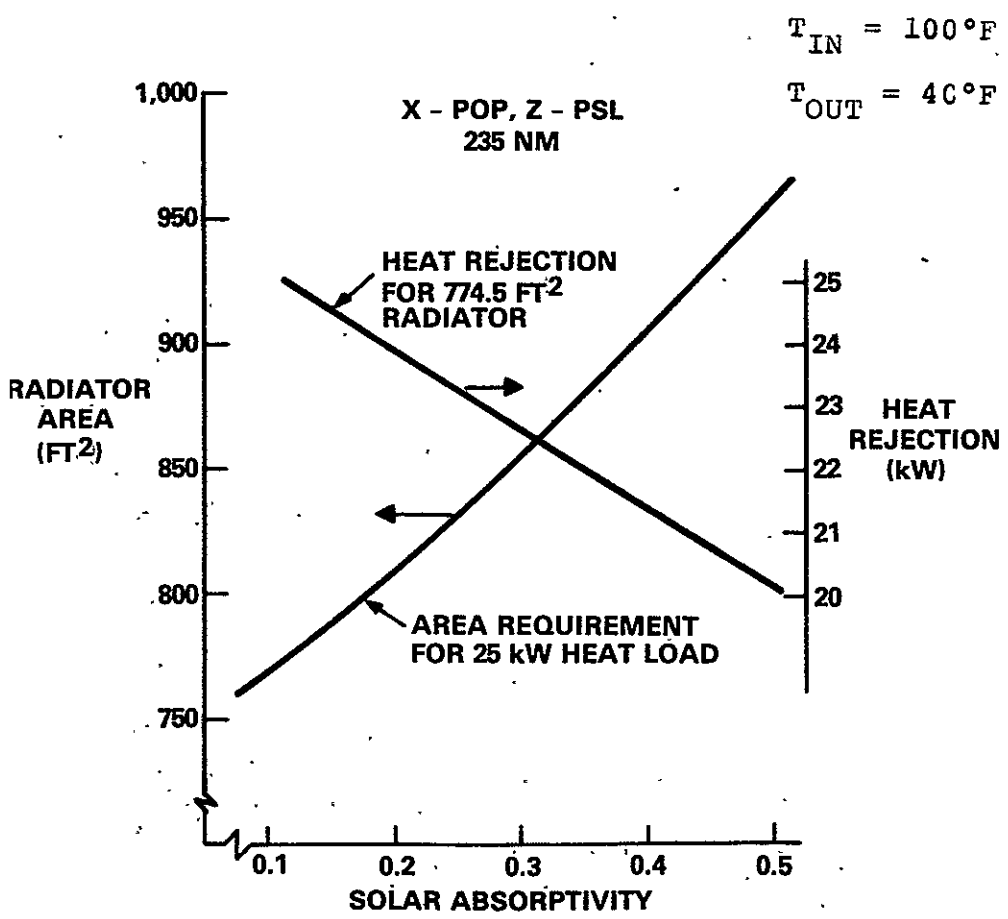

FIGURE 60
EFFECT OF SOLAR ABSORPTIVITY ON RADIATOR PERFORMANCE

G0-1078-13

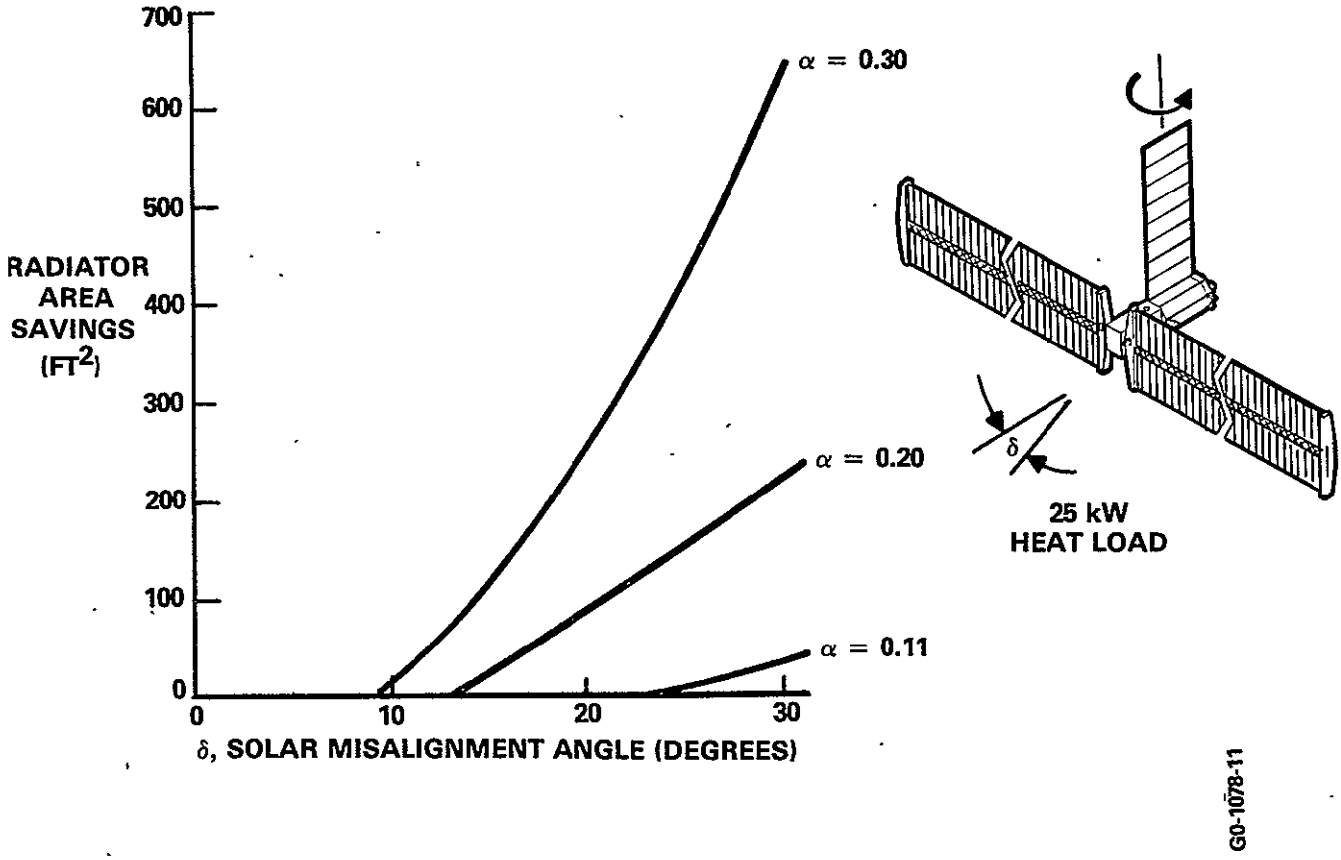

FIGURE 61
SOLAR AVOIDANCE BENEFITS

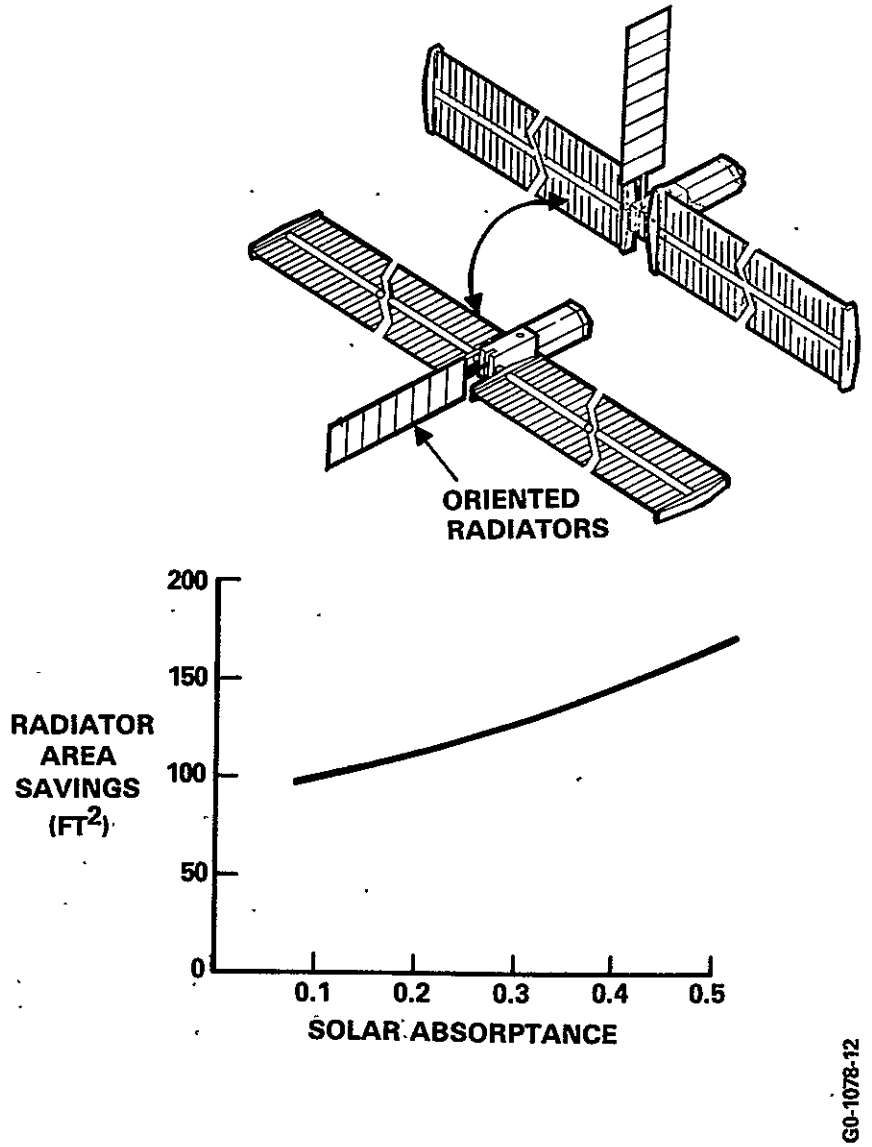

FIGURE 62 SOLAR ARRAY AVOIDANCE BENEFITS

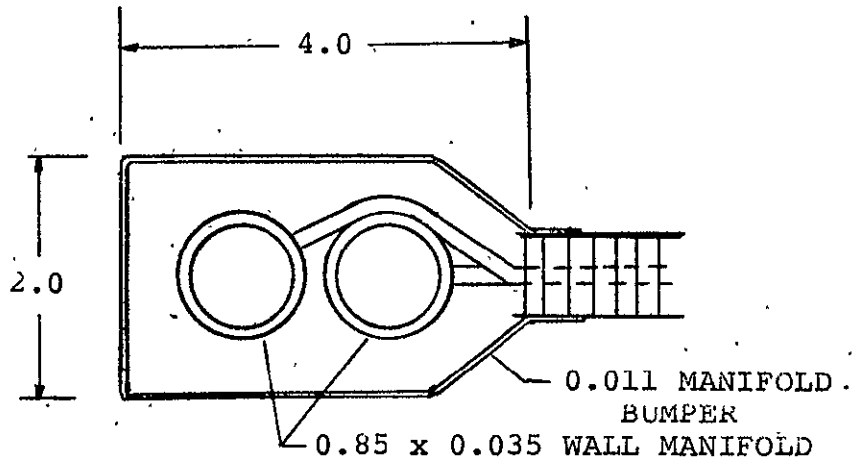

A-A MANIFOLD DETAIL

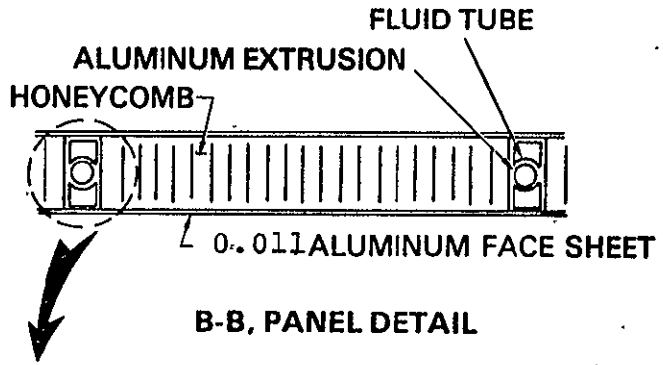

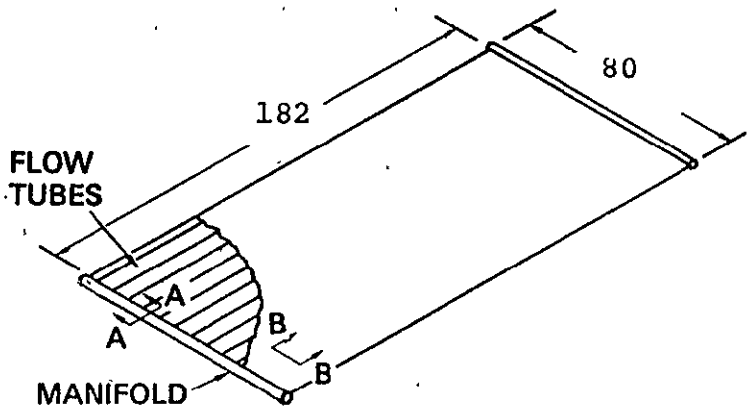

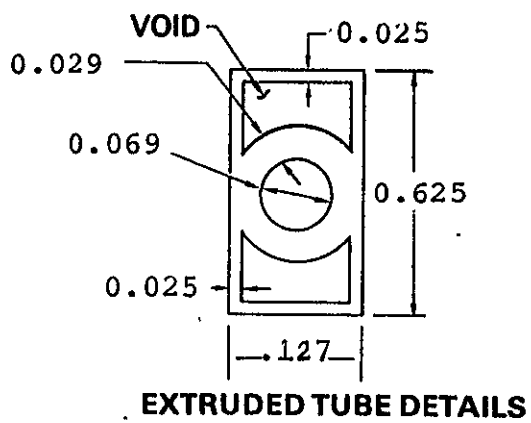

FIGURE 63 RADIATOR PANEL PRELIMINARY DESIGN

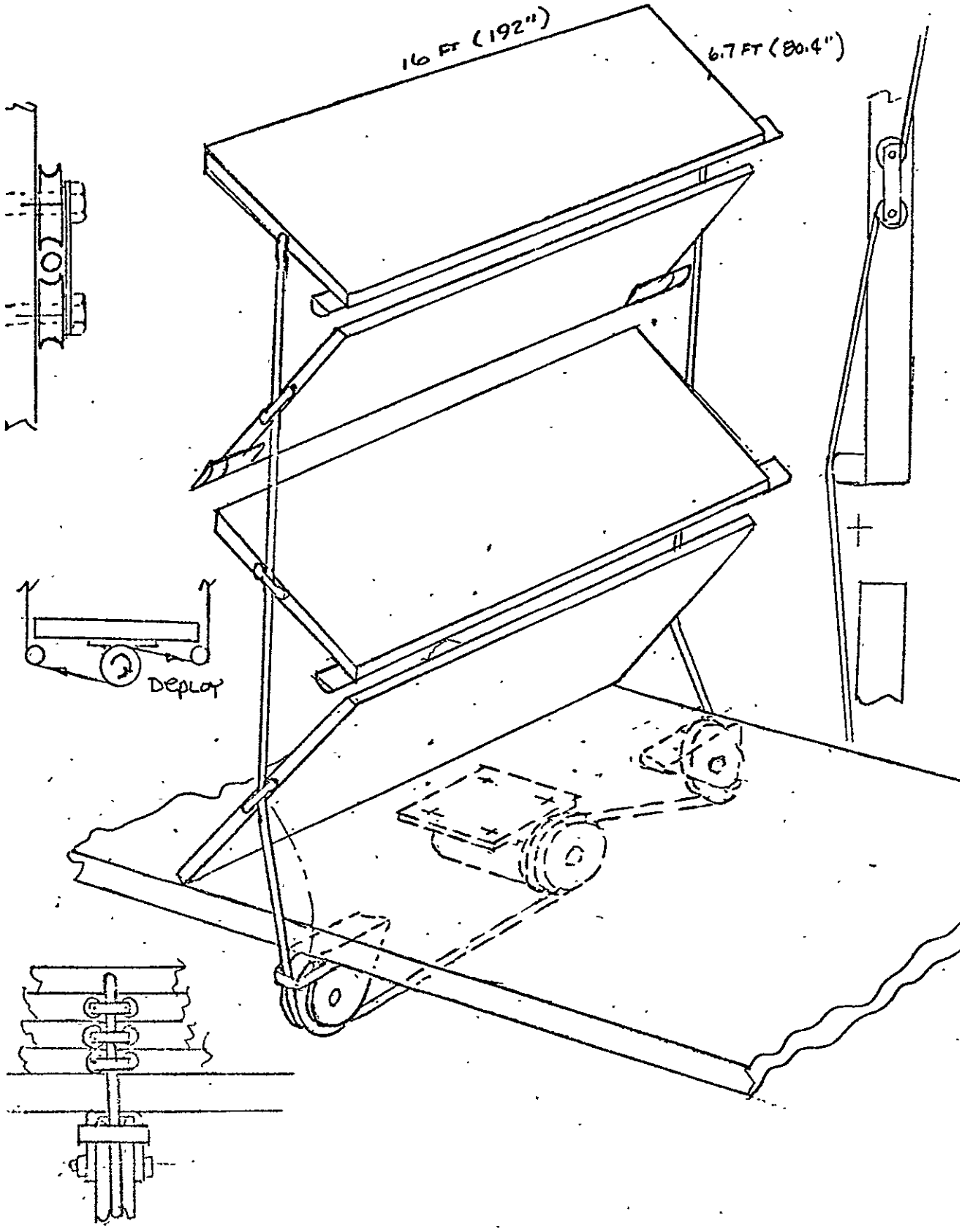

FIGURE 64

DRUM AND CABLE DEPLOYMENT SYSTEM

VOUGHT CORPORATION

FIGURE 65

HINGE LINE LOADS - SPRING LOADED HINGE CONCEPT

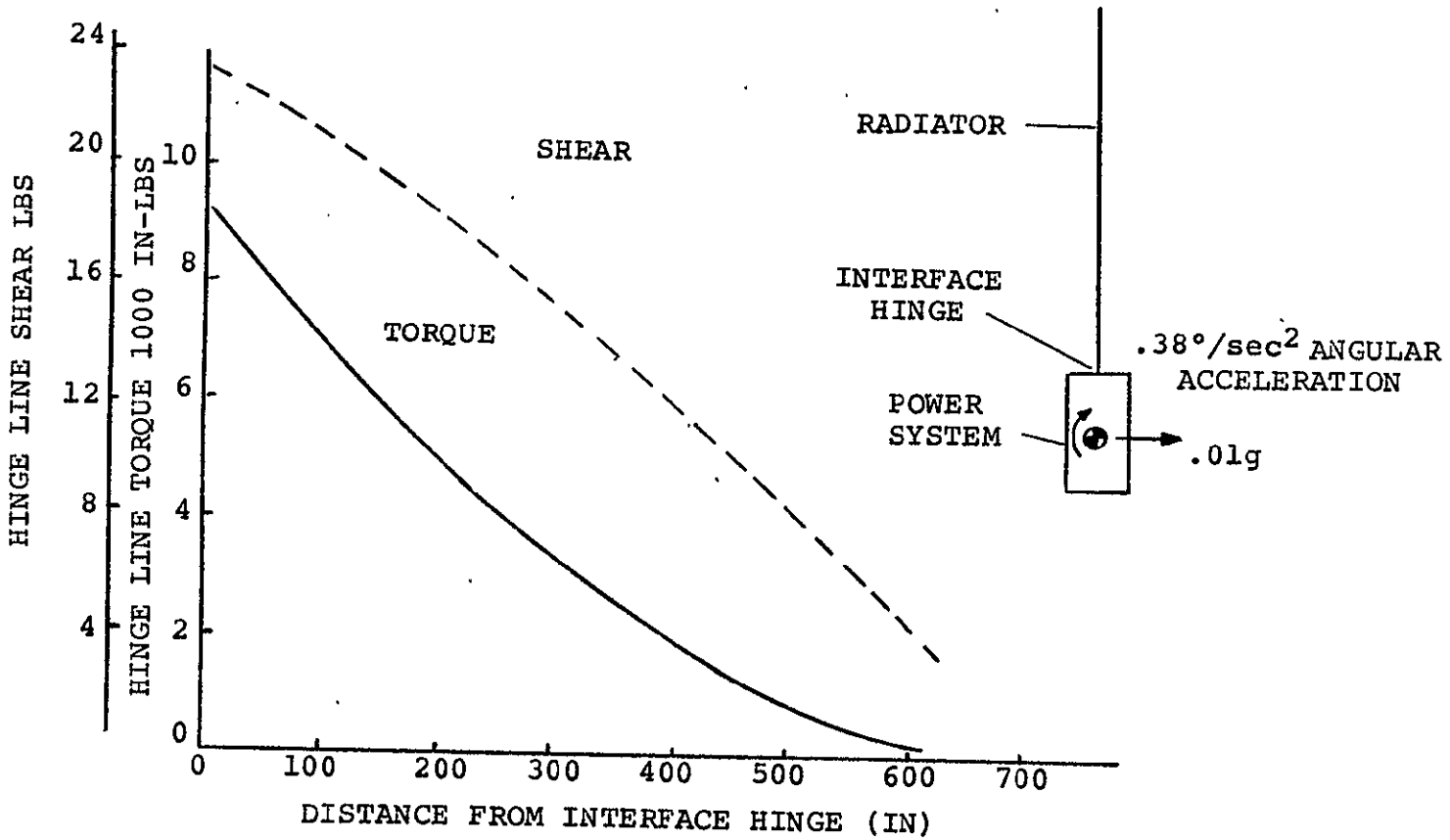

VOUGHT CORPORATION

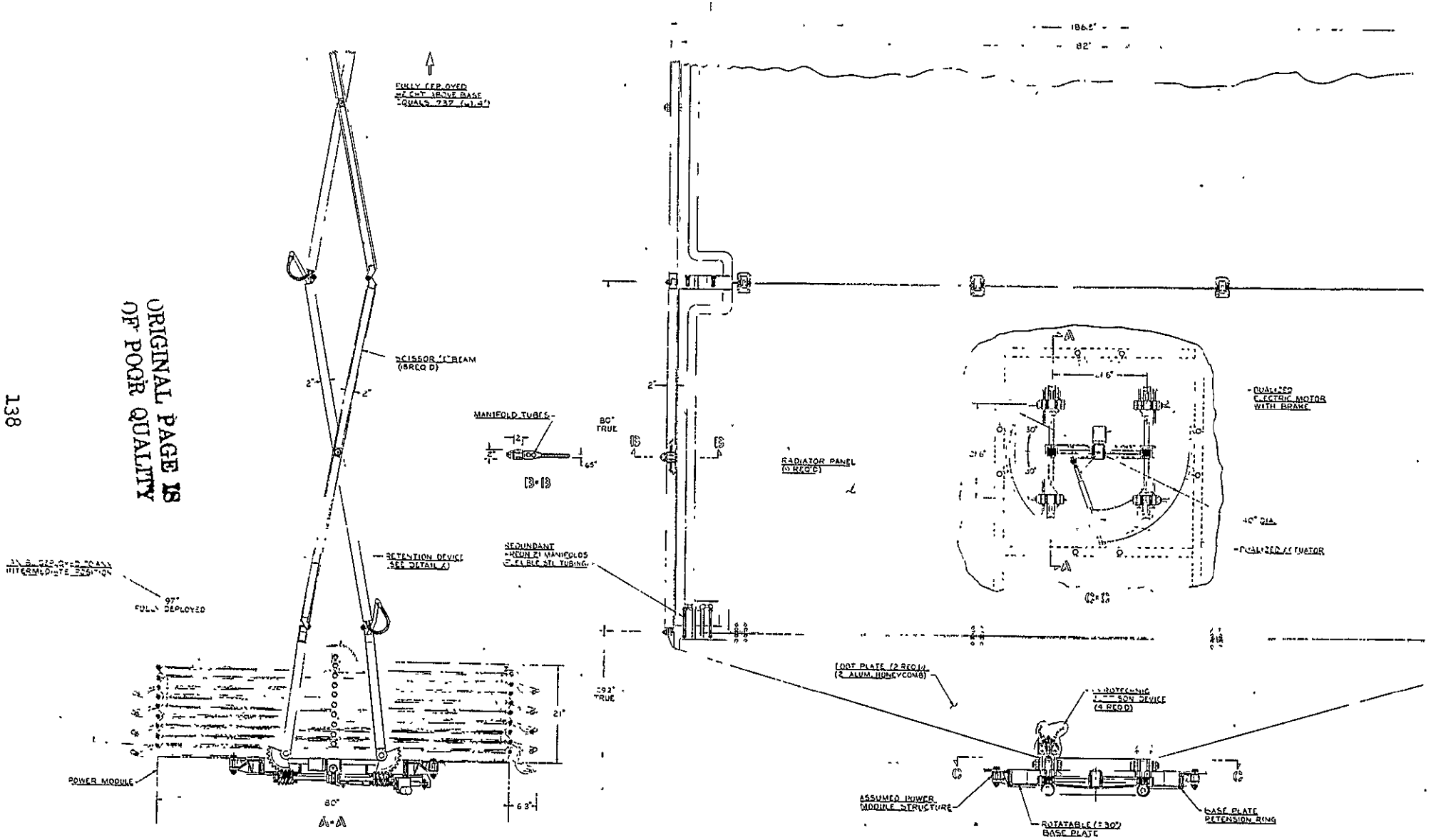

FIGURE 66 SCISSORS ARM DEPLOYMENT MECHANISM

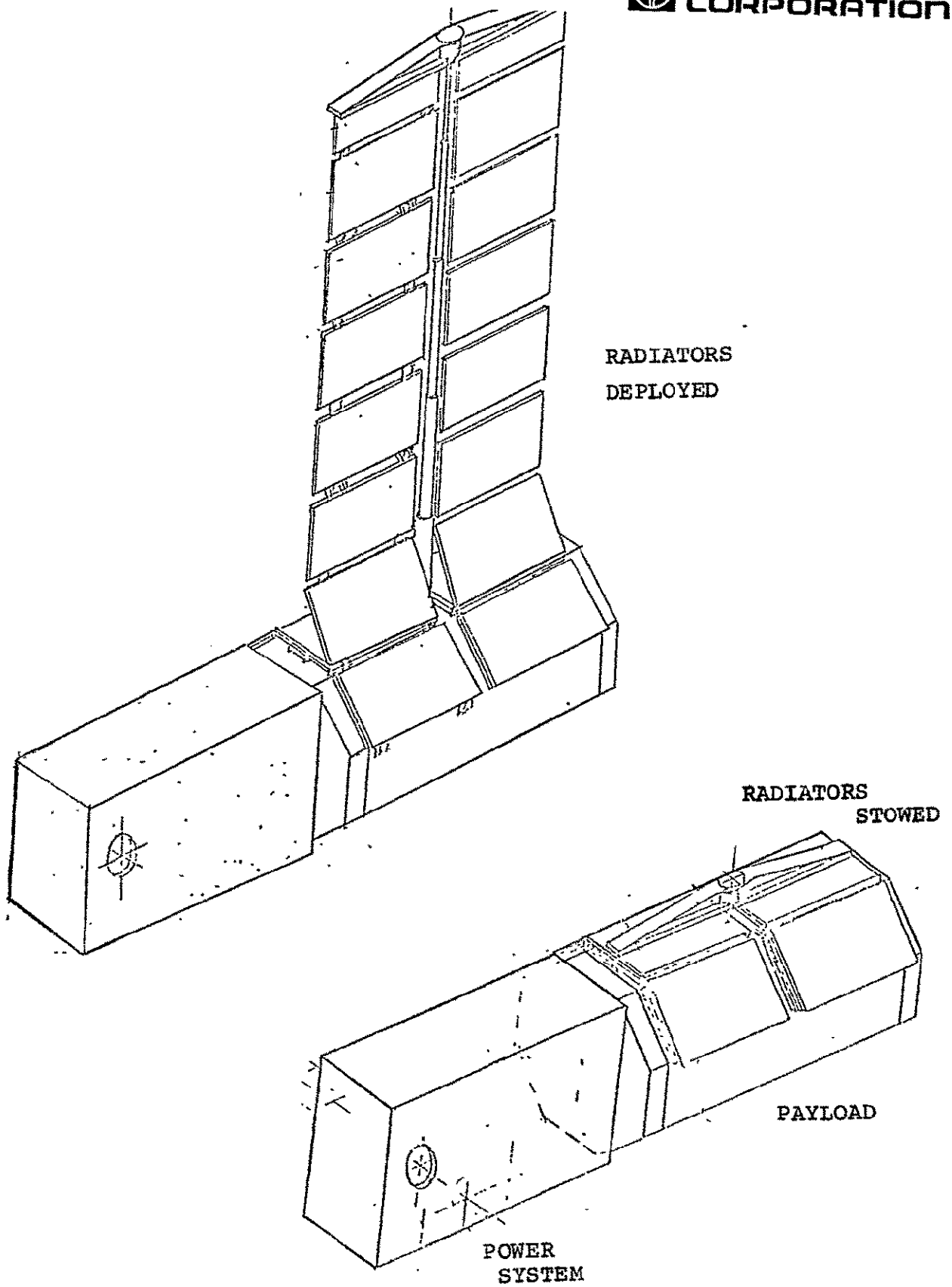

FIGURE 67 BOOM DEPLOYMENT CONCEPT

FIGURE 68 SPACE CONSTRUCTED RADIATOR ARRAY

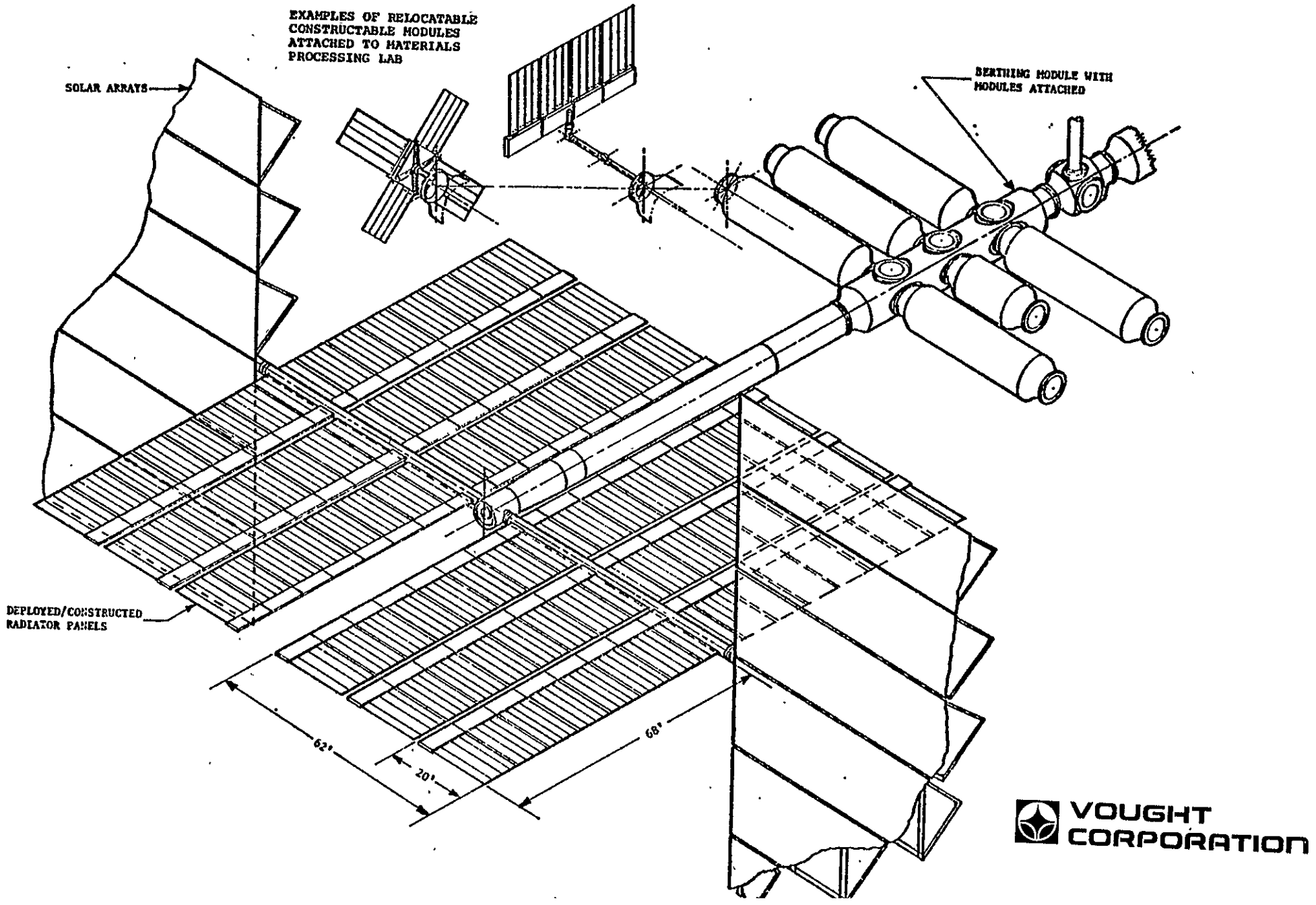

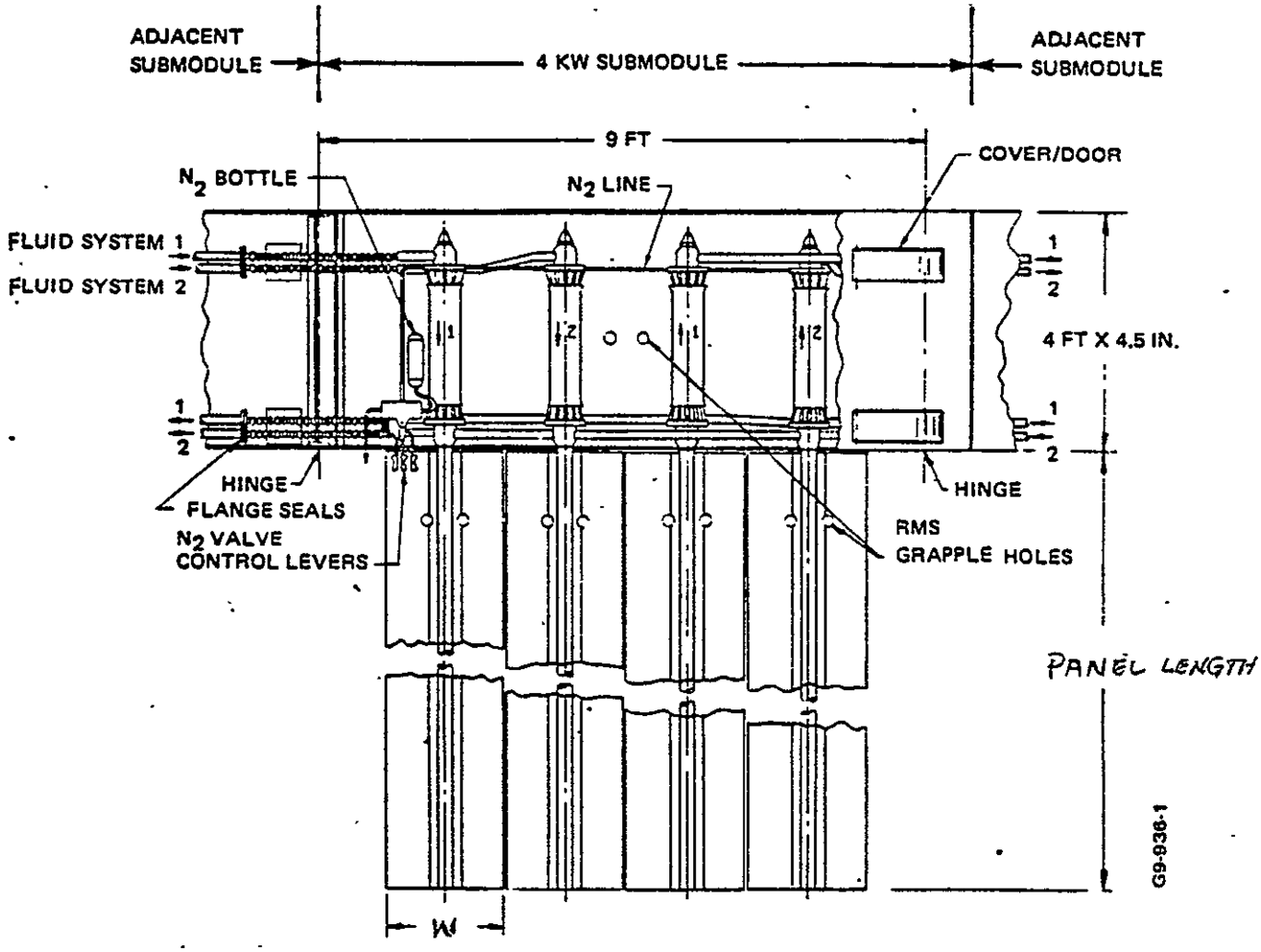

FIGURE 69 SPACE CONSTRUCTABLE RADIATOR SUBMODULE

FIGURE 70

SPACE CONSTRUCTABLE RADIATOR WEIGHT

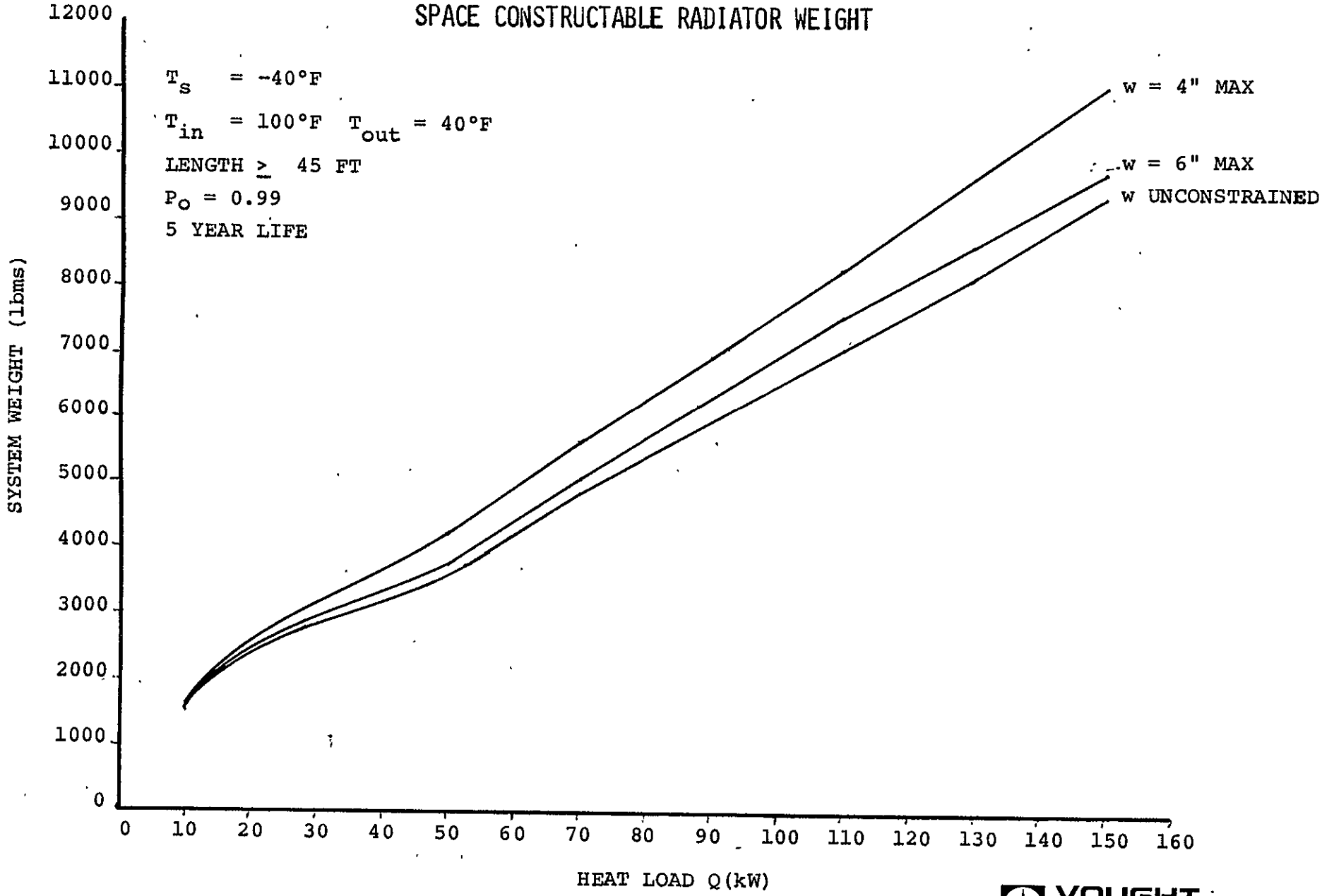

VOUGHT CORPORATION

FIGURE 71

SPACE CONSTRUCTABLE RADIATOR WEIGHT

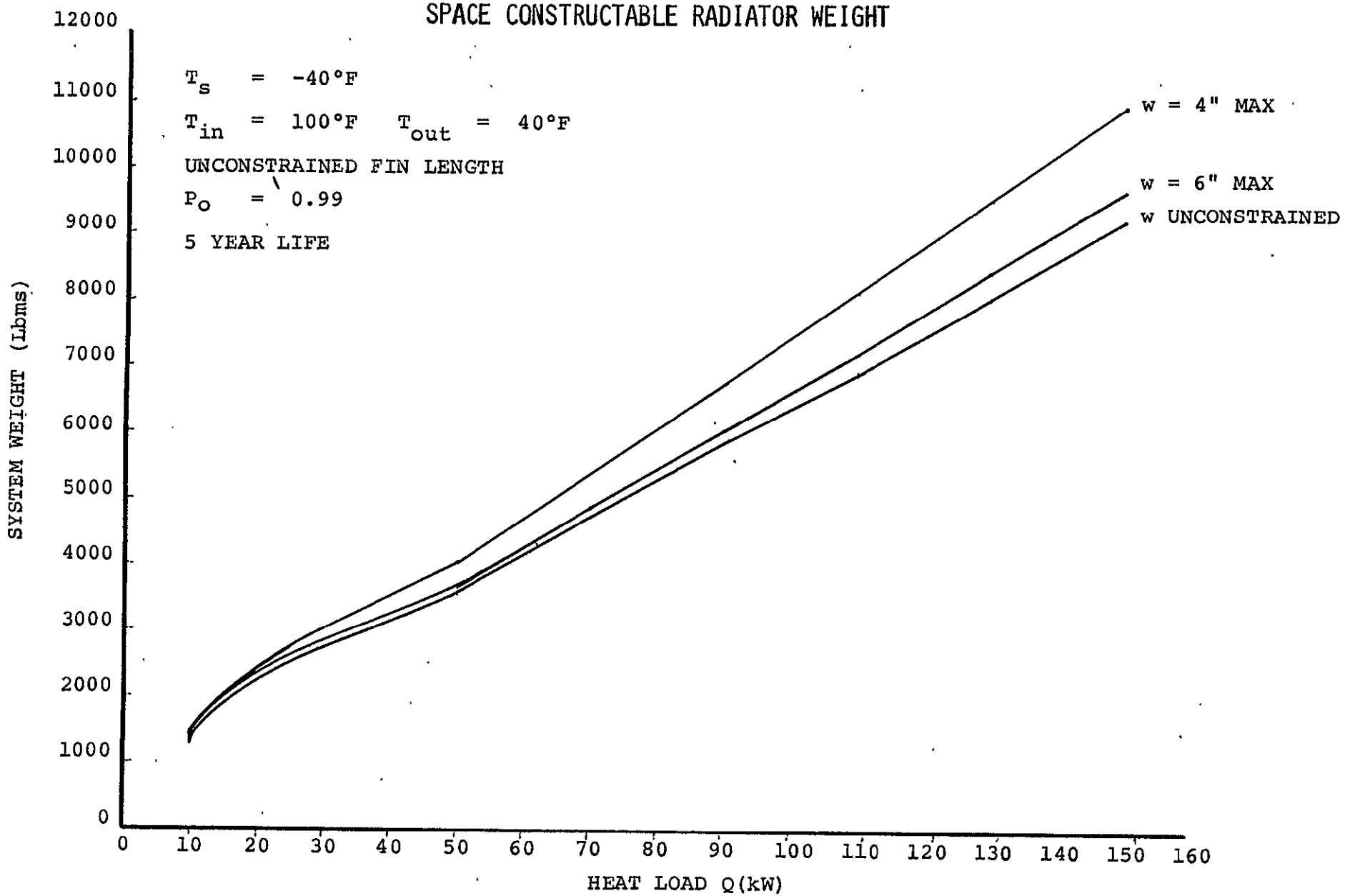

VOUGHT CORPORATION

VOUGHT CORPORATION

FIGURE 72
DEPLOYED RADIATOR
25KW POWER MODULE
FREQUENCY = 0.11 CPS

FIRST MODE

---- UNDEFORMED

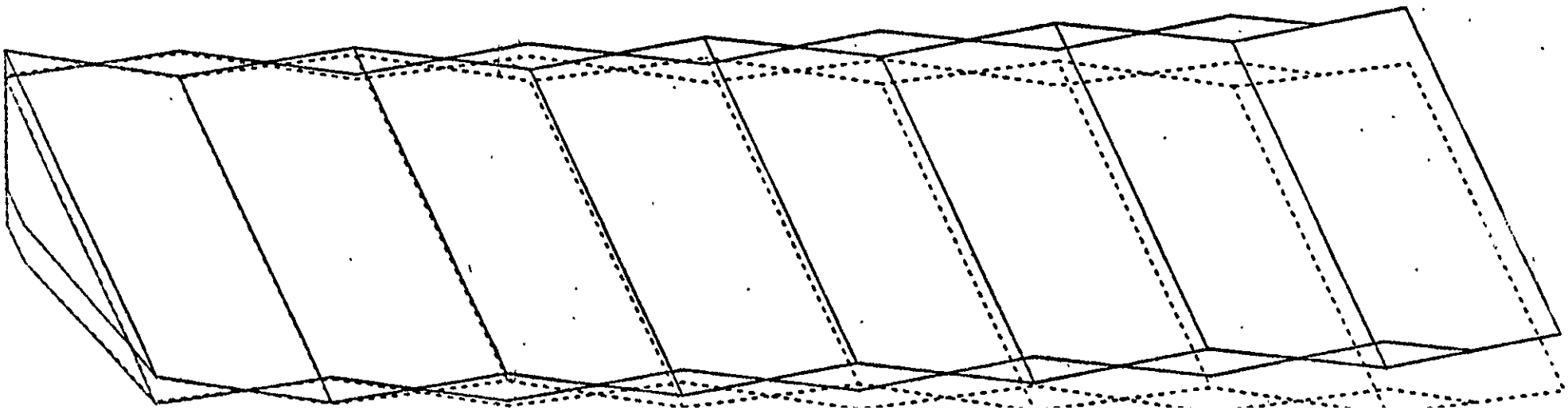

FIGURE 73
DEPLOYED RADIATOR
25KW POWER MODULE
FREQUENCY = 0.49 CPS

SECOND MODE

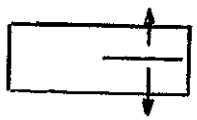

---- UNDEFORMED

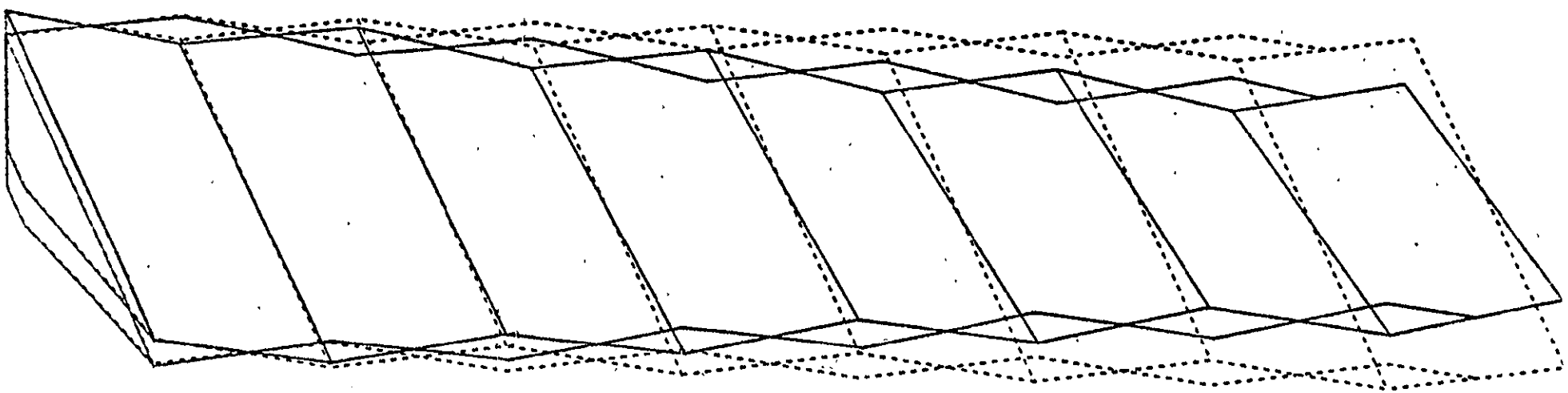

FIGURE 74
DEPLOYED RADIATOR
25KW POWER MODULE
FREQUENCY = 0.49 CPS

VOUGHT CORPORATION

THIRD MODE

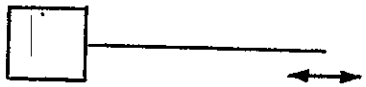

---- UNDEFORMED

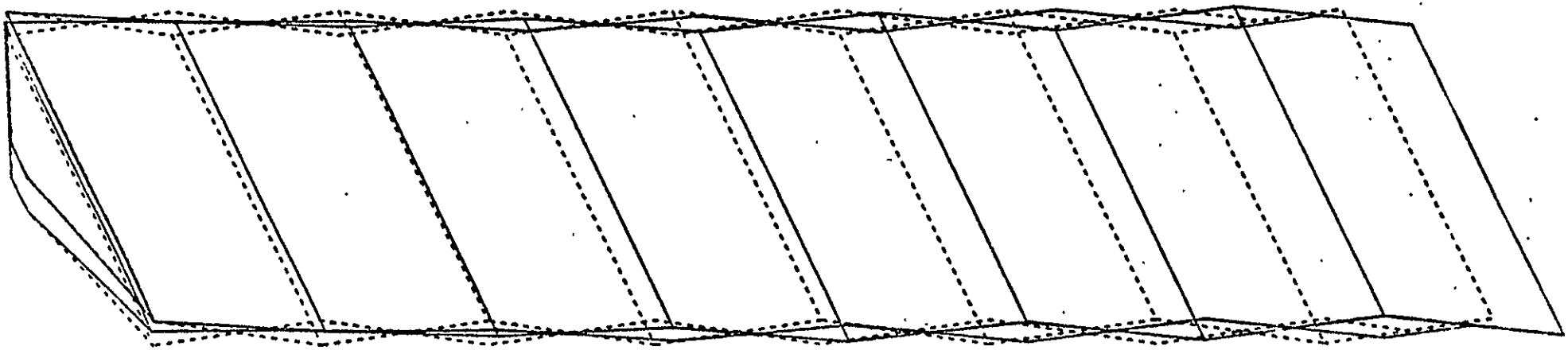

FIGURE 75
DEPLOYED RADIATOR
25KW POWER MODULE
FREQUENCY = 0.56 CPS

VOUGHT CORPORATION

FOURTH MODE

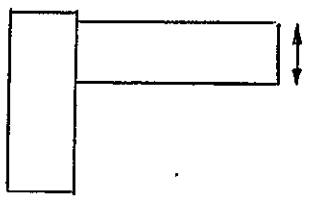

---- UNDEFORMED

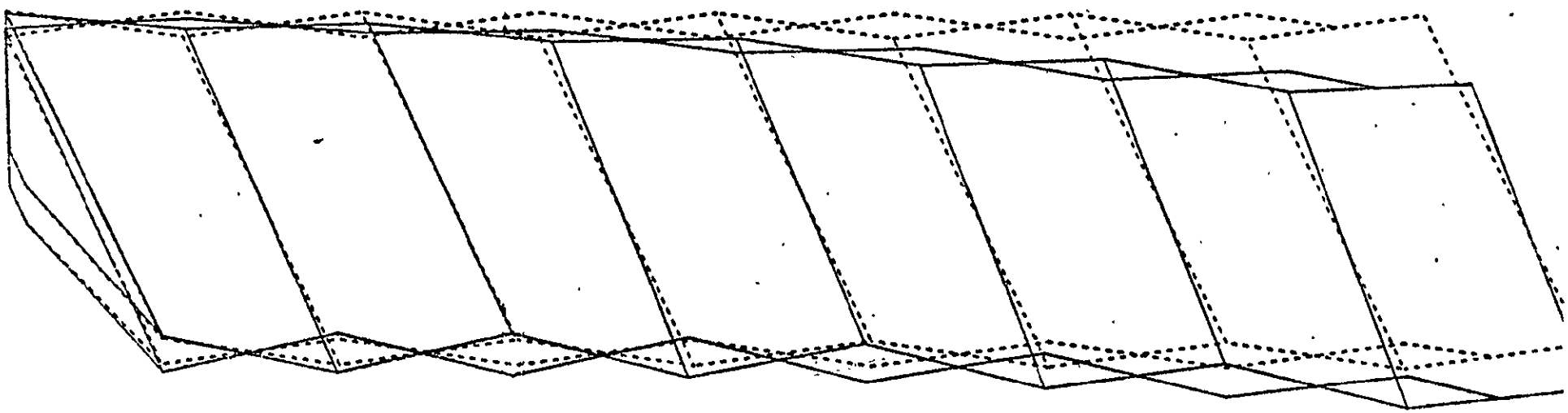

FIGURE 76
PARTIALLY DEPLOYED RADIATOR - 45 DEGS.
25KW POWER MODULE
FREQUENCY = 0.12 CPS

VOUGHT CORPORATION

FIRST MODE

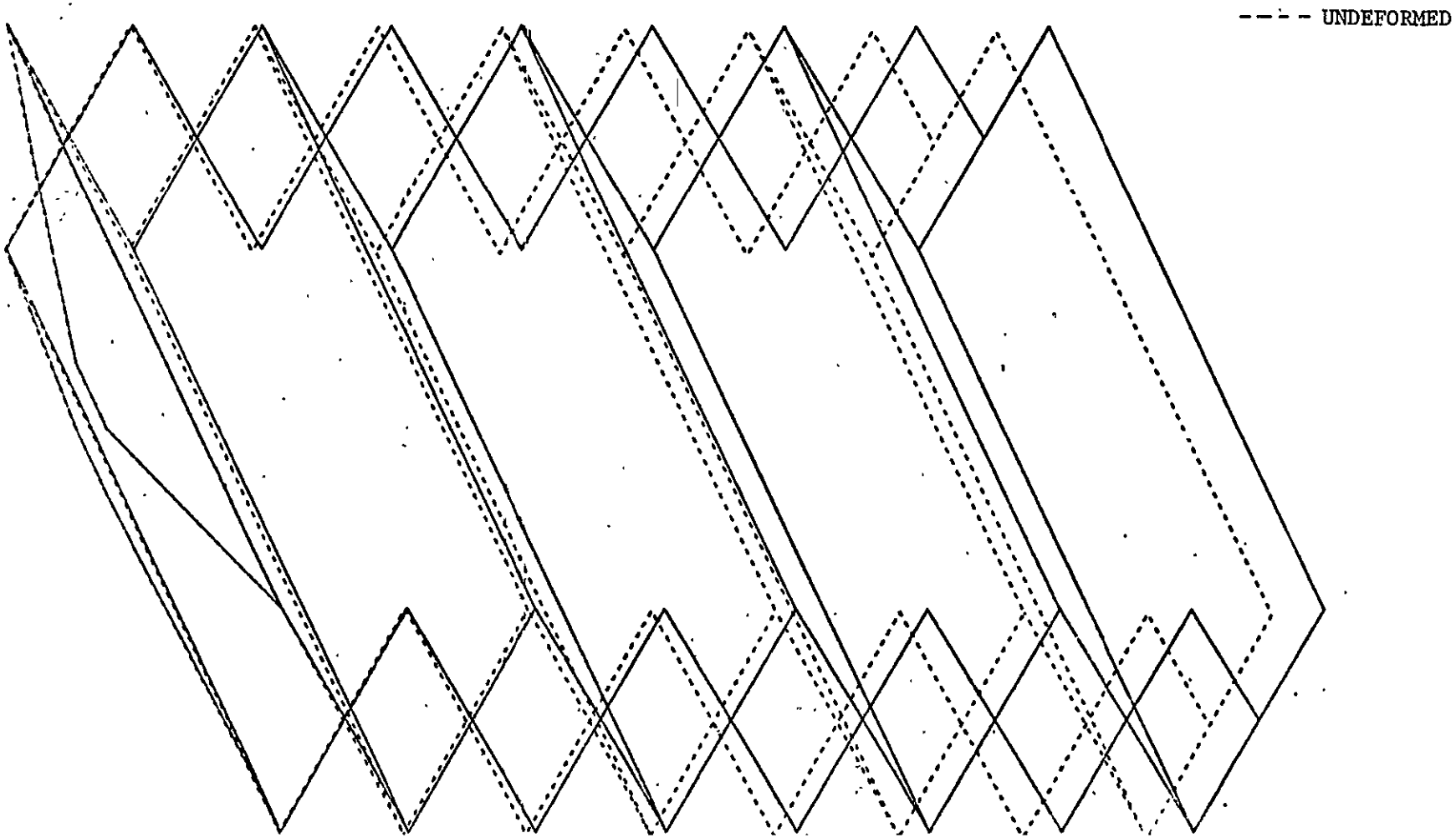

FIGURE 77
PARTIALLY DEPLOYED RADIATOR - 45 DEGS.
25KW POWER MODULE
FREQUENCY = 0.21 CPS

VOUGHT CORPORATION

SECOND MODE

- - - - UNDEFORMED

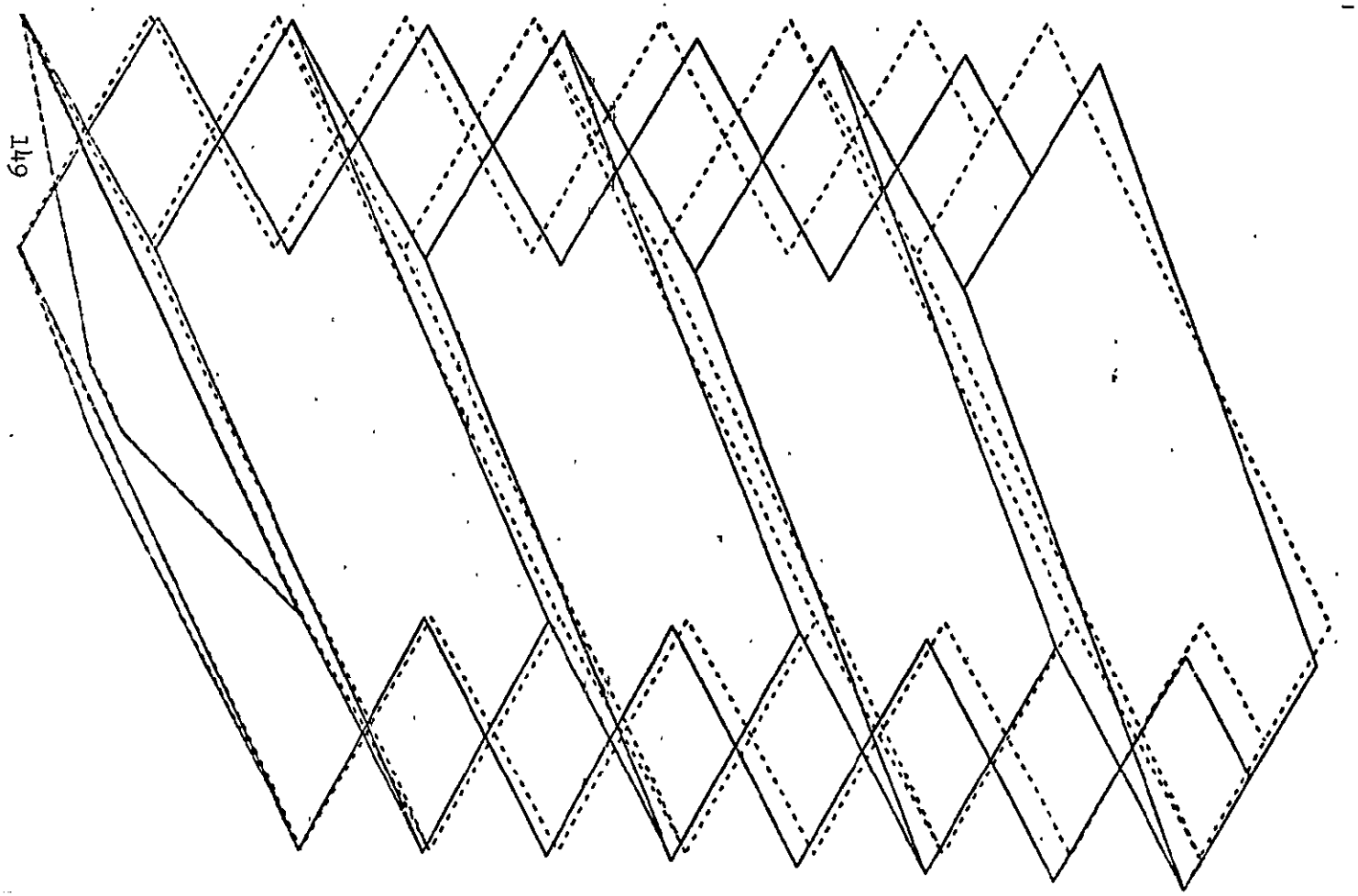

FIGURE 78
PARTIALLY DEPLOYED RADIATOR - 45 DEGS.
25KW POWER MODULE
FREQUENCY = 0.29 CPS

VOUGHT CORPORATION

THIRD MODE

---- UNDEFORMED

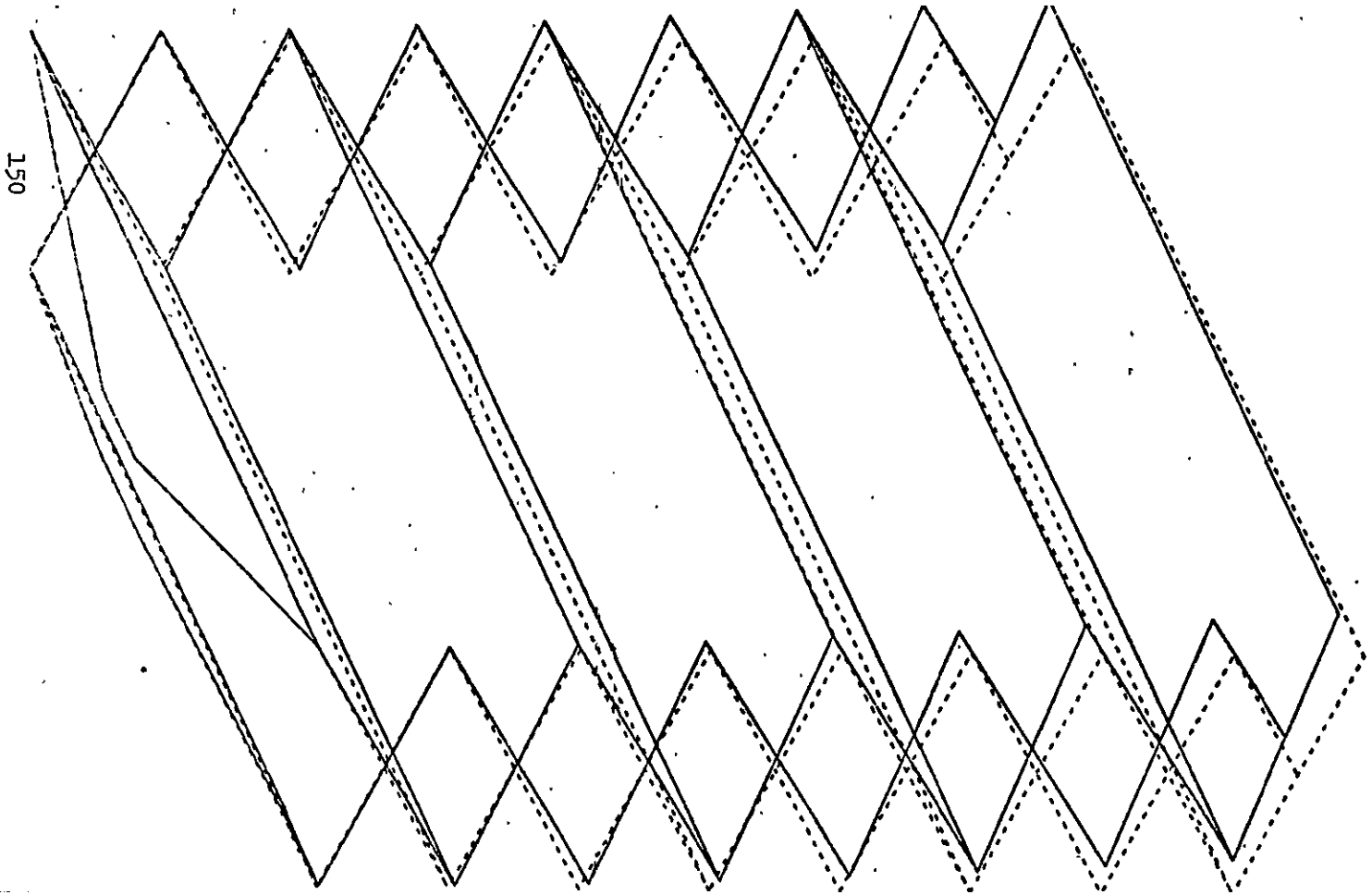

FIGURE 79

PARTIALLY DEPLOYED RADIATOR - 45 DEGS.
25KW POWER MODULE
FREQUENCY = 0.78 CPS

VOUGHT CORPORATION

FOURTH MODE

---- UNDEFORMED

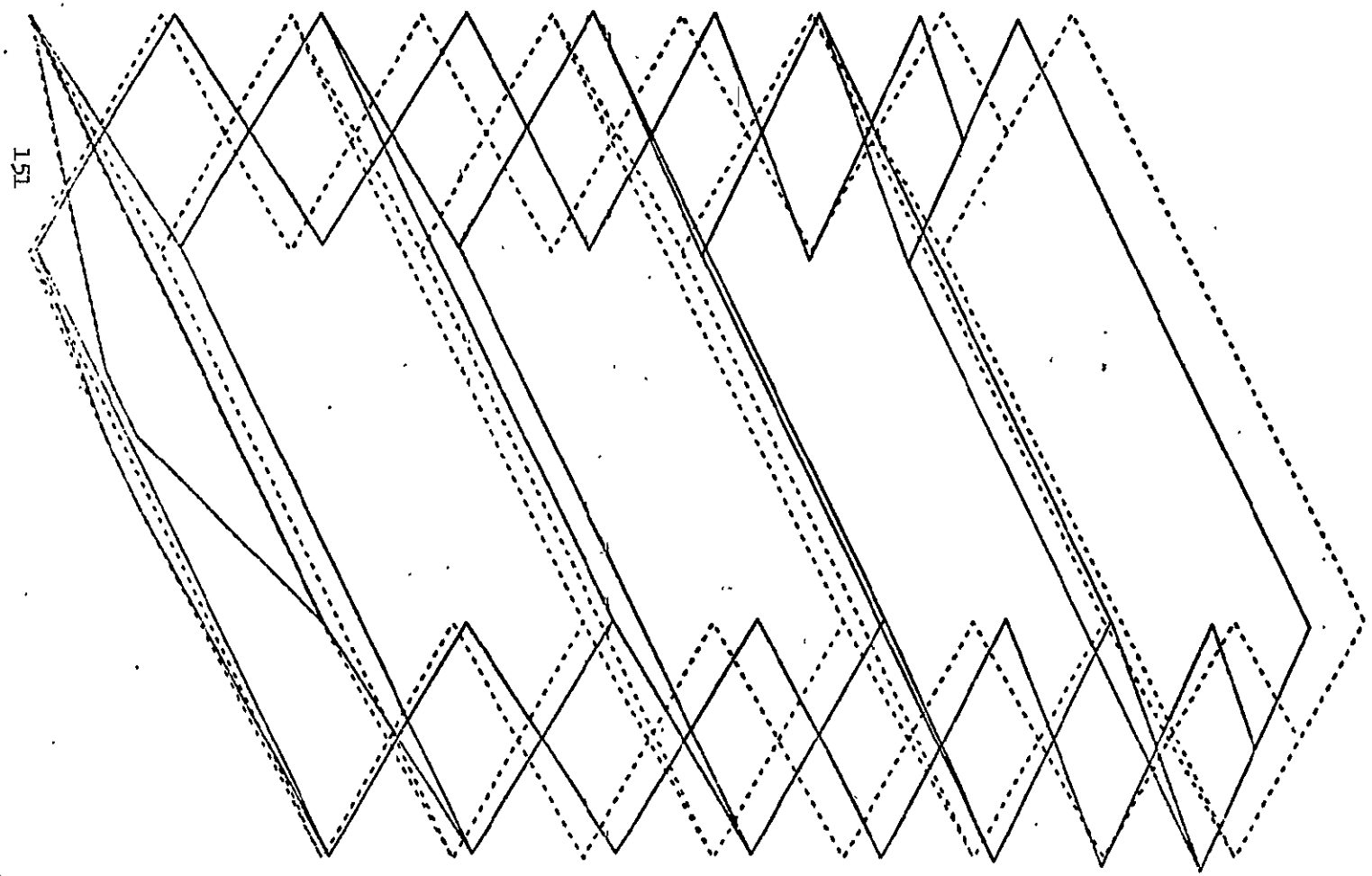

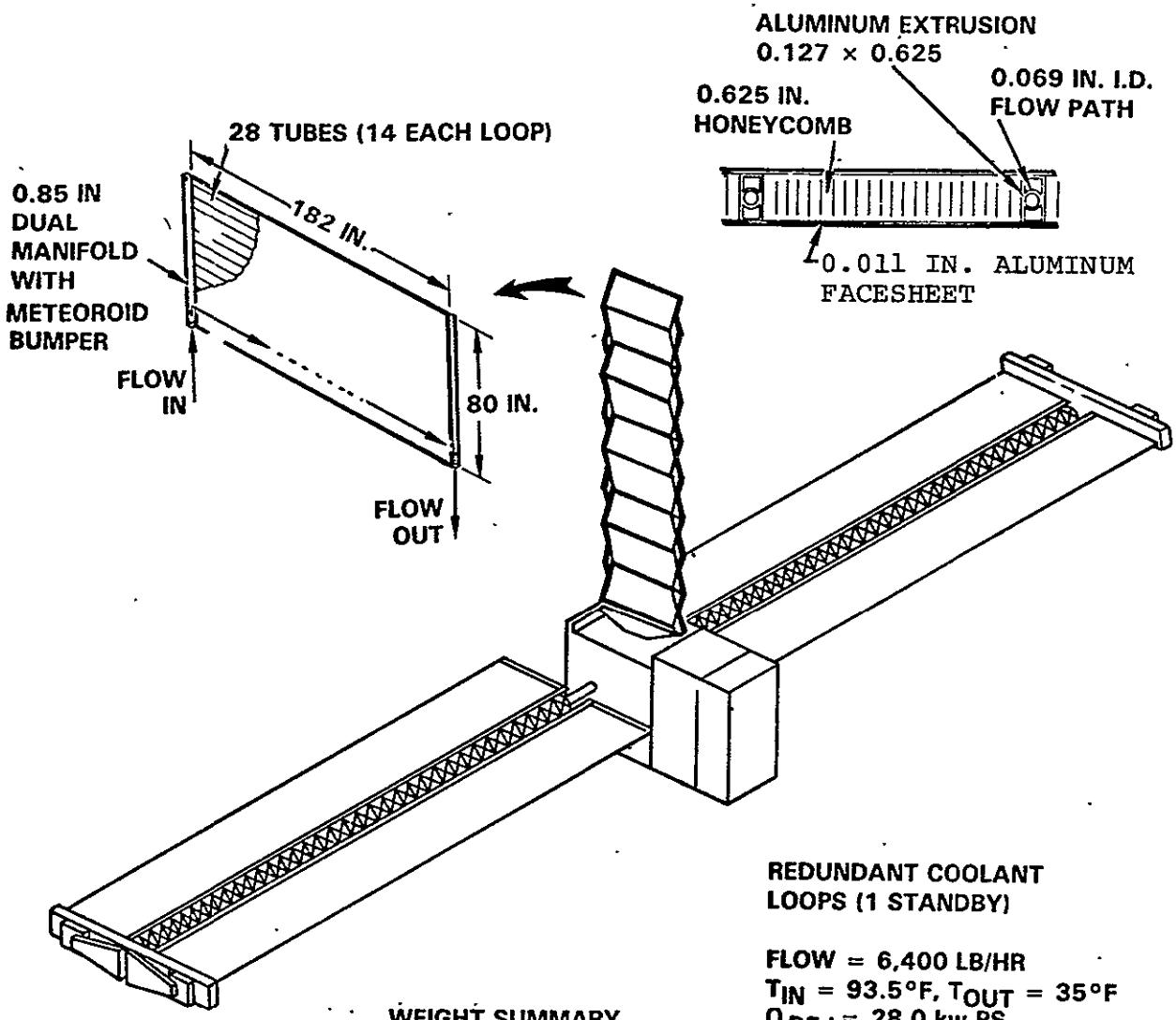

REDUNDANT COOLANT
LOOPS (1 STANDBY)

FLOW = 6,400 LB/HR
T_{IN} = 93.5°F, T_{OUT} = 35°F
Q_{REJ} = 28.0 kw PS
9 kw PAYLOAD
DEPLOYED NATURAL
FREQUENCY = 0.11 HZ

WEIGHT SUMMARY

RADIATOR PANELS (9)	1,322 LB
INTER PANEL FLEX HOSES (40)	80 LB
SCISSORS ARMS (2 × 0.3 IN. WEB I BEAM)	234 LB
DEPLOYMENT BASE – (SOLAR AVOIDANCE) (GEARS, MOTOR, LATCHES, ETC)	247 LB
	1,883 LB

G0-1078-28

FIGURE 80 TCS PRELIMINARY DESIGN SUMMARY

VOUGHT

FIGURE 81

FLEX HOSE SOFT ARMOR METEOROID PROTECTION

BASED ON RITTENHOUSE EQUATION

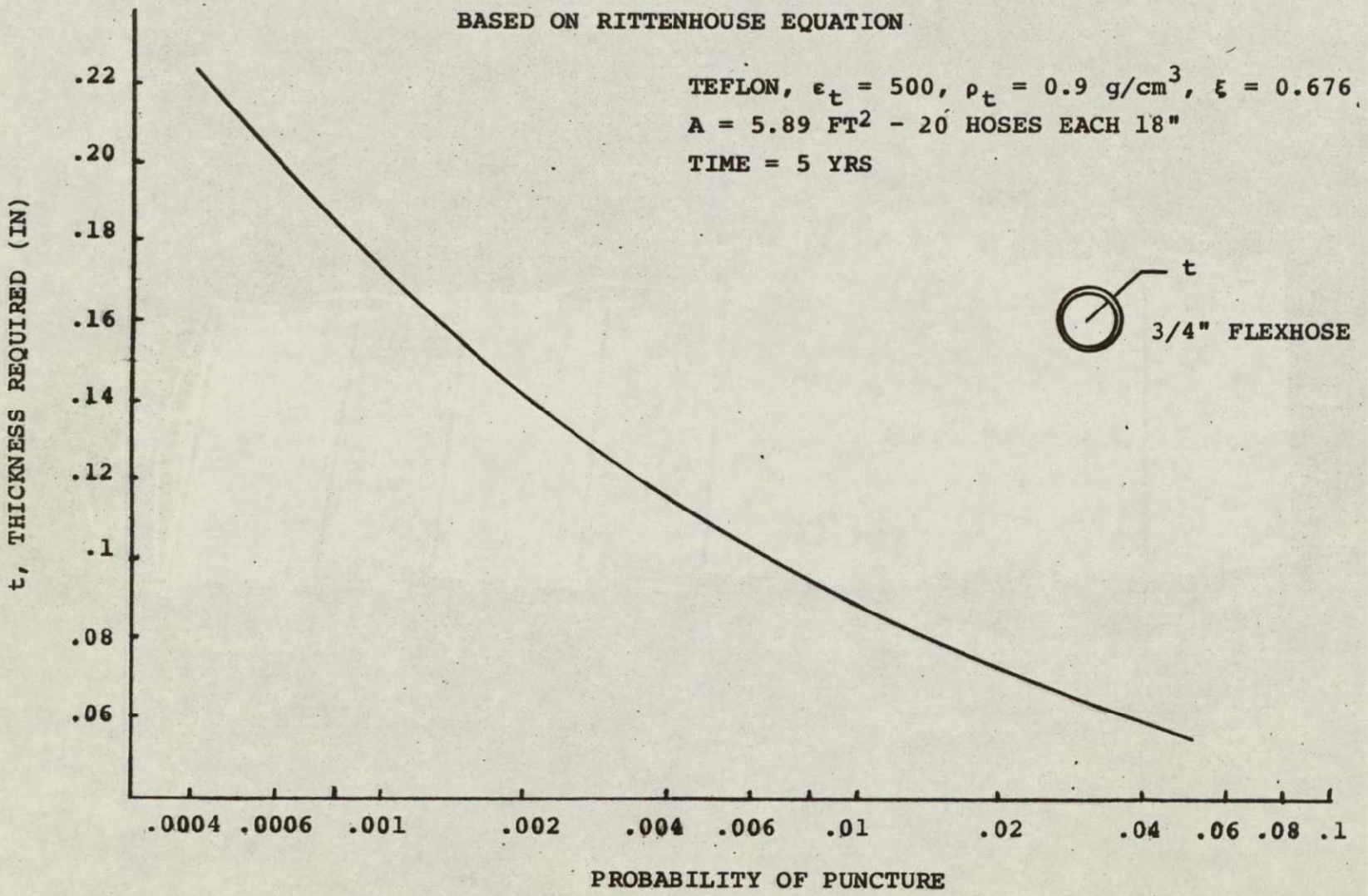

VOUGHT CORPORATION

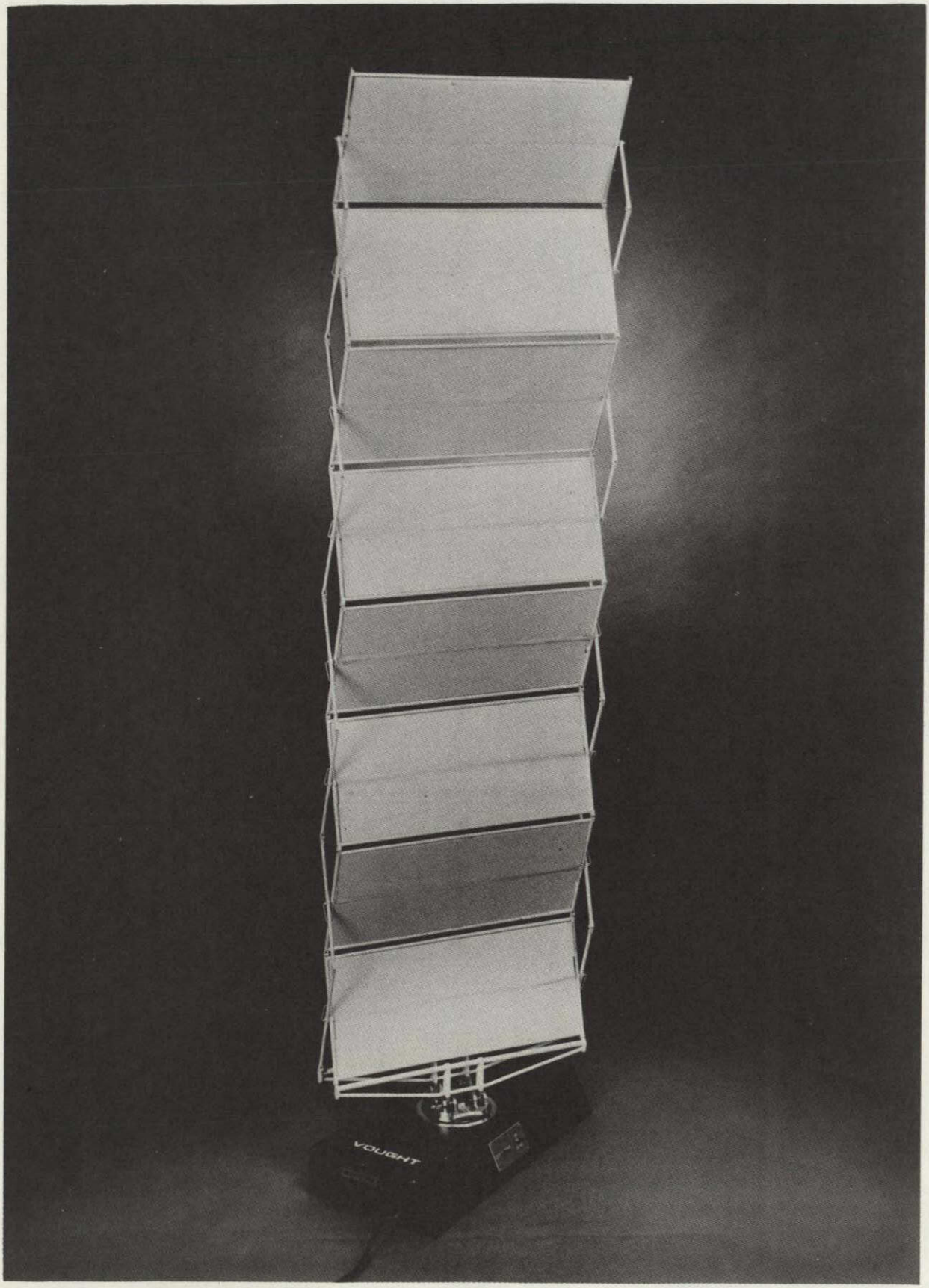

FIGURE 82 FEASIBILITY DEMONSTRATION MODEL - FULLY DEPLOYED

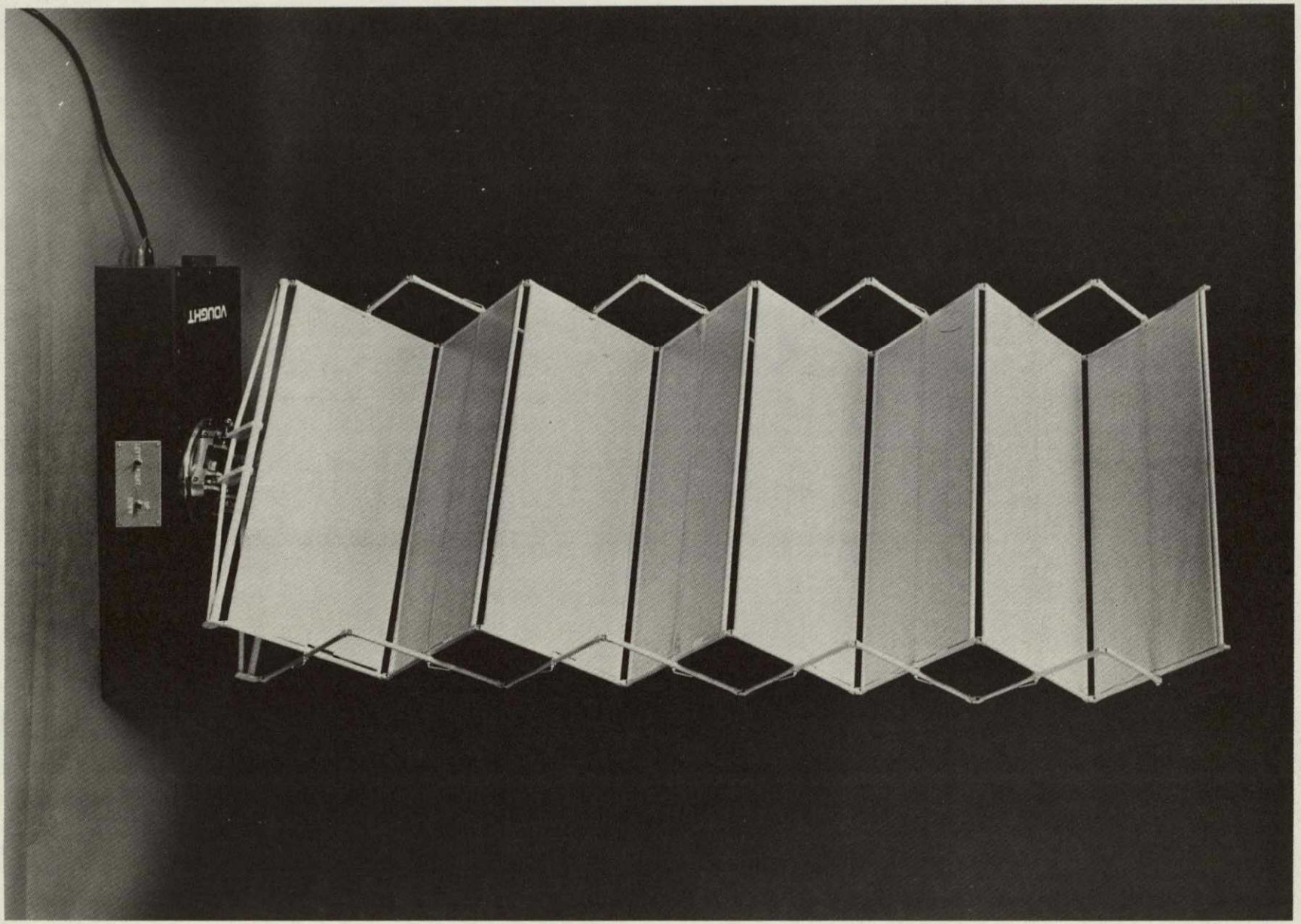

FIGURE 83 FEASIBILITY DEMONSTRATION MODEL - PARTIALLY DEPLOYED

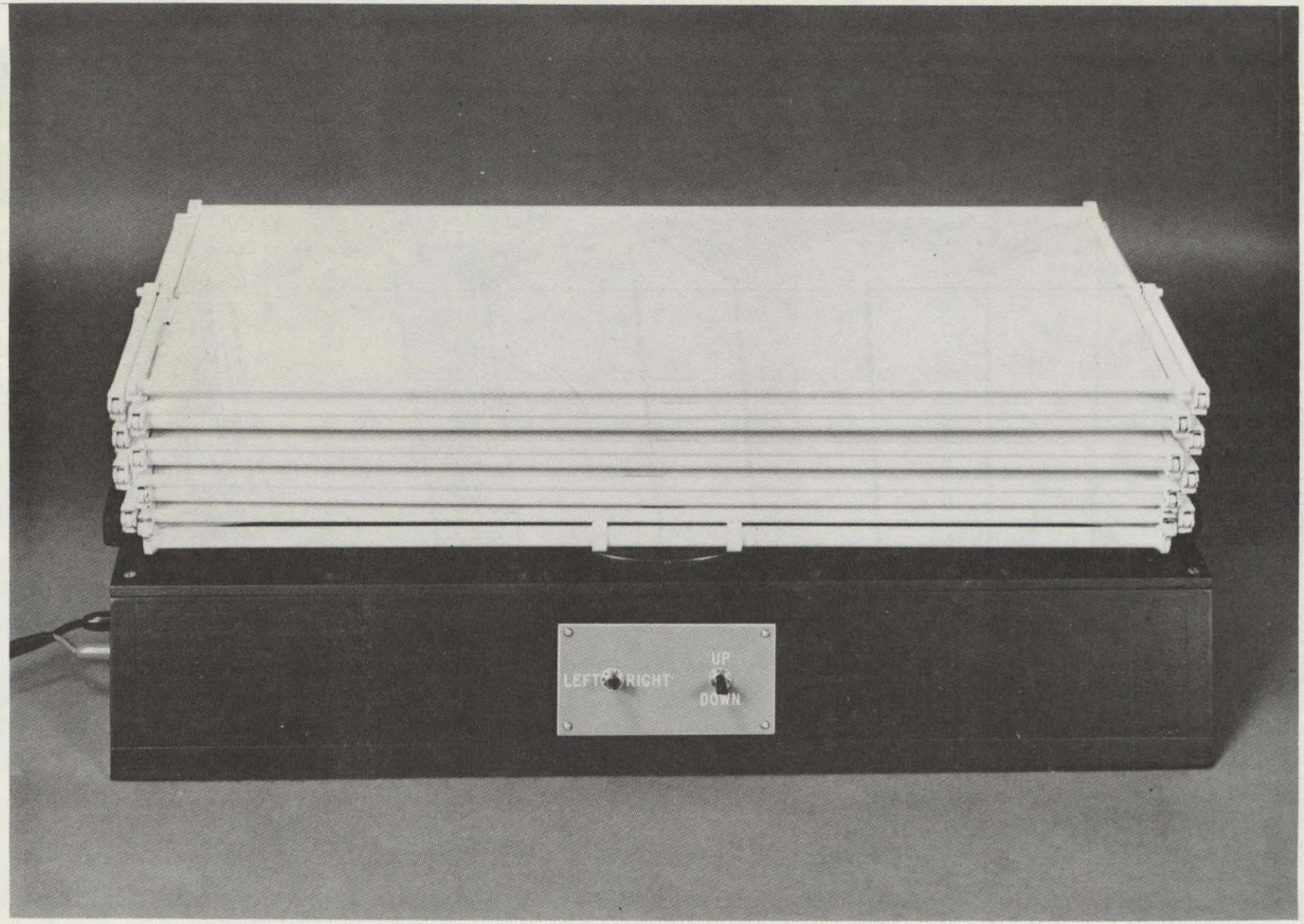

FIGURE 84 FEASIBILITY DEMONSTRATION MODEL - STOWED POSITION

APPENDIX A

RADIATOR/DEPLOYMENT MECHANISM PRELIMINARY DESIGN

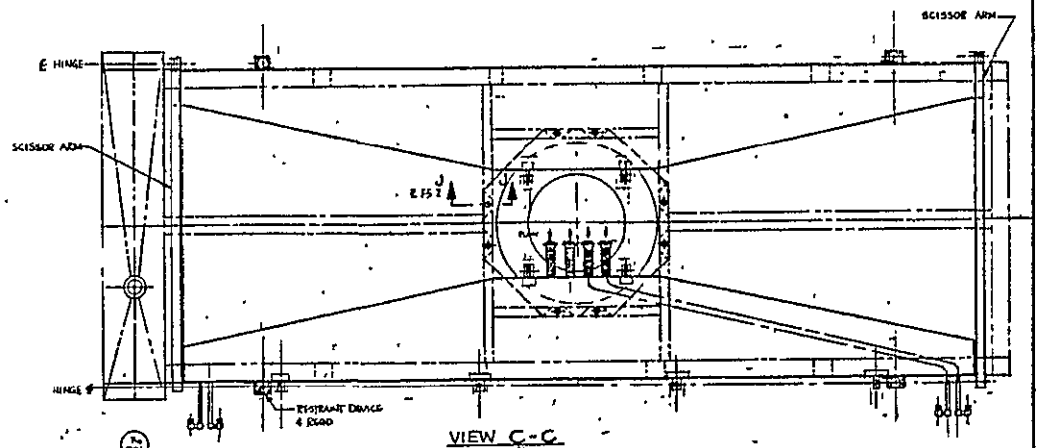

VIEW C-C

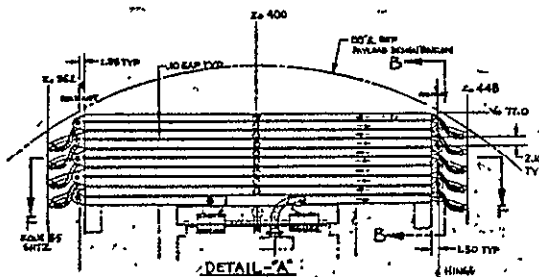

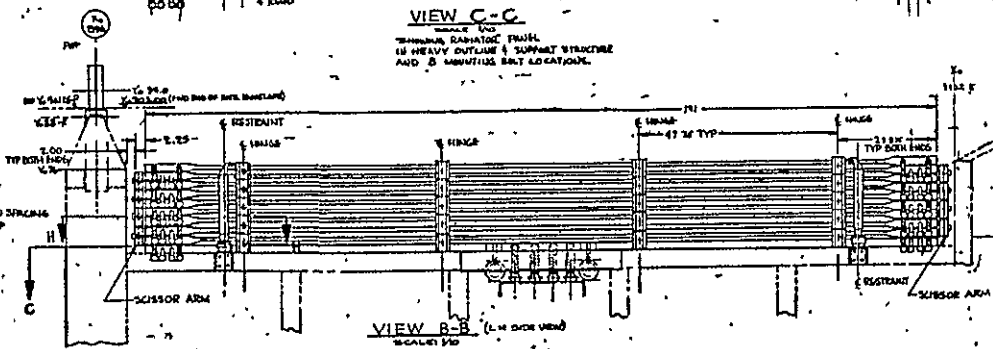

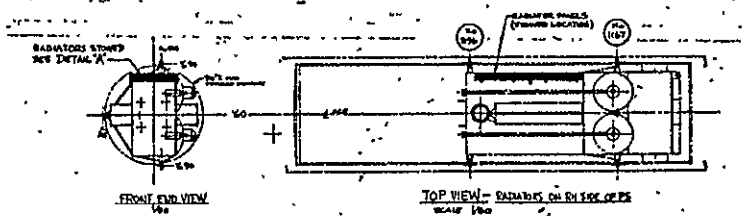

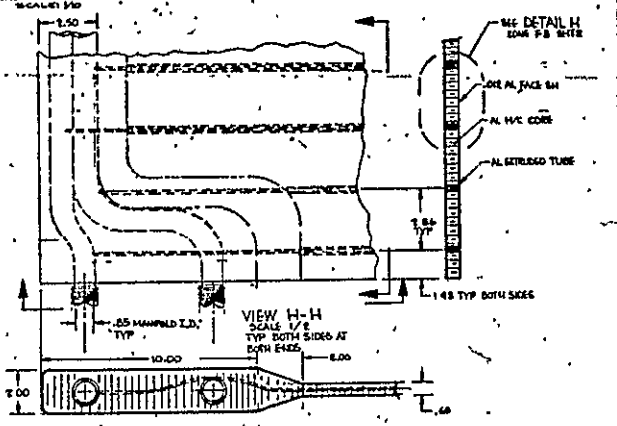

FOLDOU RAMS

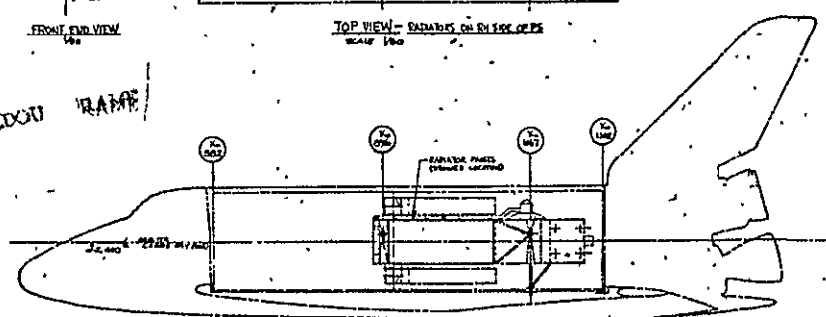

FOLD- RAMS

158 A

158B

VOUGHT CORPORATION			
RADIATOR CONFIGURATION FOR SCISSOR HINGE DEPLOY PARALLEL PUMPED FLUID CONCEPT			
E 80378	221-60113		

DMG SS1-06113 2H

DMG SS1-06113 2H

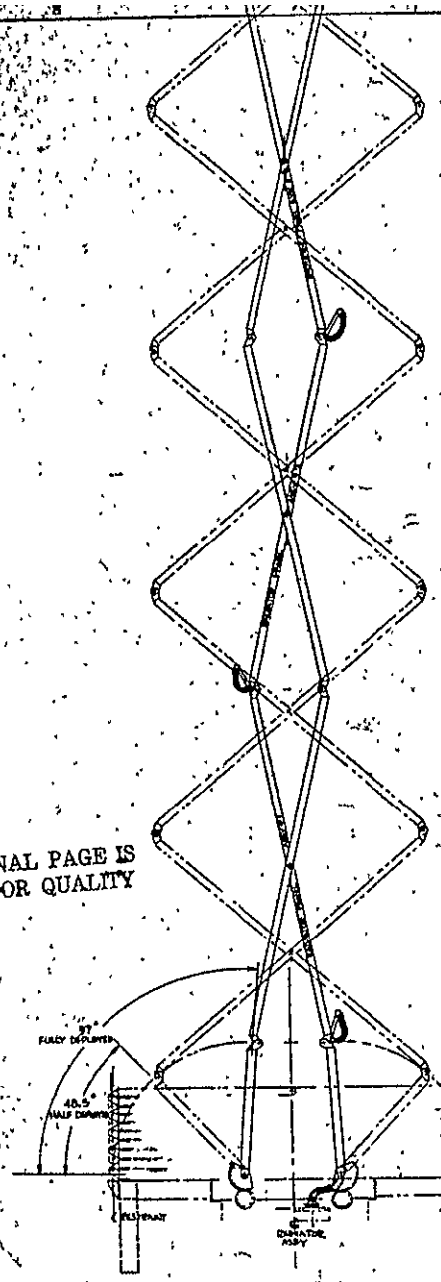

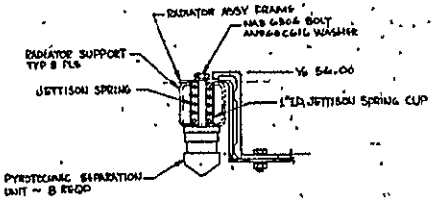

SECTION J-J
ZONE 44 SHT 1
SCALE 1/2

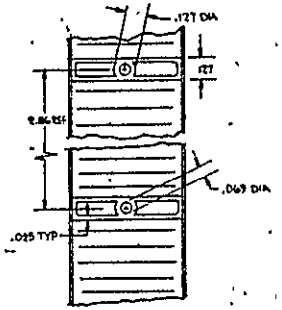

DETAIL H
ZONE D2 SHT 1
SCALE 4/1

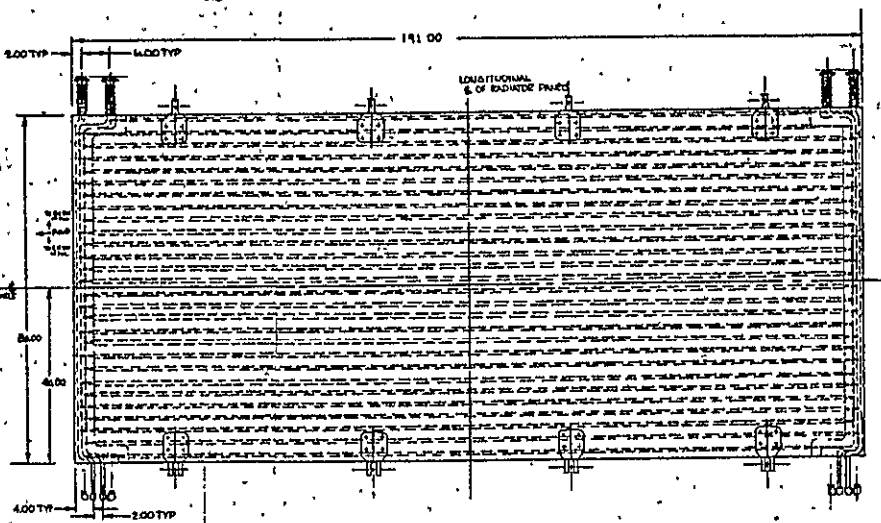

VIEW-F RADIATOR PANEL ASSY (REMOVED FOR CLR)
(ZONE D-6 SHT-1)
SCALE 1/10

DETAIL "D"
SCALE 1/6
SHOWING DEPLOYED ARRANGEMENTS

FOLDOUT FRAME

FOLDOUT FRAME

VOUGHT CORPORATION			
RADIATOR CONFIGURATION FOR SCISSOR HINGE DEPLOY PARALLEL PUMPED FLUID CONCEPT			
E180378	221-60113		

159.A

159.B

VOUGHT
CORPORATION
Post Office Box 225907 • Dallas, Texas 75265
an LTV company